Solar Wind, Suprathermal and Energetic Particles

Bob Wimmer

Institute of Experimental and Applied Physics

Christian-Albrechts-University of Kiel, Germany

wimmer@physik.uni-kiel.de

2021 PKU Summer School, July 8, 2021

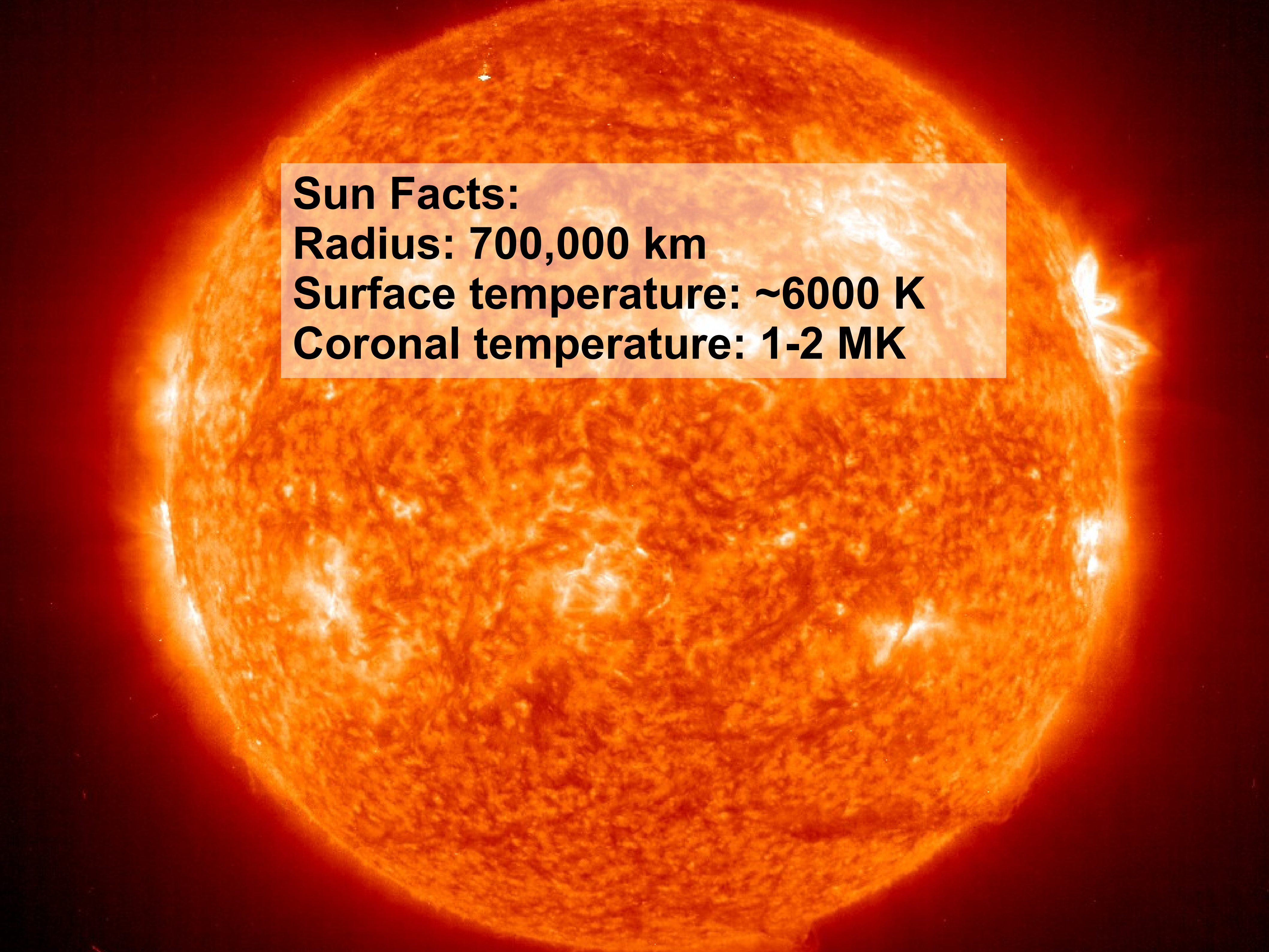
Sun Facts:
Radius: 700,000 km
Surface temperature: ~6000 K
Coronal temperature: 1-2 MK

Early solar wind history: Birkeland, Fitgerald, Lodge (late 19th century)

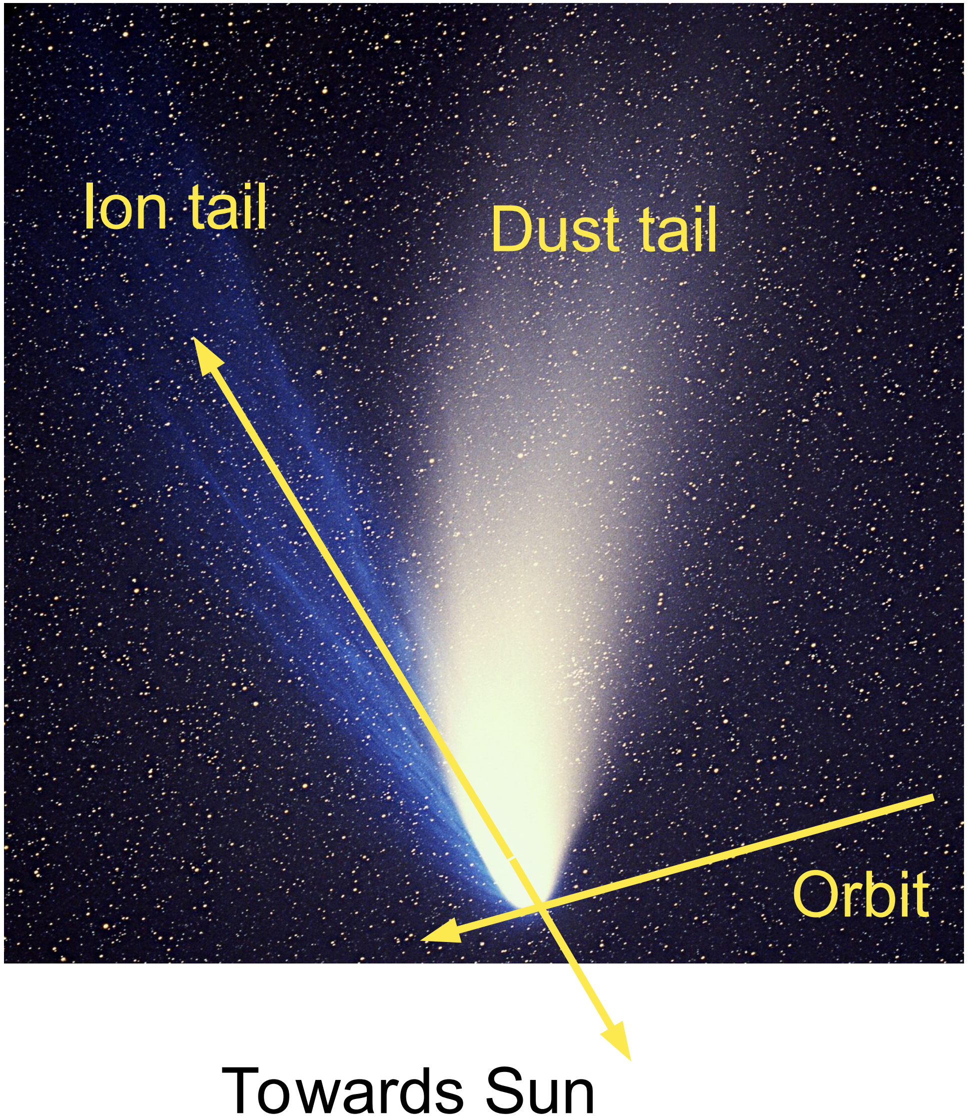

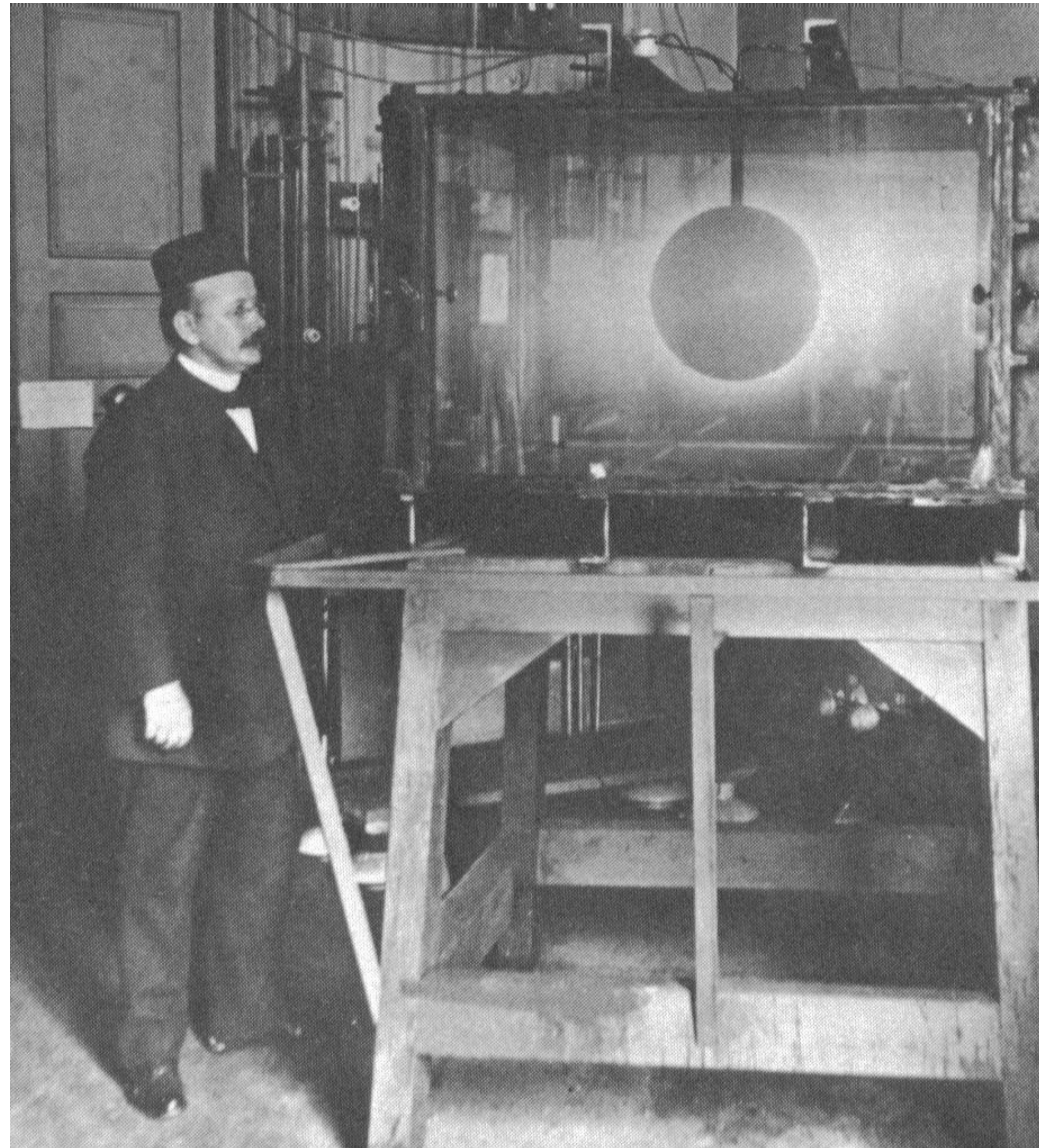

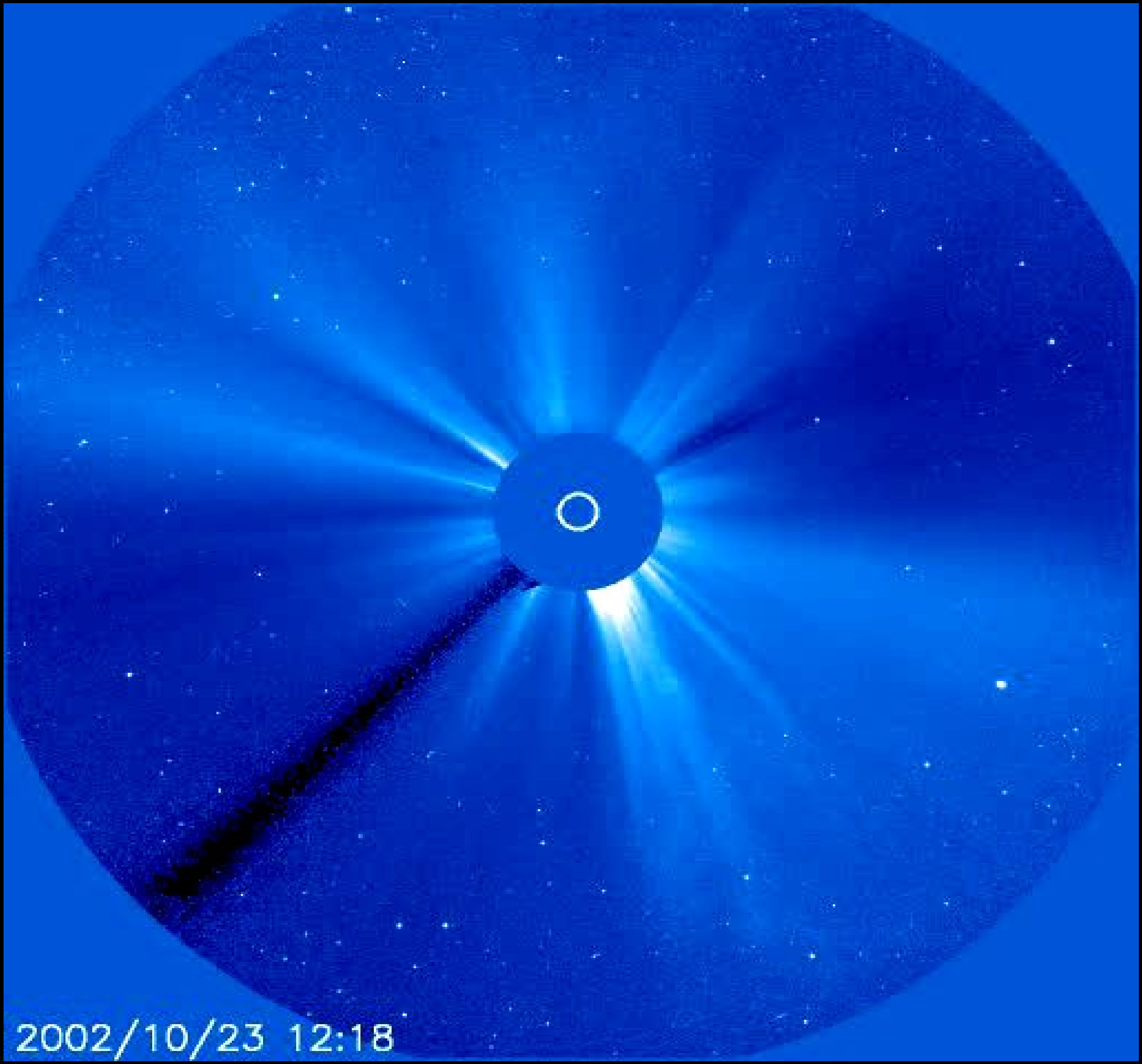
2002/10/23 12:18

Sources of the Solar Wind

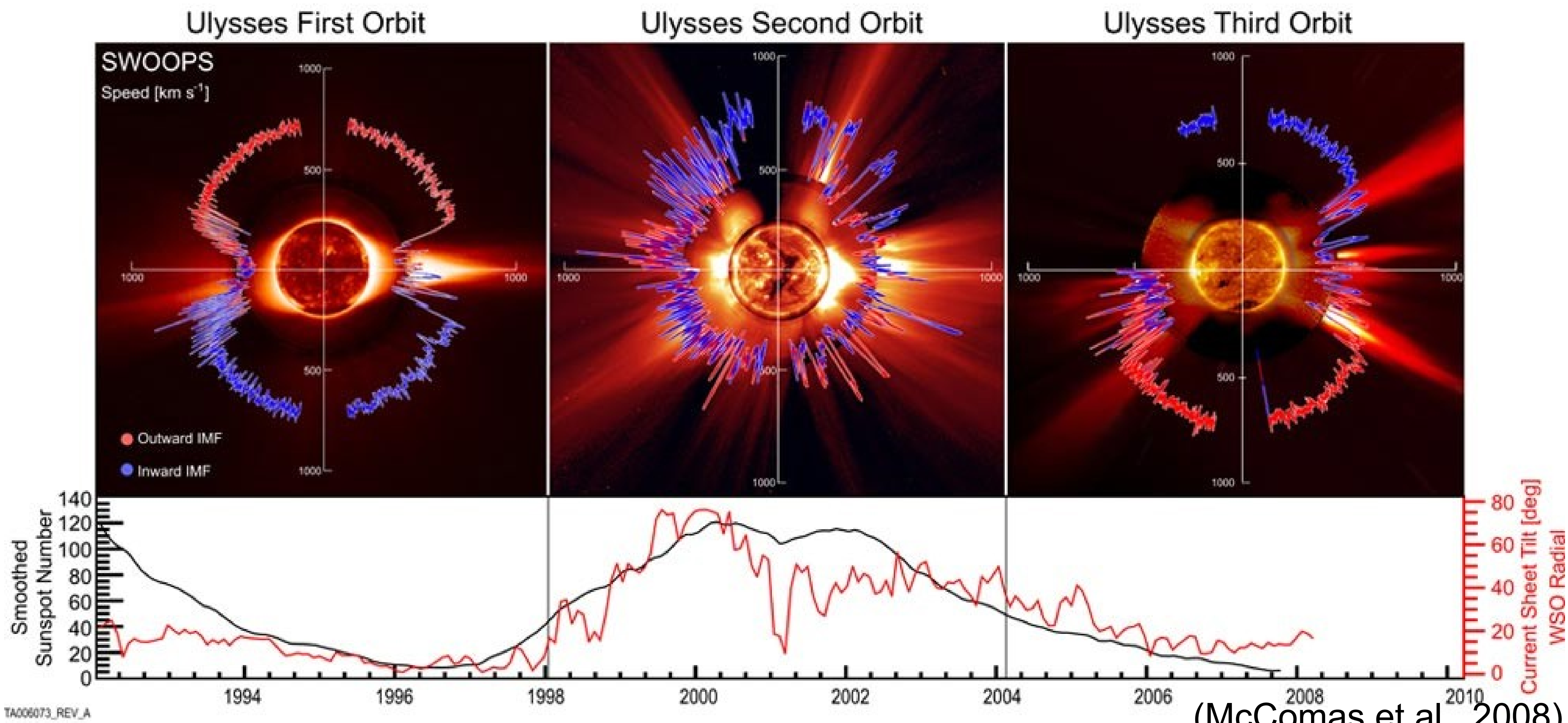

(McComas et al., 2008)

Fast wind from coronal holes

Slow wind from streamer-belt region

Fast wind from coronal holes

Three Types of Solar Wind (SW)

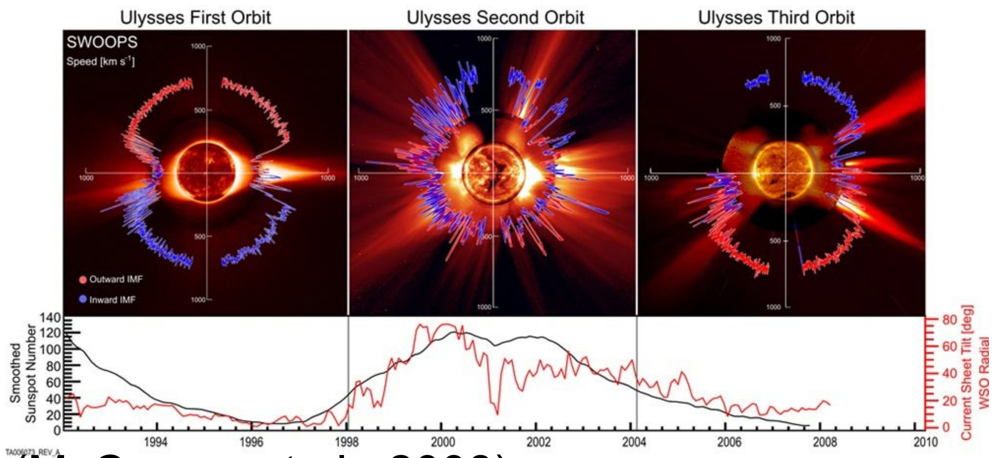

(McComas et al., 2008)

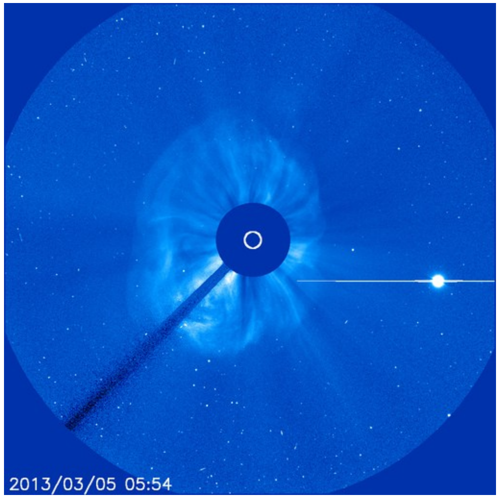

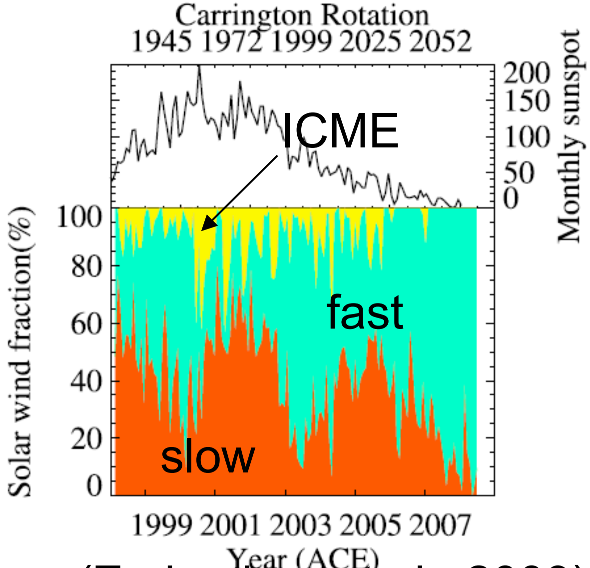

(Zurbuchen et al., 2009)

Fast solar wind from coronal holes
- Fairly uniform but strong turbulence, „young“ SW

Slow solar wind from unknown regions in streamer belt
- Highly variable, dynamically „old“
- Active regions, interchange reconnection, S-web

(Interplanetary) Coronal Mass ejections **(I)CMEs**
- Highly variable but very low turbulence

Composition as a Tracer:

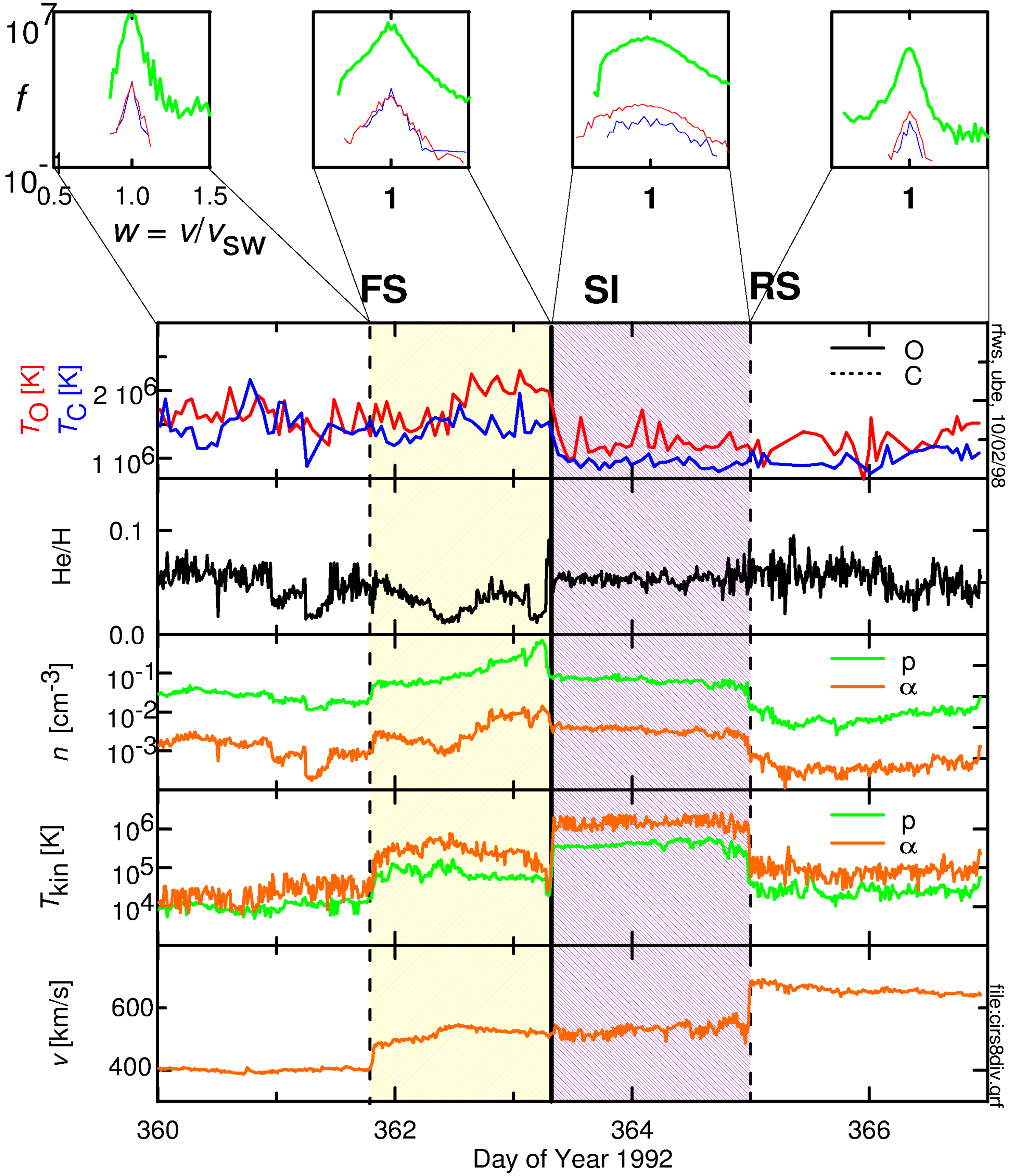

Individual streams can be identified in-situ by many independent methods:
- magnetic field
- plasma data
- specific entropy
- composition

Composition is not altered by kinetic processes and remains conserved once it has been set in chromosphere and corona. **Excellent tracer!**

Composition variable, especially in slow wind.

Three Types of Solar Wind (SW)

	v [km/s]	T [K]	n [/cm^3]	δB/B	Elem. Compos.	<Q>
Fast	500 - 750	10^5	5	high	Small bias, ~constant	low
Slow	300 - 500	$5\ 10^4$	10	low	Large bias, variable	high
ICME	300 - 2500	$2\ 10^4$	5 - 50	Very low	variable	mixed

Numbers are only typical values at 1 AU, in fact quite variable. Elemental composition is organized according to First Ionization Potential (FIP). Elements with low FIP are enriched relative to elements with high FIP.

Processes affecting composition:

FIP Enhancements seen in
- solar wind,
- energetic particles,
- active regions,
- coronal abundances,
- coronae of other stars.

FIP effect:
Separation of ions from neutrals.

Acts mainly in chromosphere.

Time scales:
- diffusion is slowest process
- 100 km diameter flux tube
- T ~ 4'000 K
==> diffusion time is order of days!

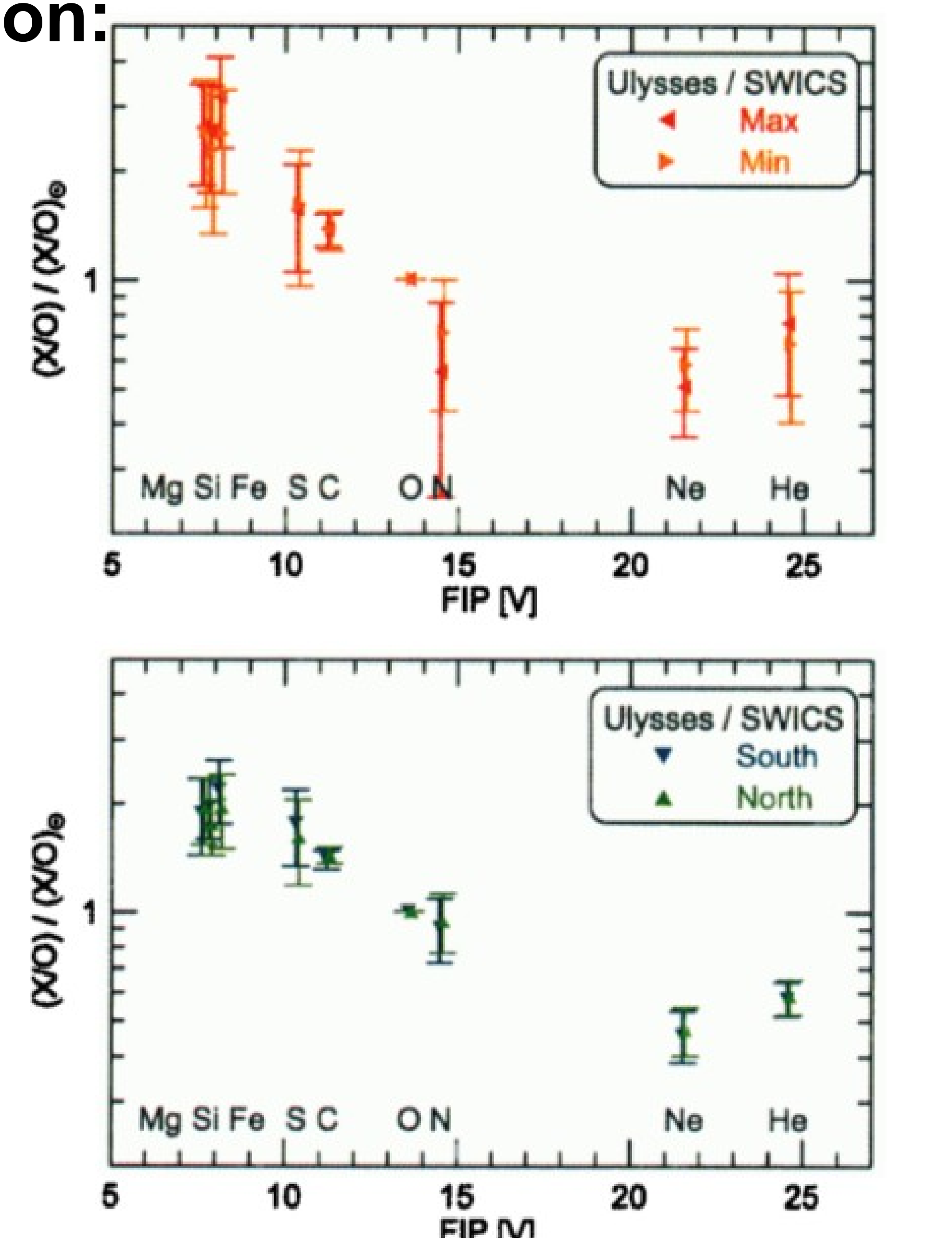

v. Steiger et al. (2000)

Processes affecting composition:

FIP Enhancements seen in
- solar wind,
- energetic particles,
- active regions,
- coronal abundances,
- coronae of other stars.

FIP effect:
Separation of ions from neutrals.

Acts mainly in chromosphere.

Time scales:
- diffusion is slowest process
- 100 km diameter flux tube
- T ~ 4'000 K
==> diffusion time is order of days!

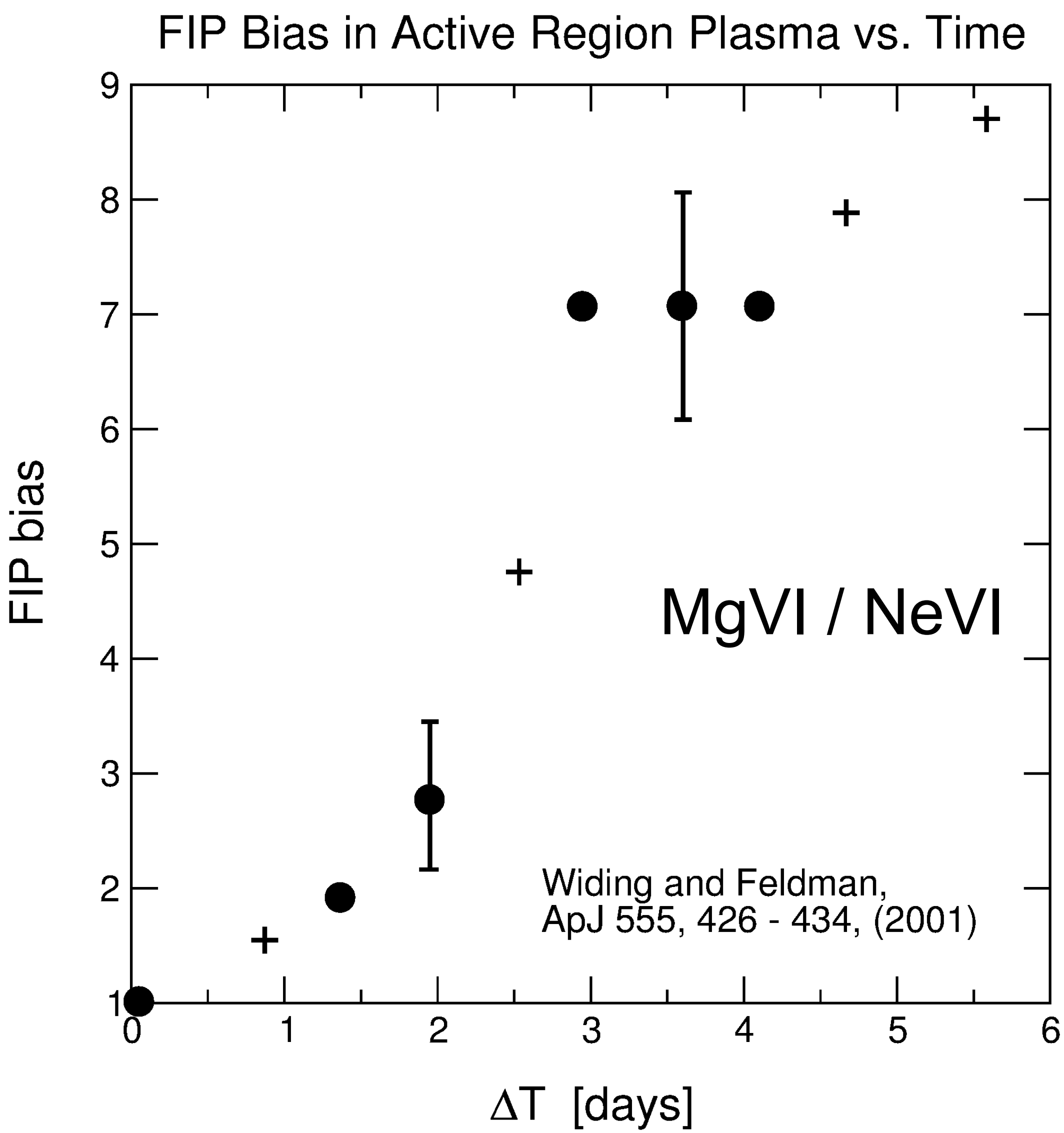

Composition as a Tracer:

Charge states freeze in in the solar wind expansion process

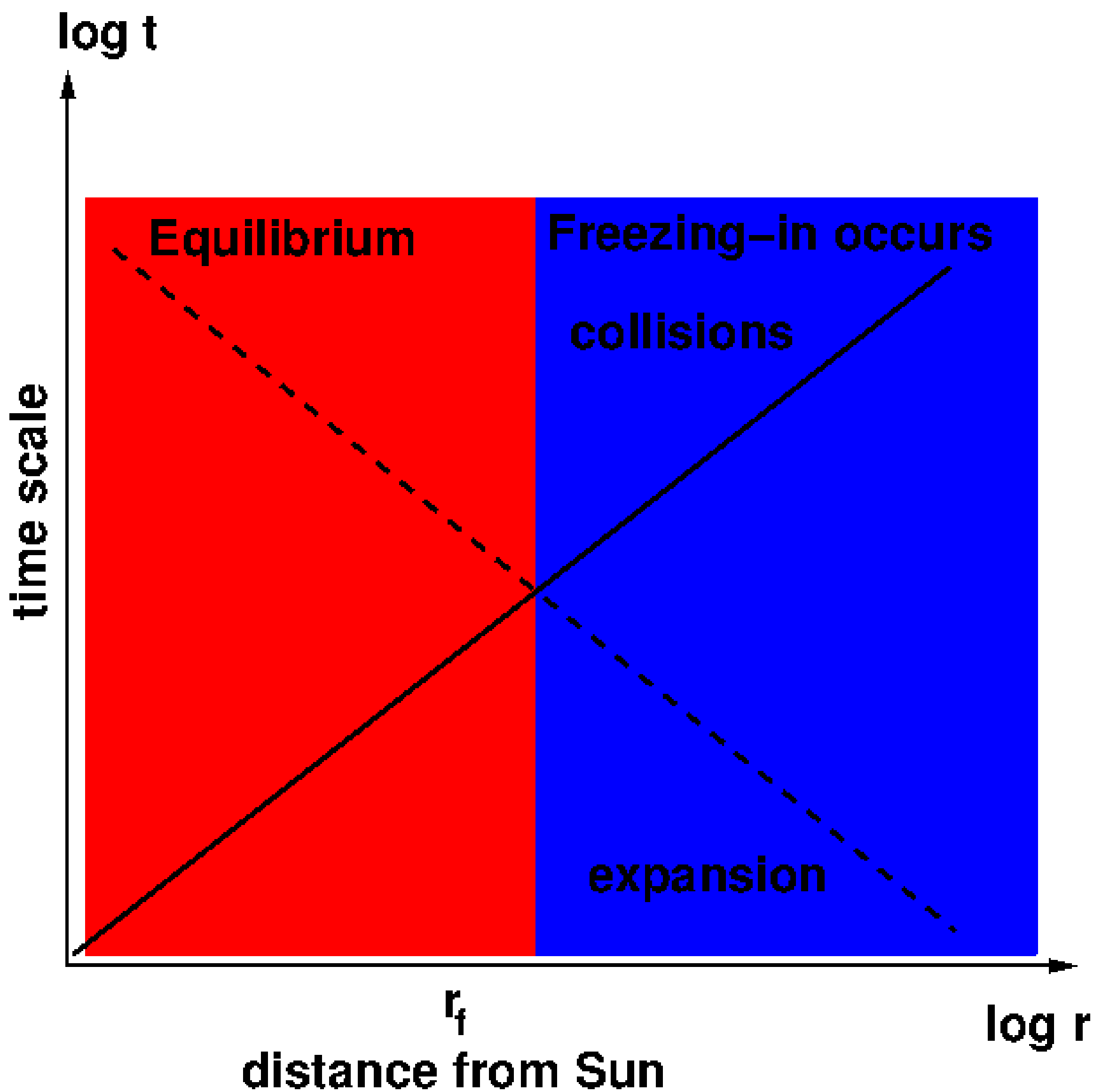

In situ charge states have lost all memory of what happened in deep corona.
They retain memory of their last charge modification (charge states frozen in) in the upper corona.

Solar wind is heated and accelerated in the corona, density decreases with height above the photosphere.

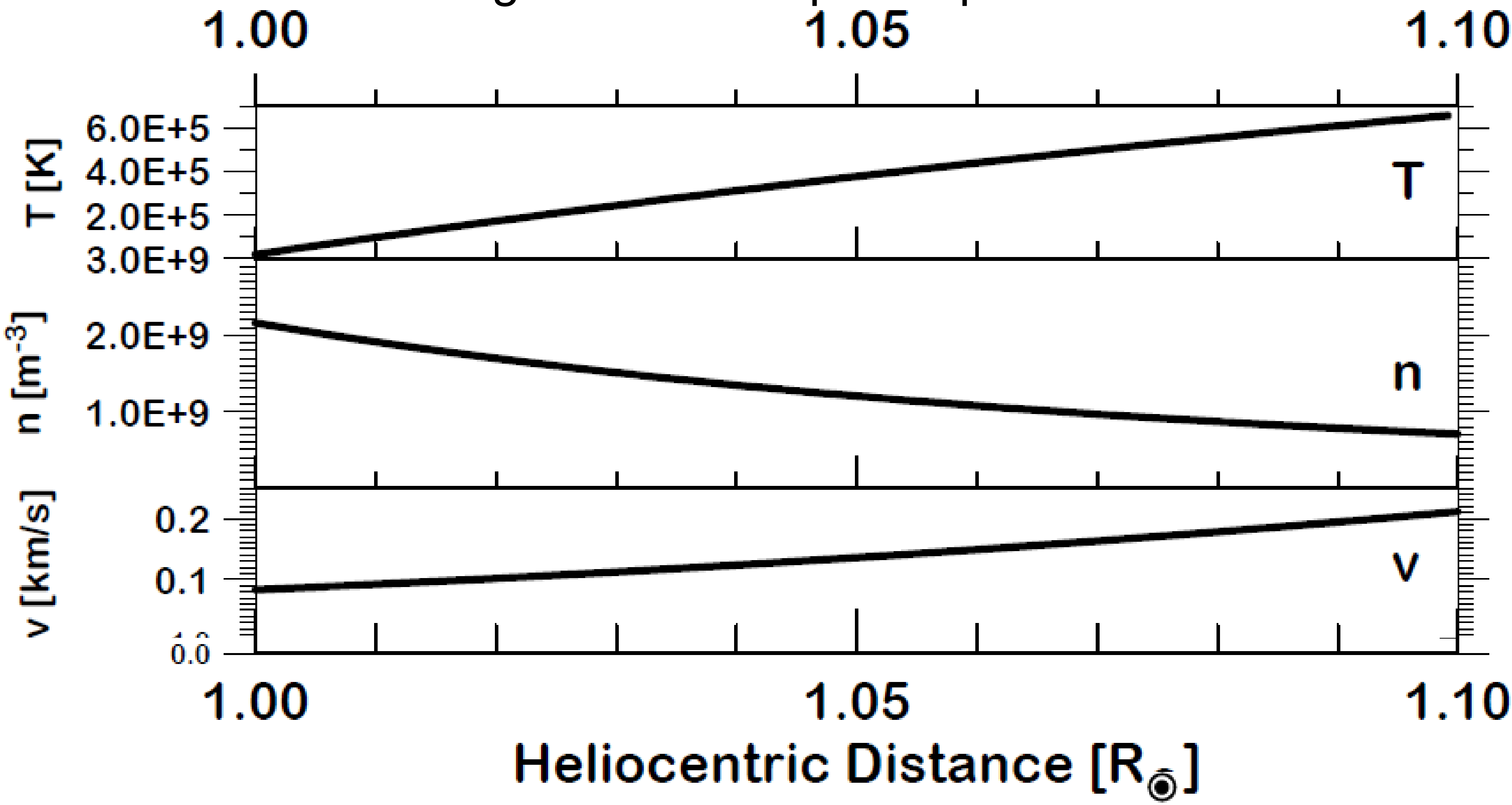

⇒ typical time scales change!

(Bochsler, 2007)

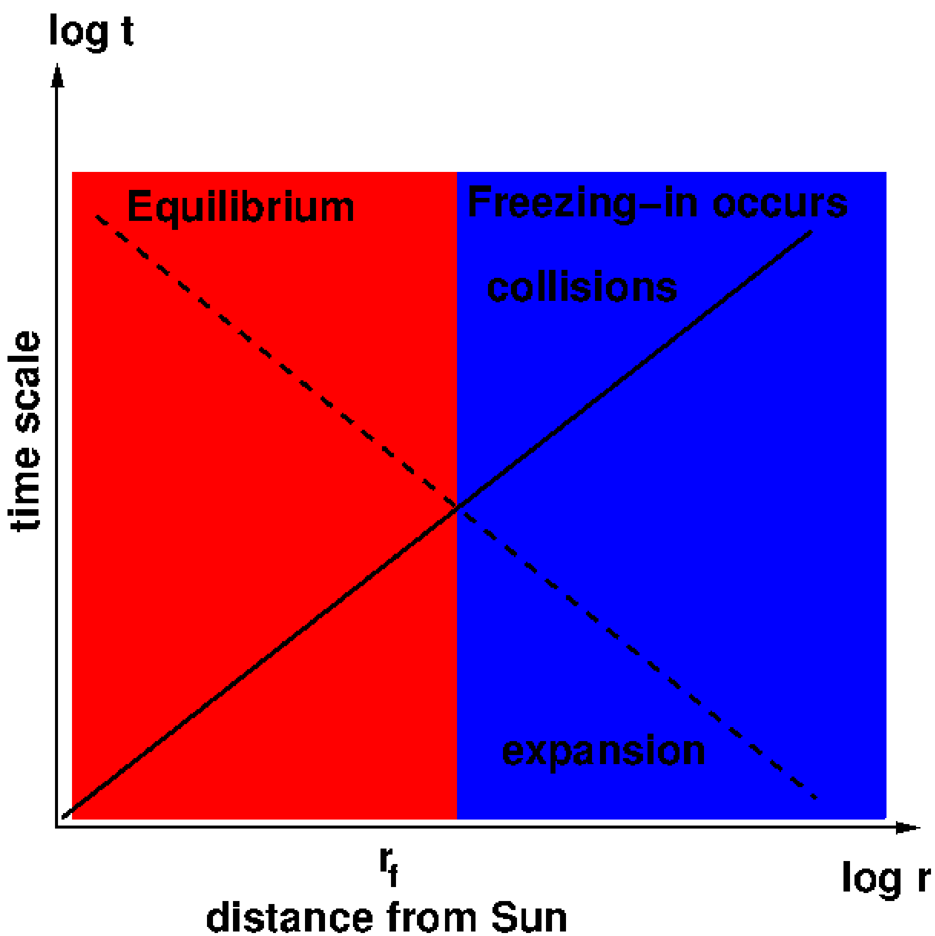

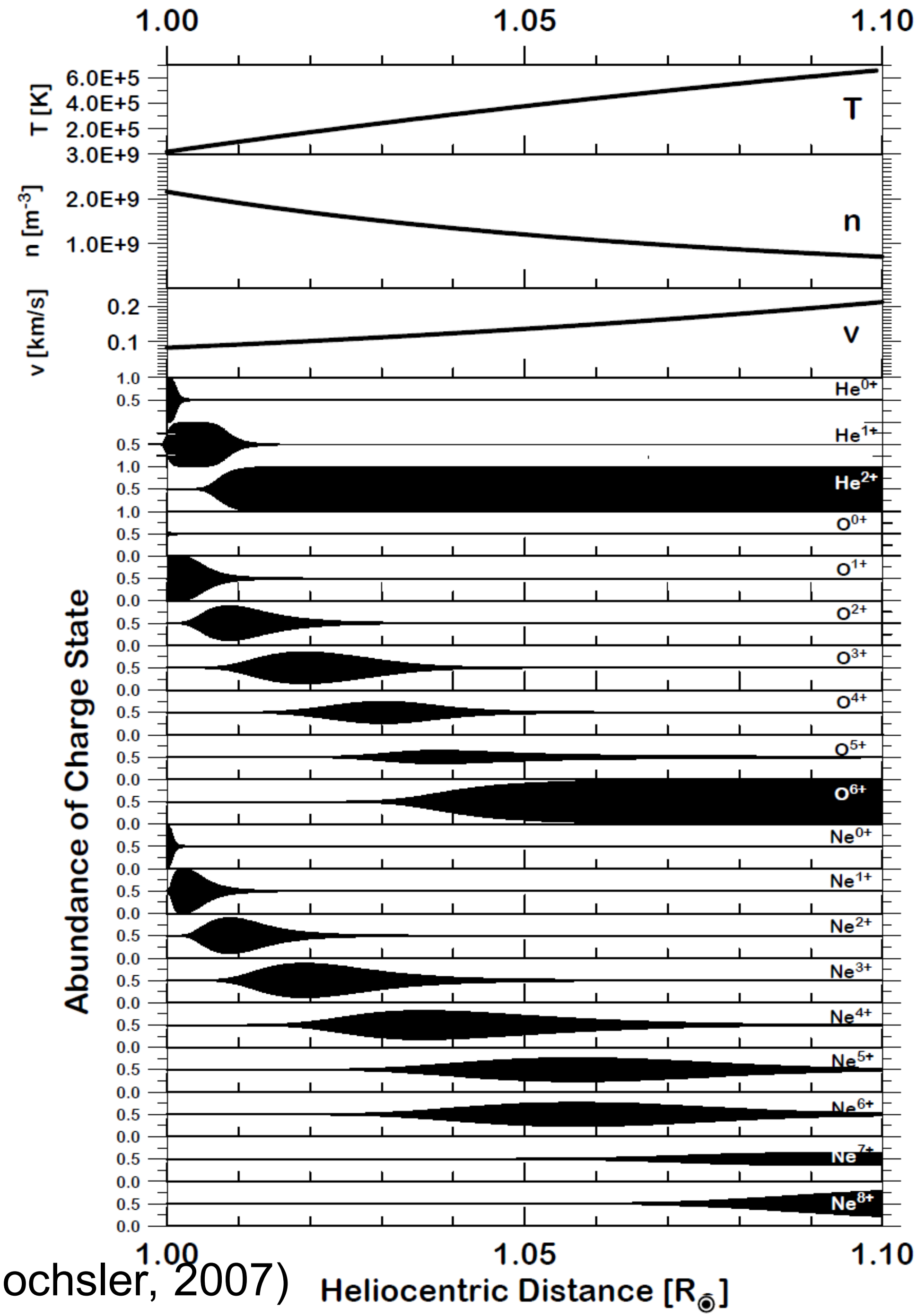

Solar wind charge states are frozen in close to the Sun.

(Bochsler, 2007)

Heavy-Ion Charge-State Composition

Continuity equation for O^{6+}

recombination

$$\frac{\partial n_6}{\partial t} + \vec{\nabla}\left(n_6 \vec{u}_6\right) = n_e \left[n_5 C_5 \; - \; n_6 \left(R_6 + C_6\right) \; + \; n_7 R_7\right]$$

ionization

$$\begin{aligned}
\frac{\partial n_0}{\partial t} + \vec{\nabla}\left(n_0 \vec{u}_0\right) &= n_e \left[- n_0 C_0 \; + \; n_1 R_1\right], \\
\frac{\partial n_1}{\partial t} + \vec{\nabla}\left(n_1 \vec{u}_1\right) &= n_e \left[n_0 C_0 \; - \; n_1 \left(R_1 + C_1\right) \; + \; n_2 R_2\right], \\
\vdots &= \vdots \\
\frac{\partial n_i}{\partial t} + \vec{\nabla}\left(n_i \vec{u}_i\right) &= n_e \left[n_{i-1} C_{i-1} \; - \; n_i \left(R_i + C_i\right) \; + \; n_{i+1} R_{i+1}\right], \\
\vdots &= \vdots \\
\frac{\partial n_{n-1}}{\partial t} + \vec{\nabla}\left(n_{n-1} \vec{u}_{n-1}\right) &= n_e \left[n_{n-2} C_{n-2} \; - \; n_{n-1} \left(R_{n-1} + C_{n-1}\right) \; + \; n_n R_n\right] \\
\frac{\partial n_n}{\partial t} + \vec{\nabla}\left(n_n \vec{u}_n\right) &= n_e \left[n_{n-1} C_{n-1} \; - \; n_n R_n\right].
\end{aligned}$$

How to measure solar wind composition Example: SWICS (Ulysses & ACE)

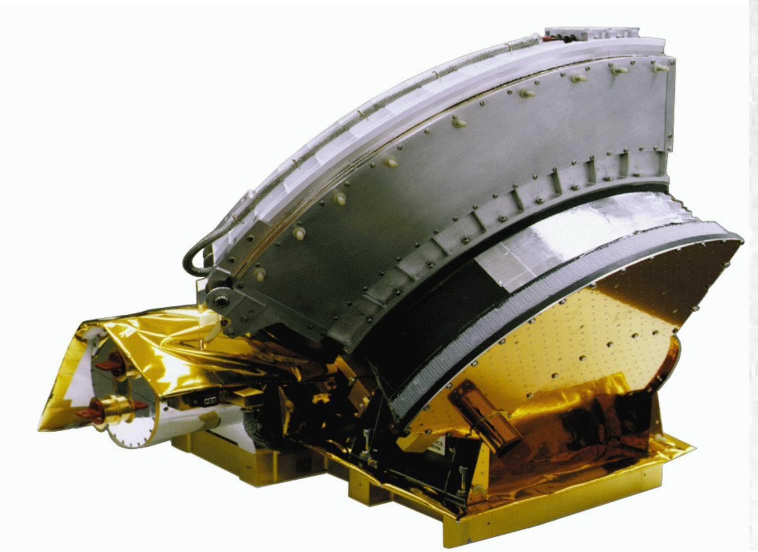

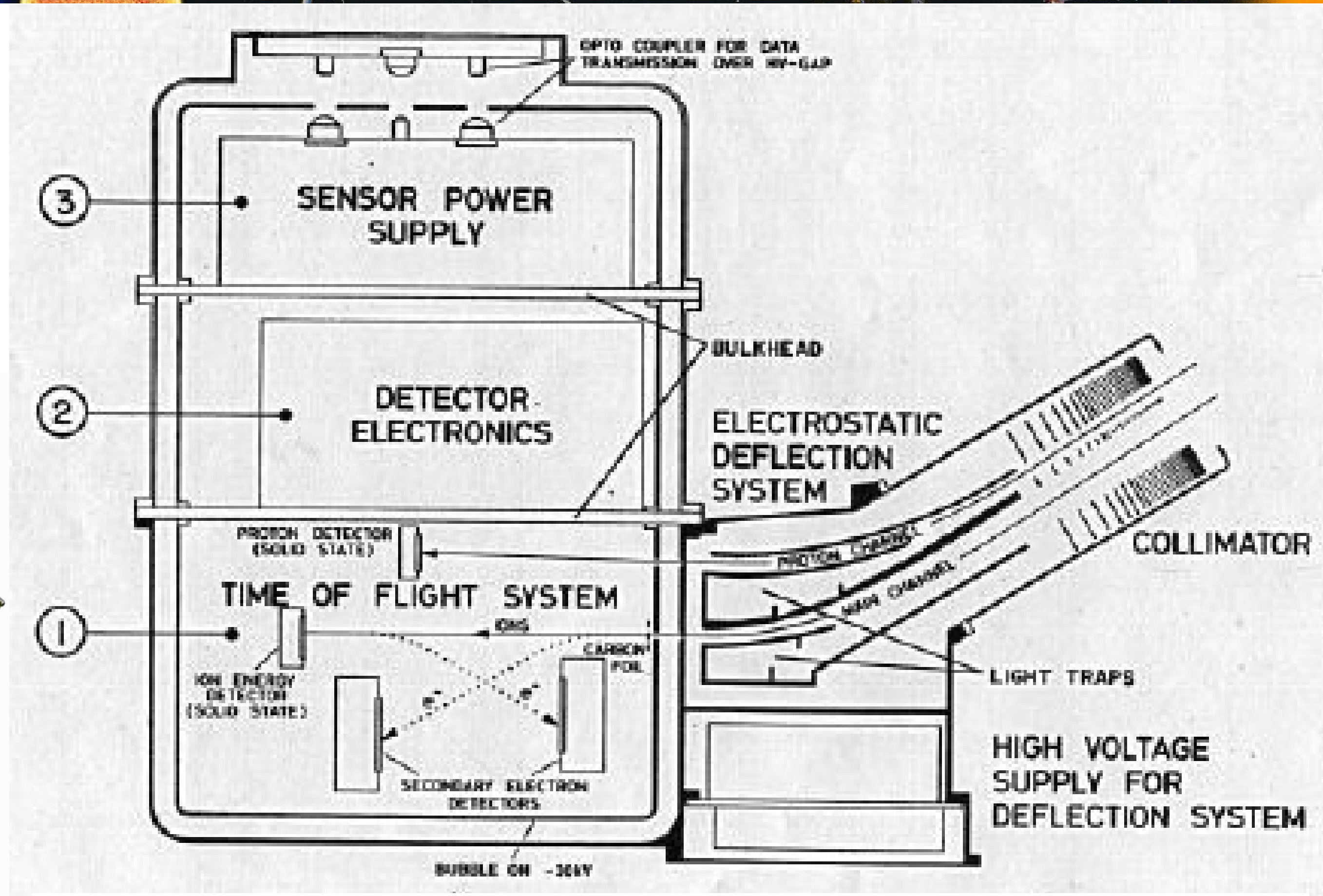

CTOF on SOHO, PLASTIC on STEREO, and HIS on Solar Orbiter work in a similar manner.

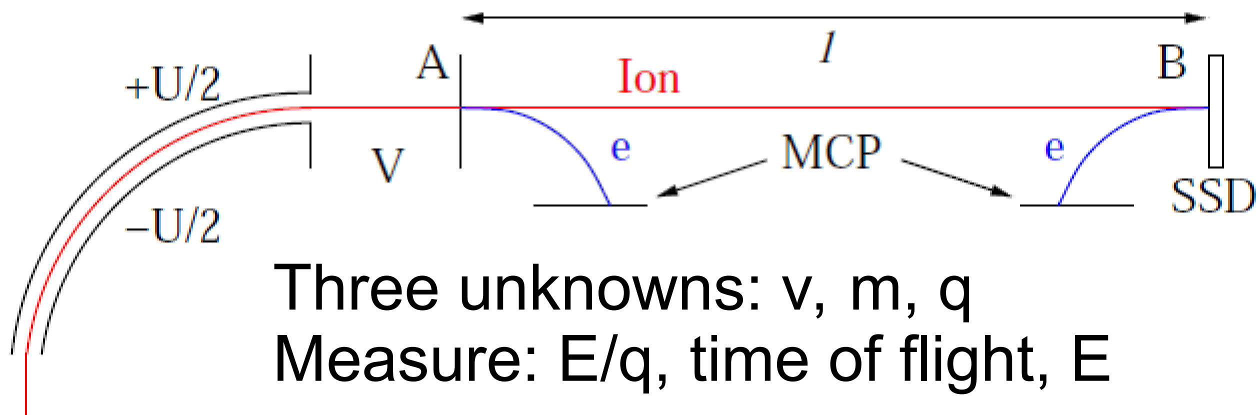

Three unknowns: v, m, q
Measure: E/q, time of flight, E

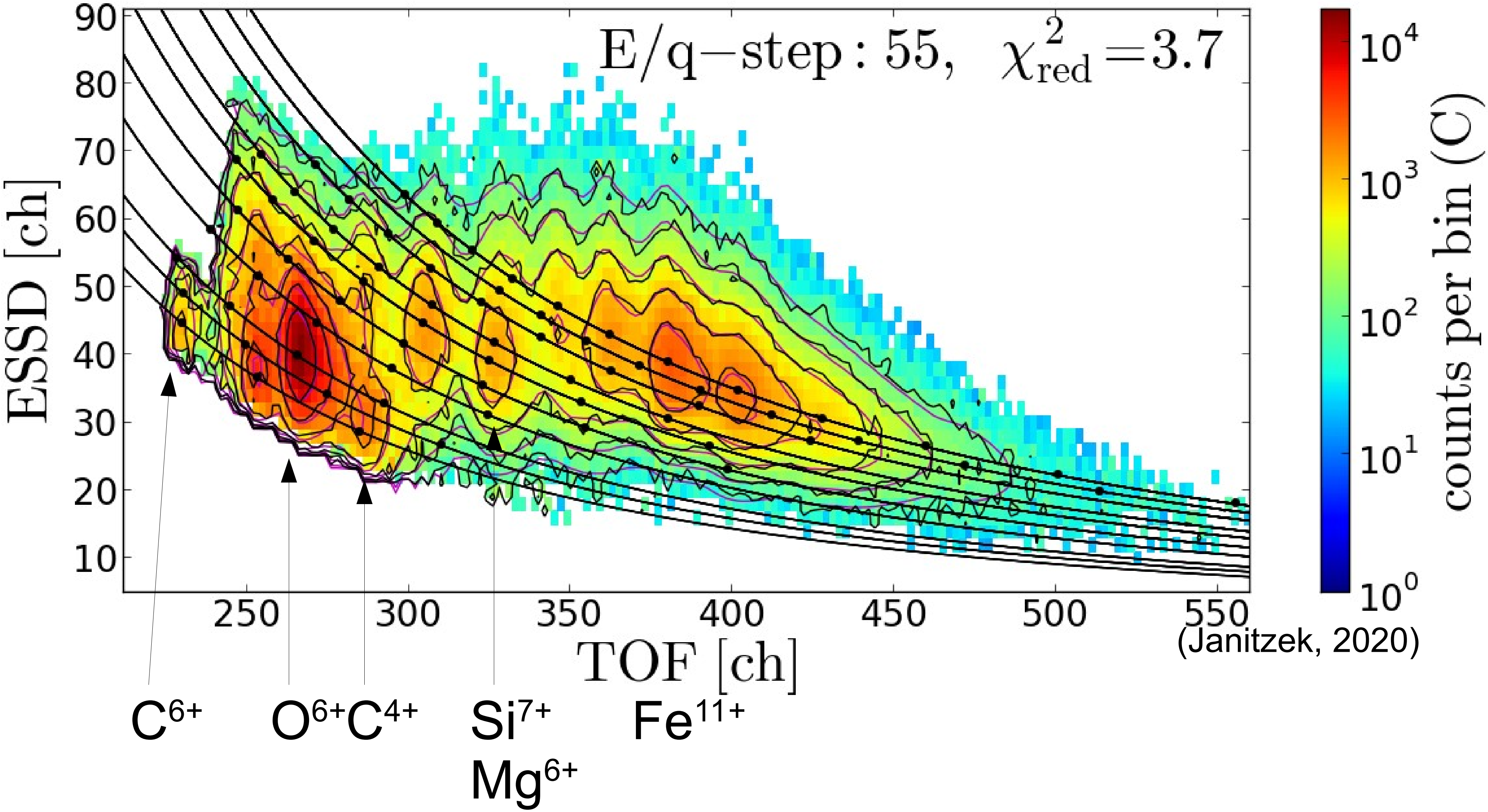
E/q−step: 55, χ^2_{red} = 3.7
ESSD [ch]
TOF [ch]
counts per bin (C)
90
80
70
60
50
40
30
20
10
250
300
350
400
450
500
550
10^4
10^3
10^2
10^1
10^0
(Janitzek, 2020)
C^{6+}
$O^{6+}$$C^{4+}$
Si^{7+}
Mg^{6+}
Fe^{11+}

Collisions determine the microphysics: differential speeds and kinetic temperatures of heavy ions

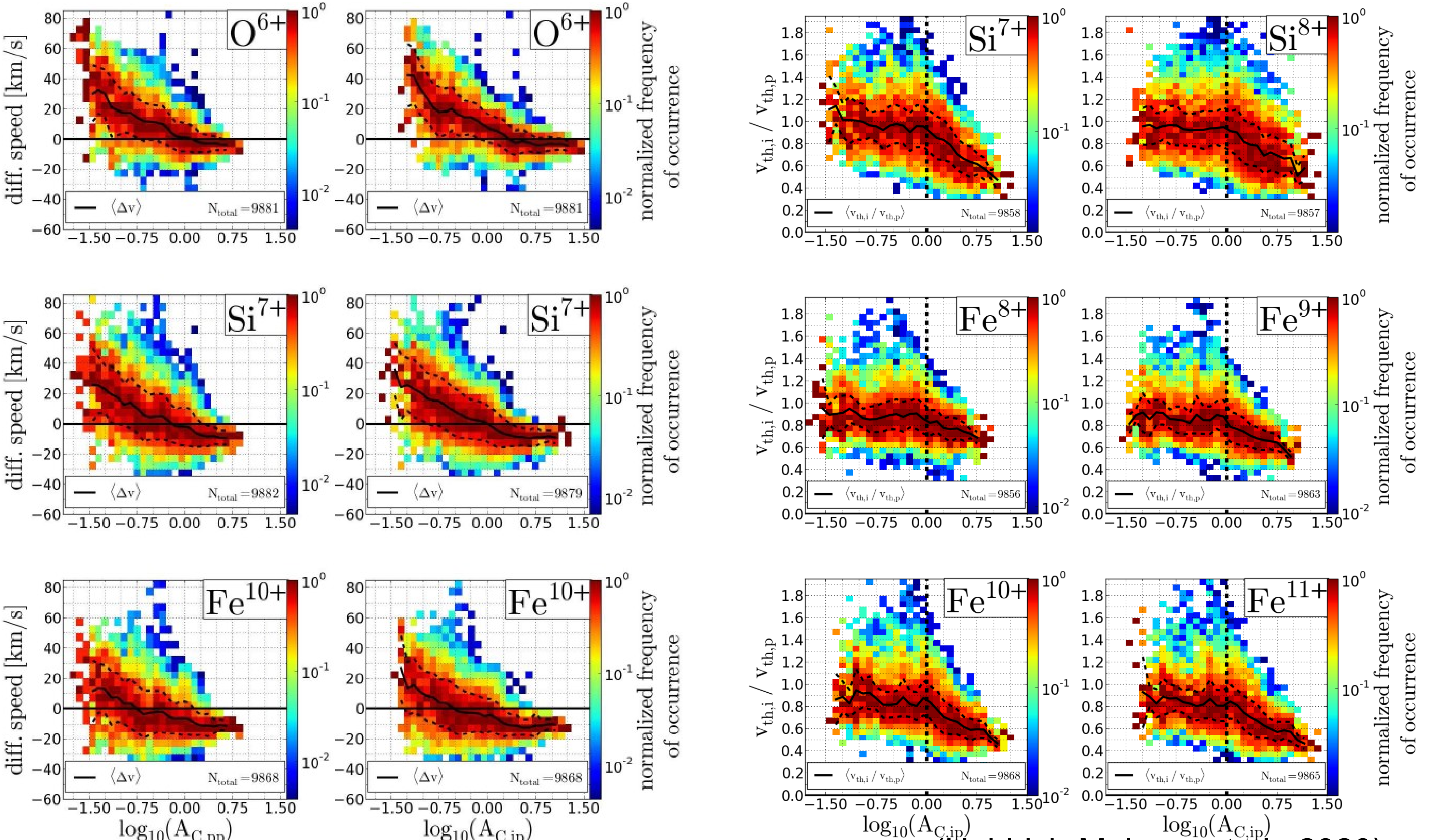

(Heidrich-Meisner et al., 2020)

Processes affecting composition:

Chromosphere and corona:
Charge-state and elemental composition somehow linked.

Slow wind hot (source?)
Fast wind cool (coronal hole)

What links the chromosphere and the corona?

Slow wind strongly FIPped
Fast wind weakly/barely FIPped

Q: Go to the ACE Science Center, get SWICS data for 2009 and convince yourself that these changes happen.

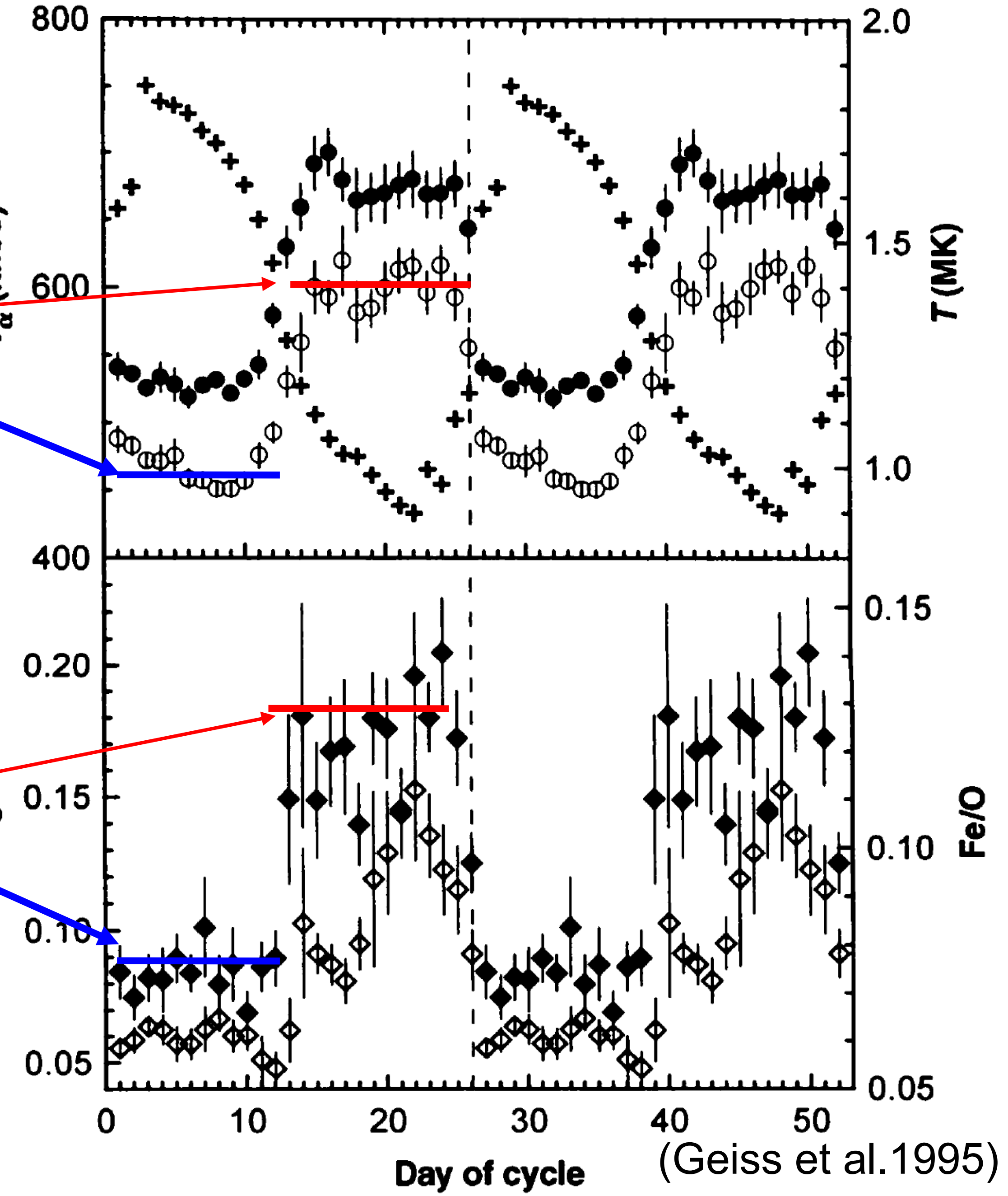

(Geiss et al.1995)

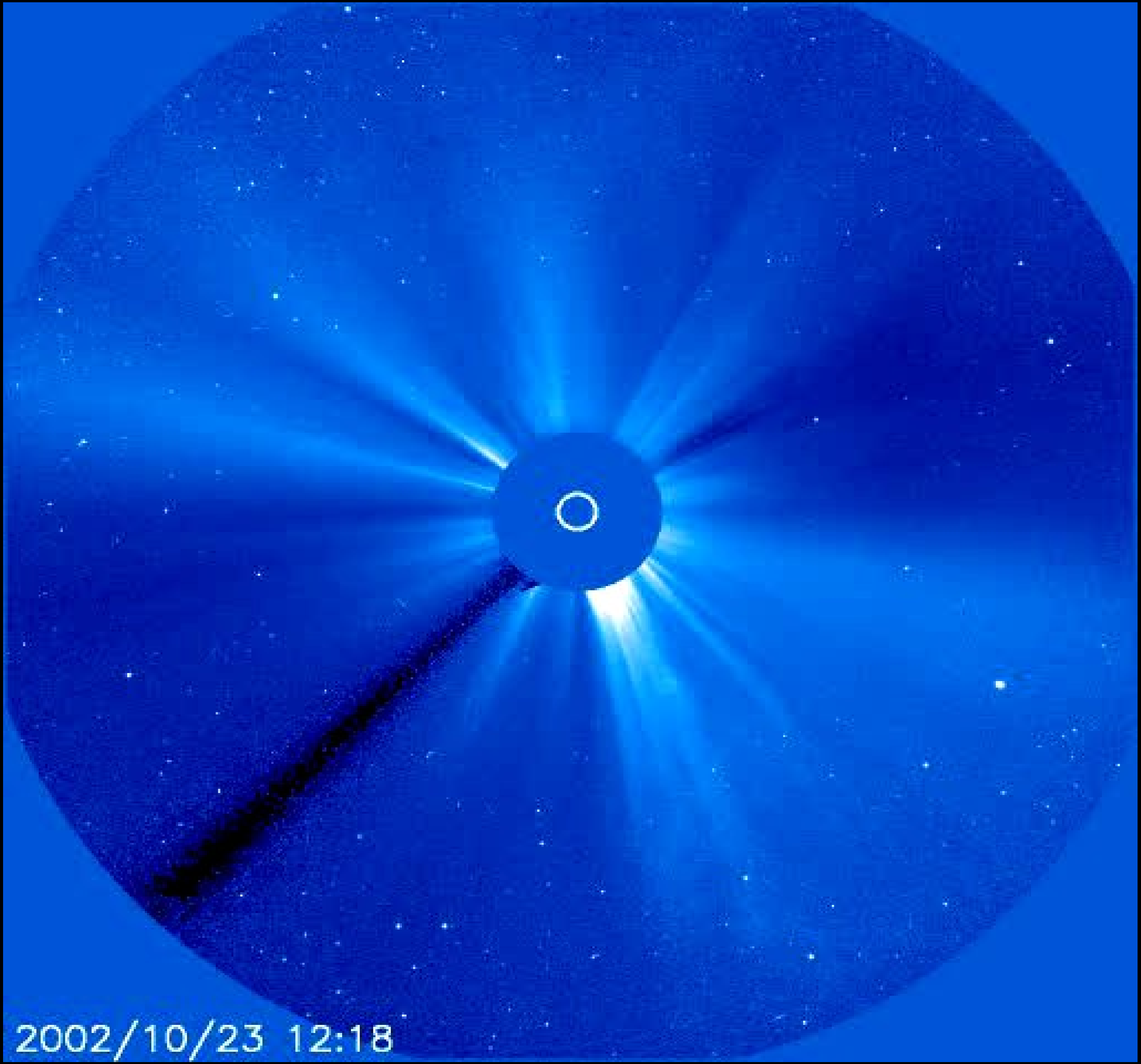
2002/10/23 12:18

The Magnetic Field in the Solar Wind

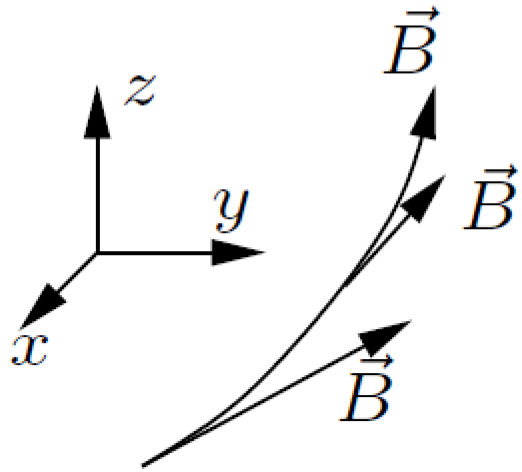

We define a fieldline as an entity for which

$$\frac{\mathrm{d}x}{B_x} = \frac{\mathrm{d}y}{B_y} = \frac{\mathrm{d}z}{B_z}$$

We define a flux tube as an entity for which the enclosed magnetic flux is conserved.

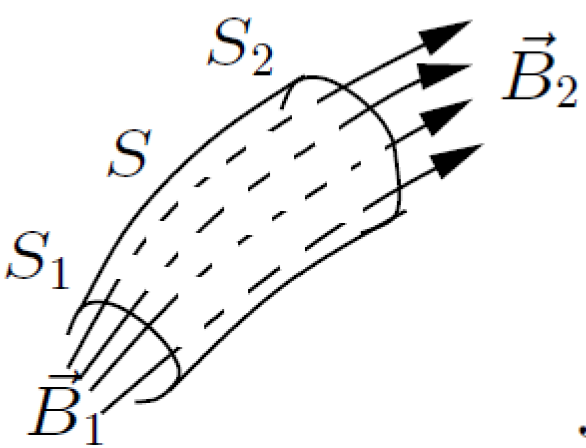

$$F_m = \int_S \vec{B} \cdot \mathrm{d}\vec{S} = \text{const.} \qquad (*)$$

Because $\vec{B} \cdot \mathrm{d}\vec{S}$ =0 for surface S,

$$\int_S \vec{B} \cdot \mathrm{d}\vec{S} = \int_{S_1} \vec{B} \cdot \mathrm{d}\vec{S} + \int_{S_2} \vec{B} \cdot \mathrm{d}\vec{S},$$

But $\int_S \vec{B} \cdot \mathrm{d}\vec{S} = \int_V \vec{\nabla} \cdot \vec{B}\mathrm{d}V,$ vanishes, which proves (*).

The Frozen-in Magnetic Field

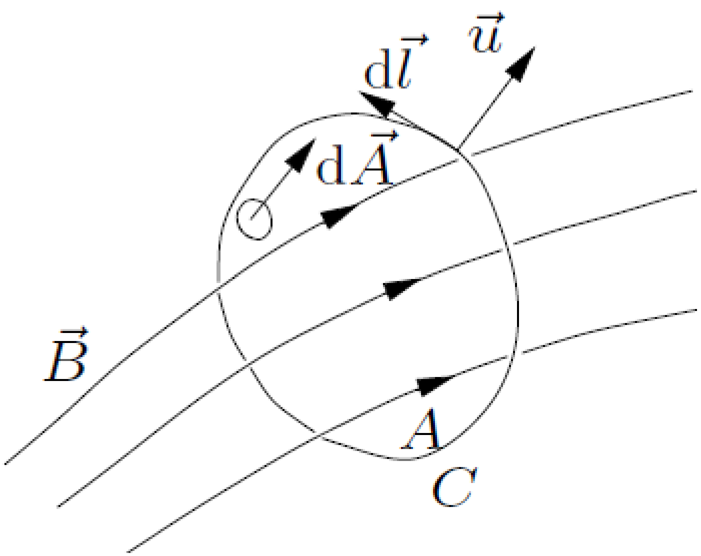

For the well-conducting solar wind, the MHD induction equation,

$$\dot{\vec{B}} = \vec{\nabla} \times \vec{u} \times \vec{B} + \frac{1}{\mu_0 \sigma} \Delta \vec{B},$$

turns into

$$\dot{\vec{B}} = \vec{\nabla} \times \vec{u} \times \vec{B},$$ which means that the flux through C does not change.

There are two ways in which the flux through C could change:

- The field, B, within C changes,
- The curve C moves with respect to B

For the first possibility we get

$$\dot{\vec{B}} \cdot \mathrm{d}\vec{A} \xrightarrow{\text{Integration over A}} \int_A \partial_t \vec{B} \, \mathrm{d}\vec{A}$$

The Frozen-in Magnetic Field II

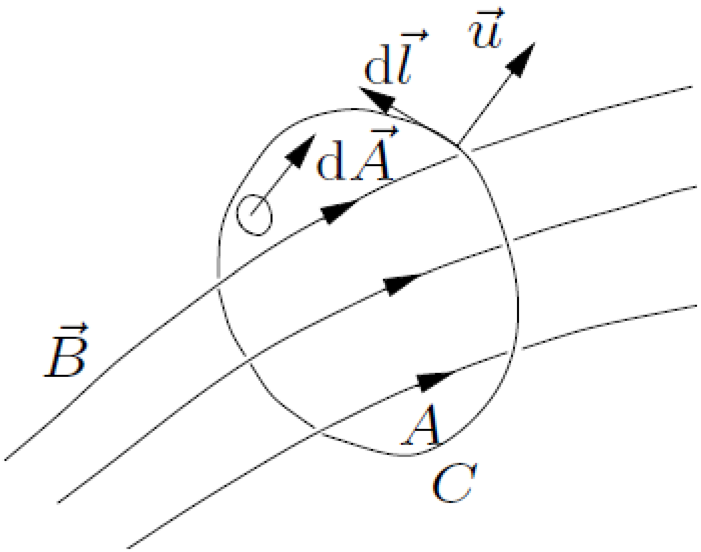

For the second case, we consider the infinitesimal displacement of curve C. The infinitesimal change in the flux is

$$\vec{B} \cdot \left(\vec{u} \times \mathrm{d}\vec{l} \right)$$

The full change in flux is obtained by integration along C. Using the identity

$$A \cdot (B \times C) = (A \times B) \cdot C$$

we get

$$\frac{\mathrm{d}}{\mathrm{d}t} \int_A \mathrm{d}\vec{A} \cdot \vec{B} = \int_A \mathrm{d}\vec{A} \cdot \frac{\partial \vec{B}}{\partial t} - \oint_C \mathrm{d}\vec{l} \cdot \left(\vec{u} \times \vec{B} \right)$$

Using Stokes' theorem, we have the induction equation in integral, so

$$\frac{\mathrm{d}}{\mathrm{d}t} \int_A \mathrm{d}\vec{A} \cdot \vec{B} = \int_A \mathrm{d}\vec{A} \cdot \left(\frac{\partial \vec{B}}{\partial t} - \vec{\nabla} \times \left(\vec{u} \times \vec{B} \right) \right) = 0.$$ QED

The Heliospheric Magnetic Field

Solar wind flows radially away from the Sun.

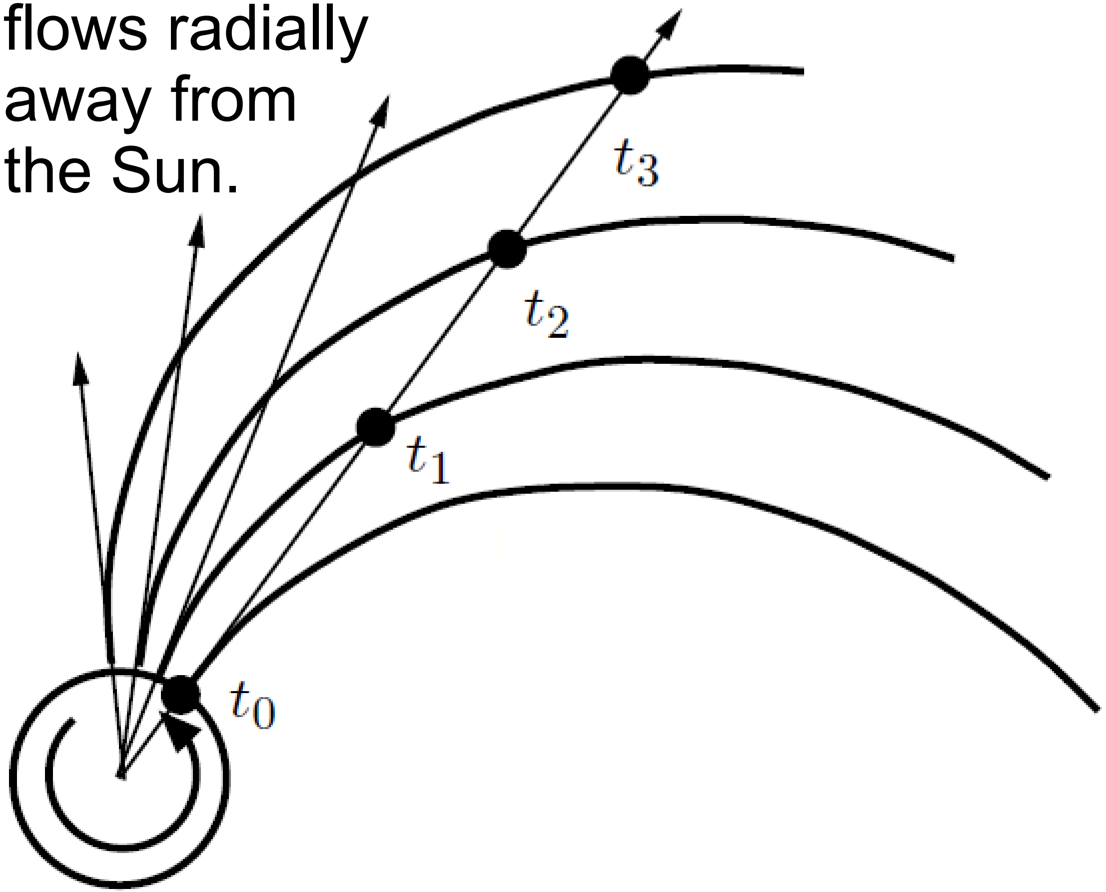

Radially expanding solar wind pulls along the frozen-in magnetic field.

This results in the formation of an Archimedean spiral.

In honor of Eugene Parker this is called the Parker spiral.

The Parker Spiral

Then the behavior of the heliospheric field is determined by the flow of the solar wind.
In a frame co-rotating with the Sun:

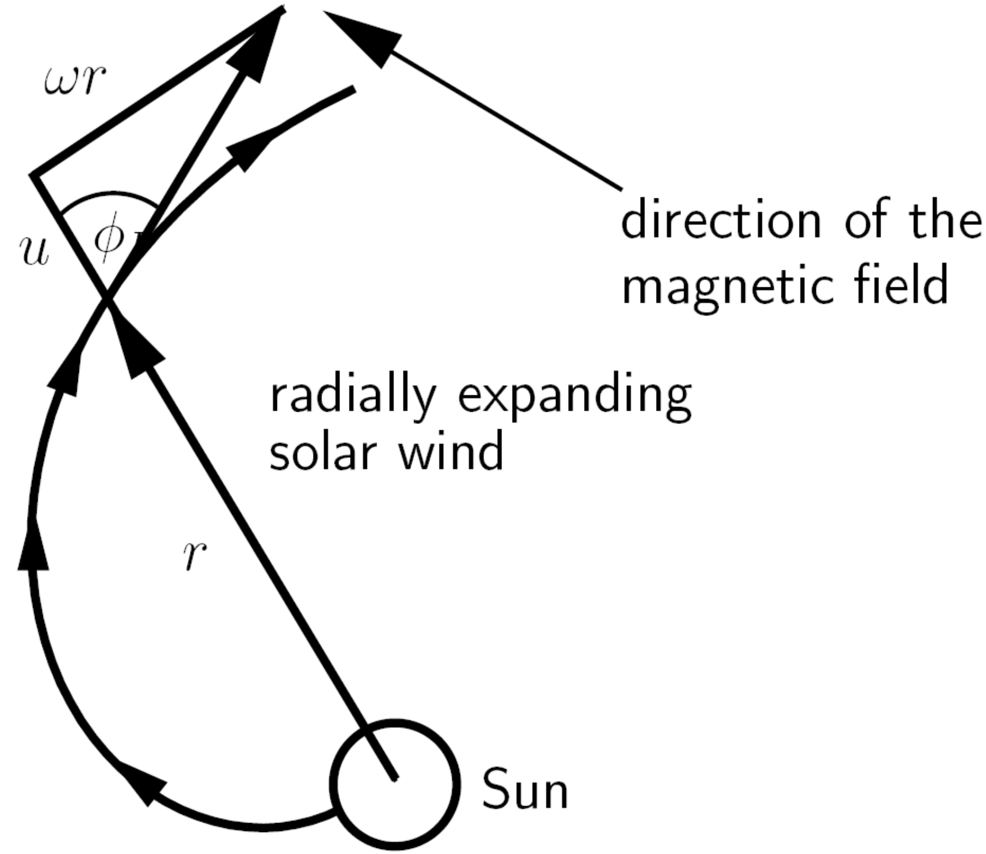

$$
\begin{aligned}
u_r &= u, \\
u_\phi &= -r\omega \sin\theta, \\
u_\theta &= 0,
\end{aligned}
$$

because the solar wind flows radially outwards from the Sun.

The so-called Parker-angle, ϕ_P, is the angle between the radial and the magnetic field directions.

$$\cos^2(\phi_P) = \frac{1}{1 + \left(\frac{\omega r \sin\theta}{u}\right)^2}$$

(typically about 45° at 1 AU)

The Heliospheric Current Sheet

Because the Sun's rotation axis is inclined wrt. ecliptic, a warped current sheet forms. This was coined the „ballerina skirt“ by Alfvén.

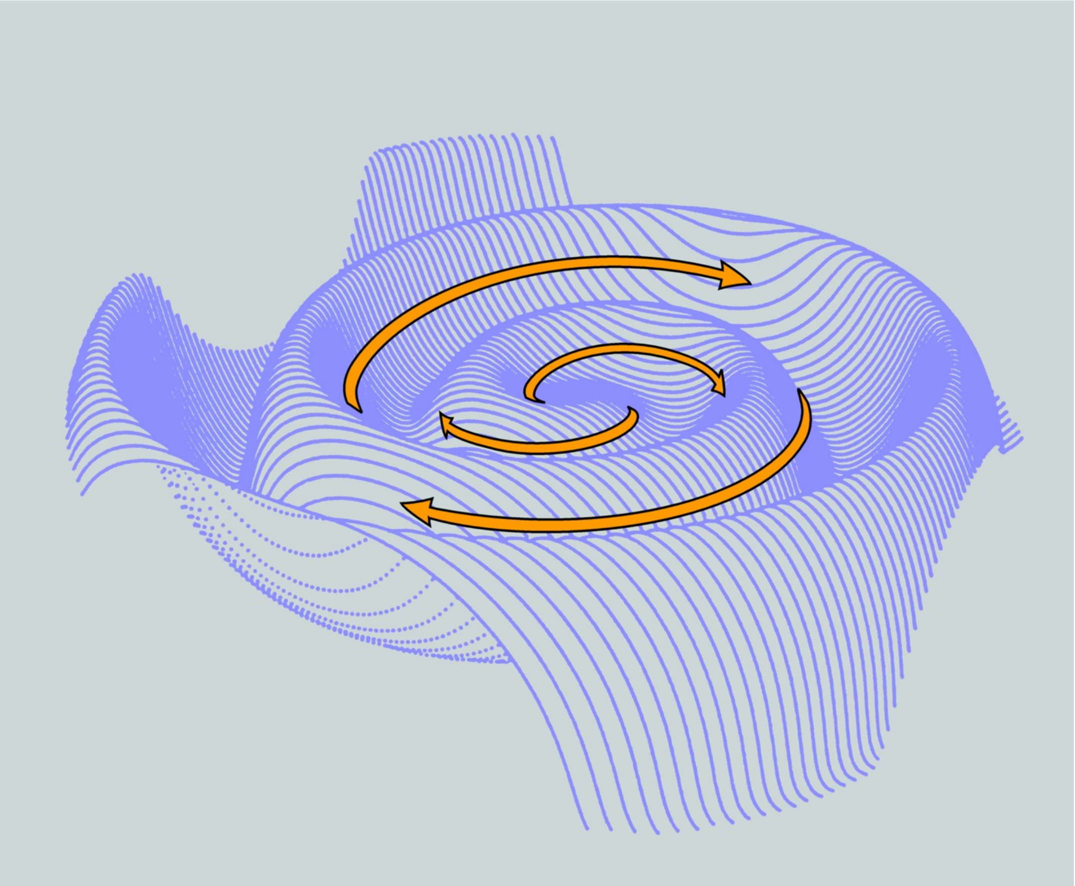

The Heliospheric Current Sheet

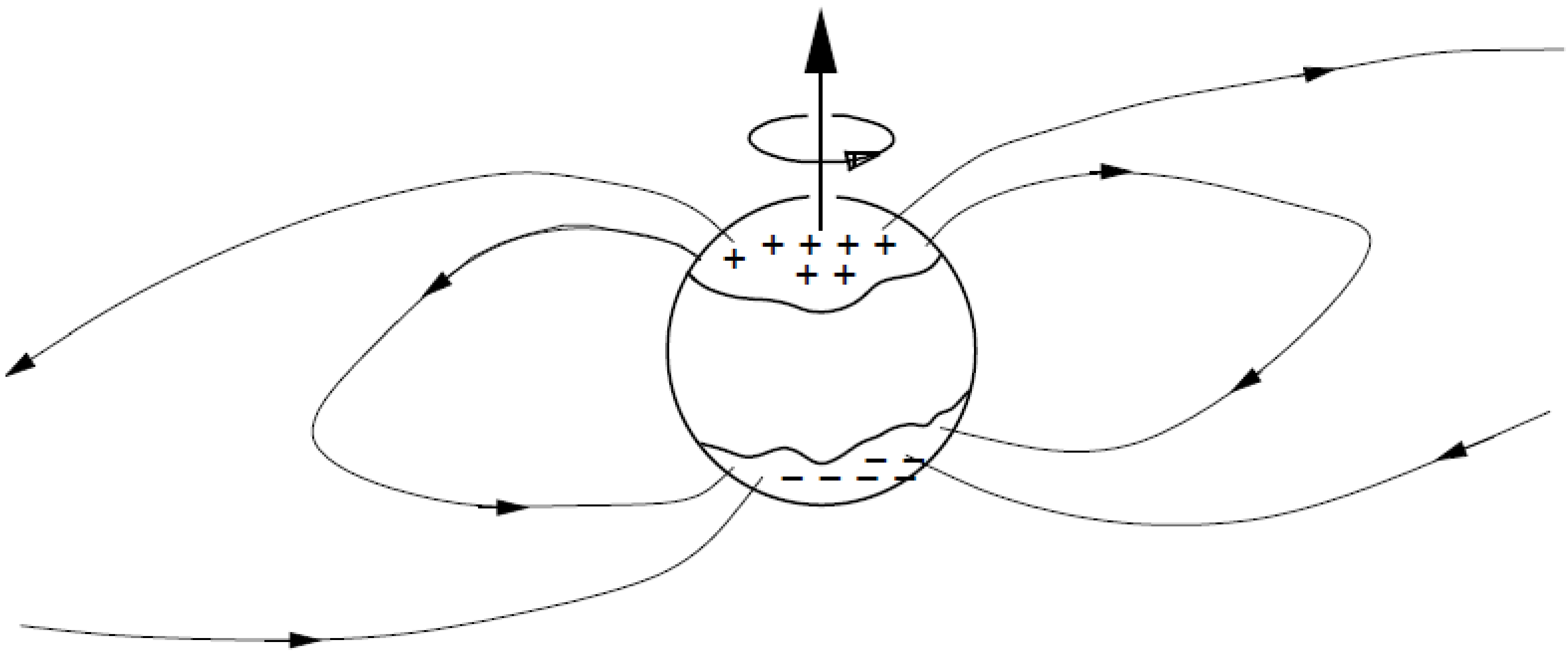

Stretching out of the magnetic field leads to formation of current sheet.

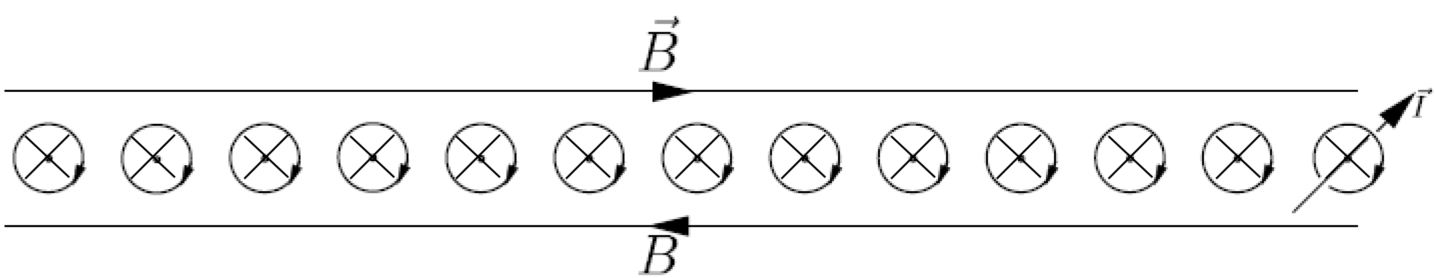

Formation of Stream Interaction Regions

When fast wind runs into slow wind, ...

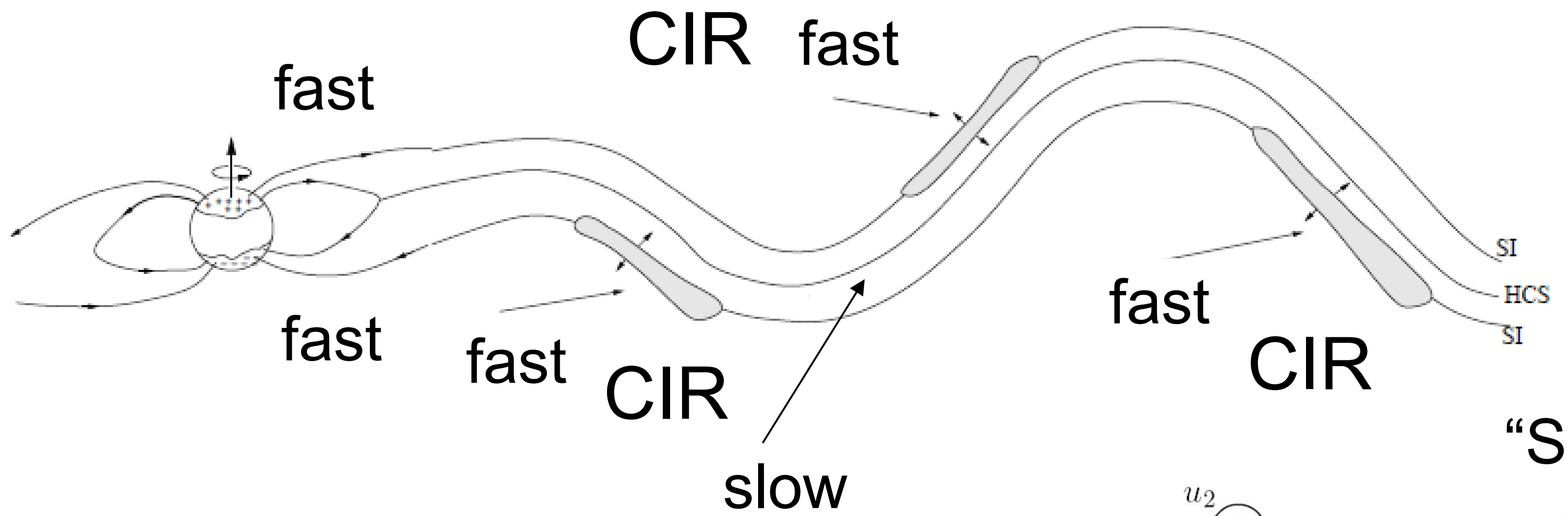

Fast wind running into slow wind leads to the formation of Corotating Interaction Regions (CIRs). Shocks form typically beyond 1 AU.

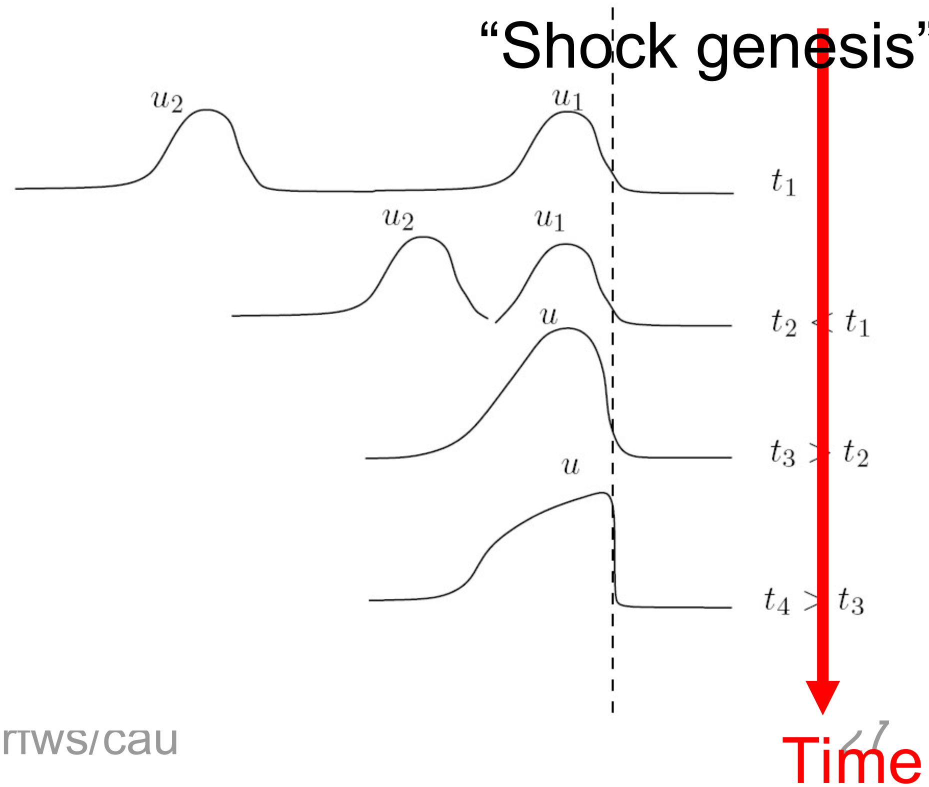

Composition as a Tracer:

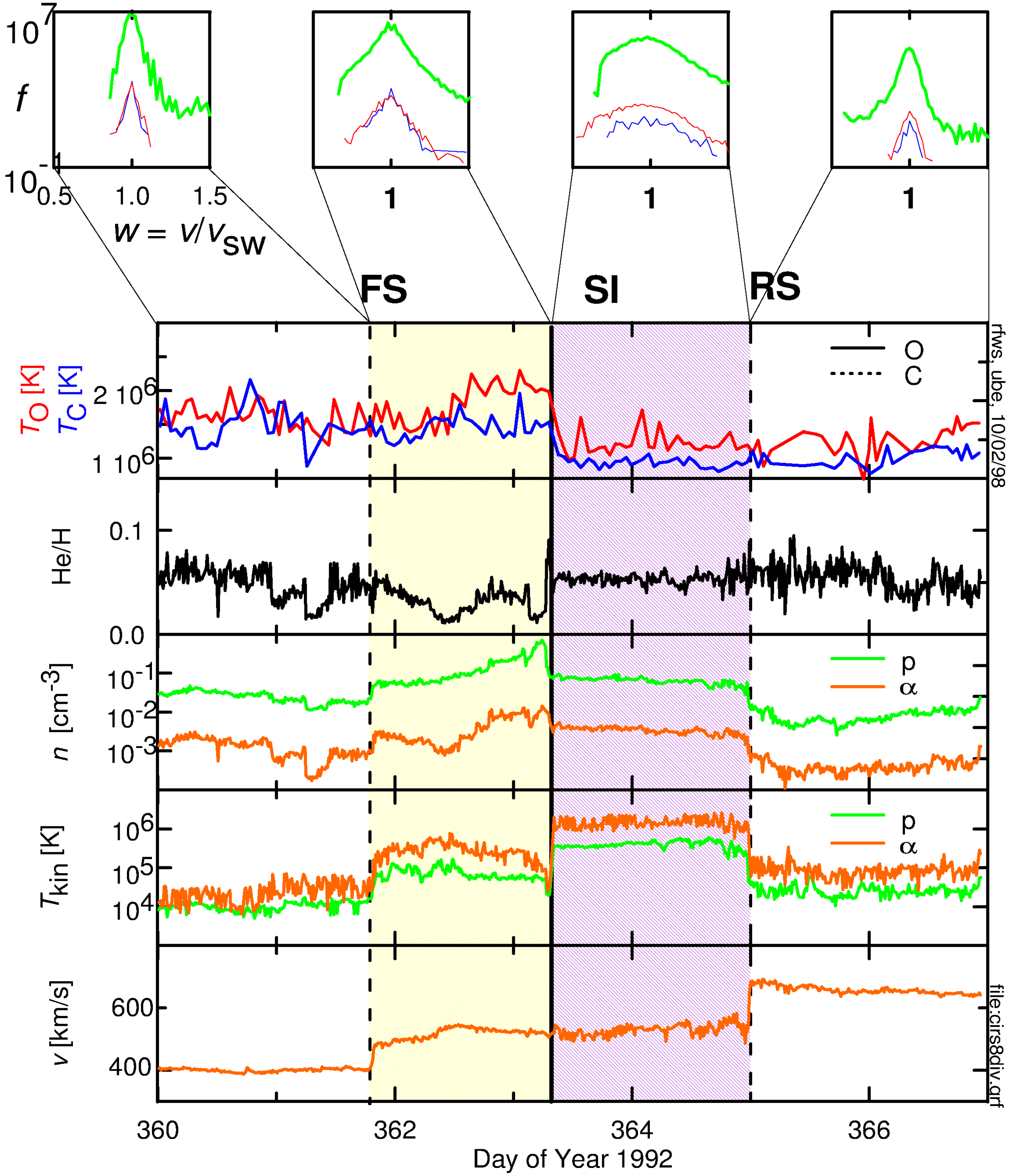

Stream Interaction Regions

Individual streams can be identified in-situ by many independent methods:
- magnetic field
- plasma data
- specific entropy
- composition

Composition is not altered by kinetic processes and remains conserved once it has been set in chromosphere and corona. **Excellent tracer!**

Composition variable, especially in slow wind.

Extreme-UV quiet Sun brightenings observed by the Solar Orbiter/EUI

Berghmans et al., https://doi.org/10.1051/0004-6361/202140380

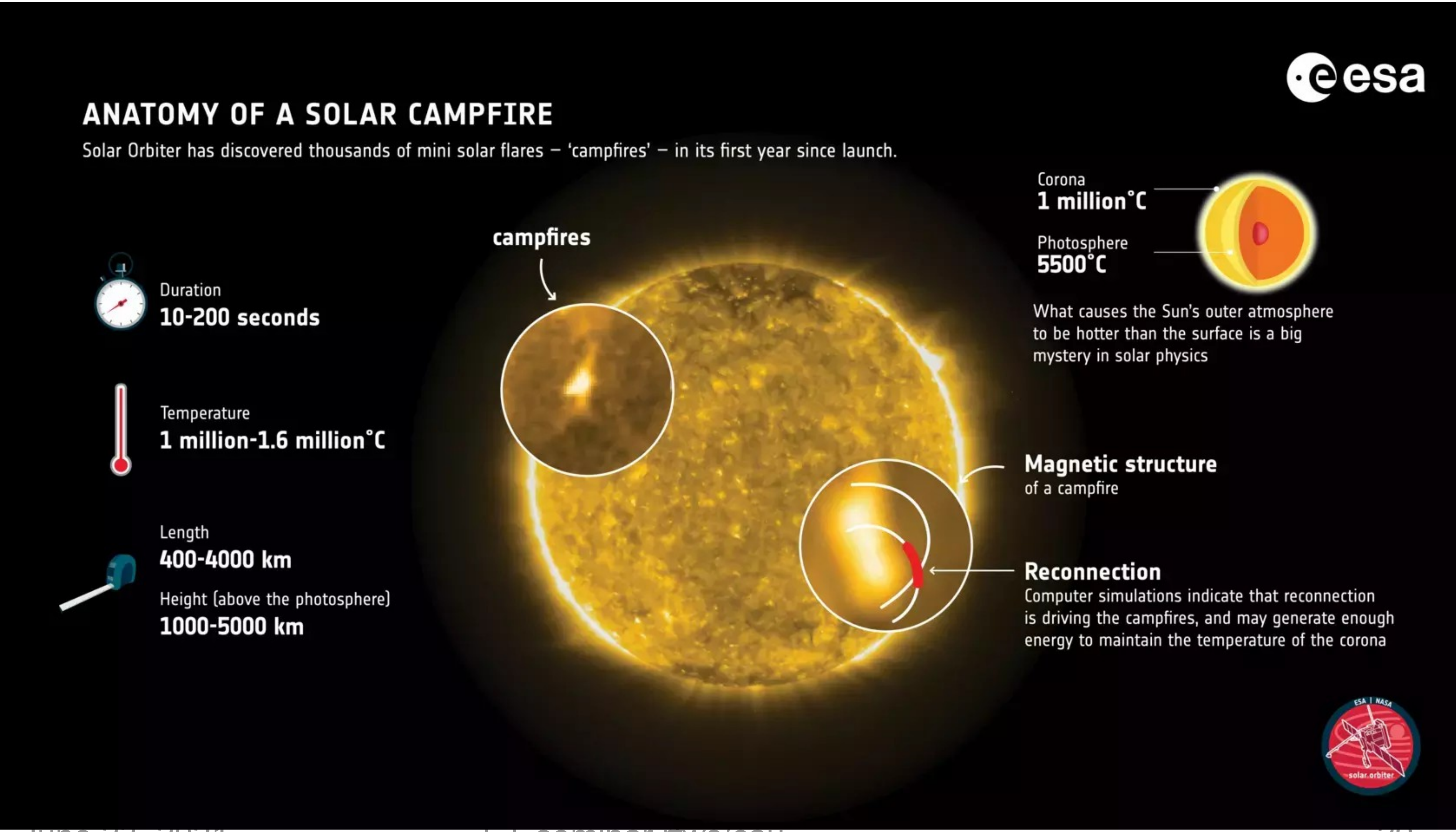

Transient small-scale brightenings in the quiet solar corona: A model for campfires observed with Solar Orbiter

Chen et al.,
https://doi.org/10.1051/0004-6361/202140638

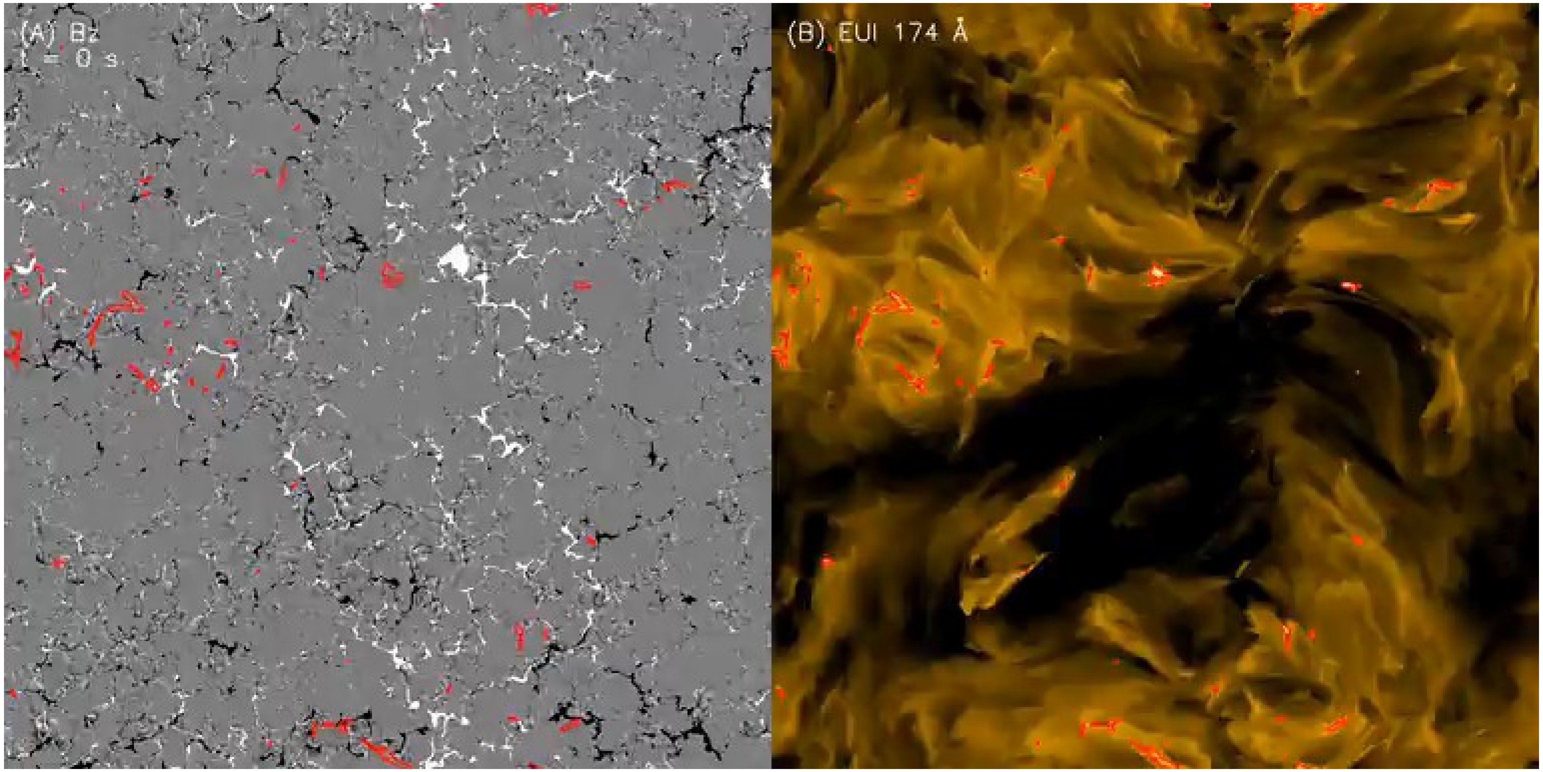

Extreme-UV quiet Sun brightenings observed by the Solar Orbiter/EUI

Berghmans et al., https://doi.org/10.1051/0004-6361/202140380

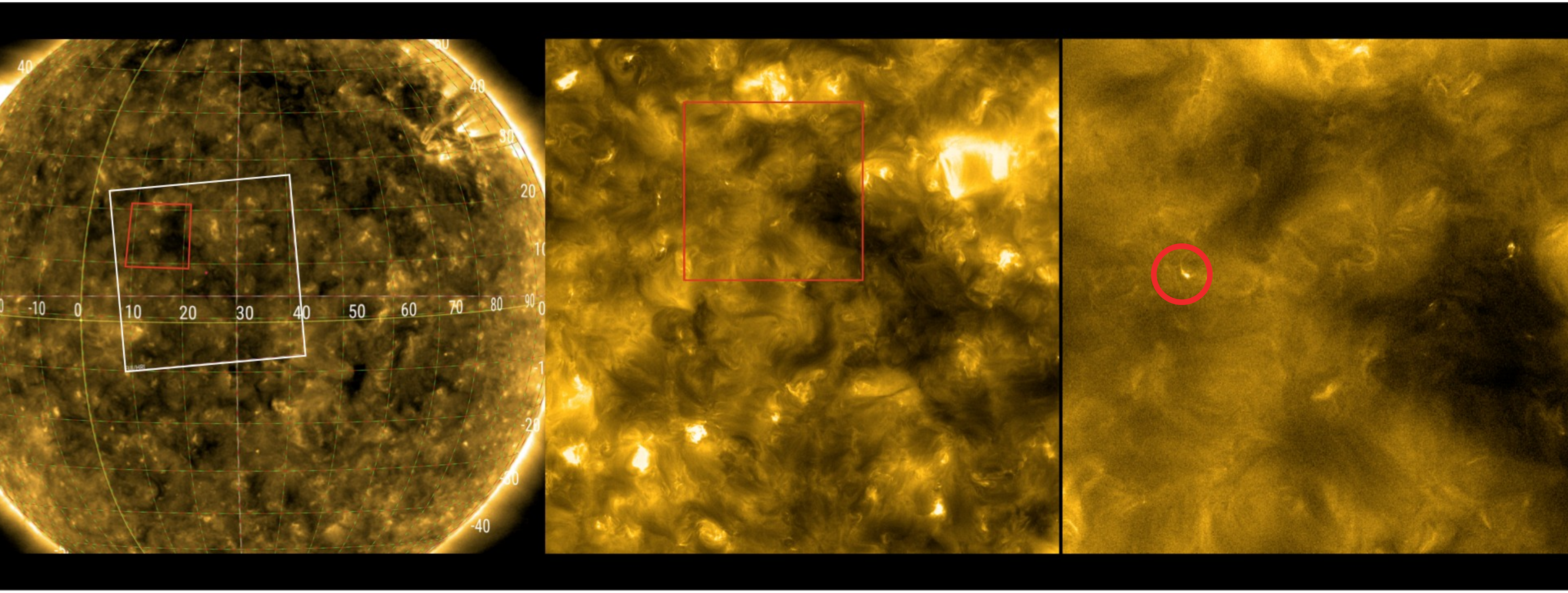

What is the size distribution of these flares?
→ Expect power law, as normal in nature.

Extreme-UV quiet Sun brightenings observed by the Solar Orbiter/EUI

Berghmans et al., https://doi.org/10.1051/0004-6361/202140380

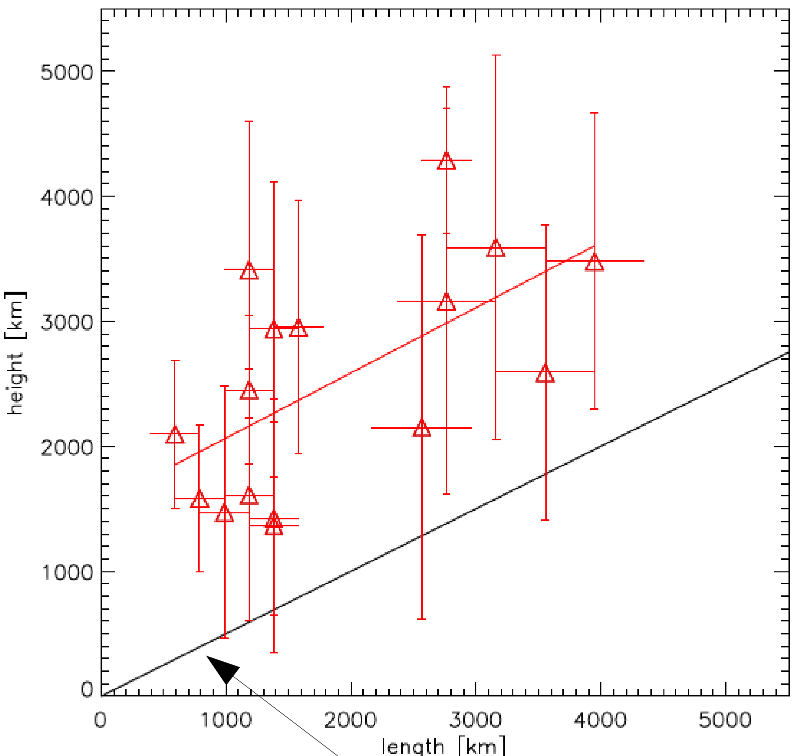

Subsample of 16 campfires also observed
with SDO/AIA allows triangulation.

1000 – 5000 km above photosphere

Located above chromospheric network

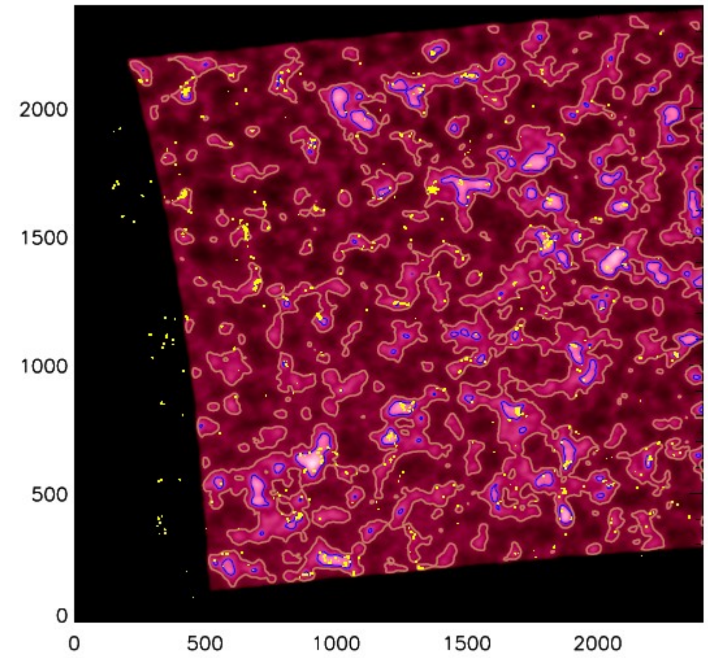

Expected for semi-circular loop.
Loops are elongated in height.

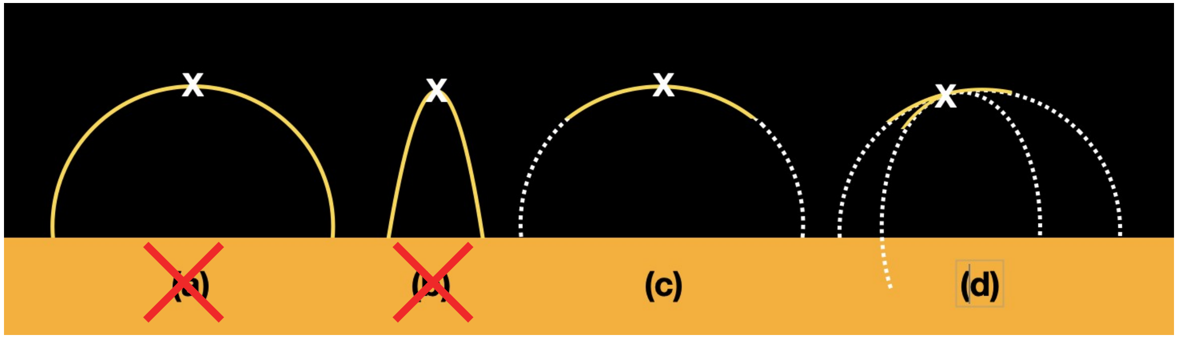

Extreme-UV quiet Sun brightenings observed by the Solar Orbiter/EUI

Berghmans et al., https://doi.org/10.1051/0004-6361/202140380

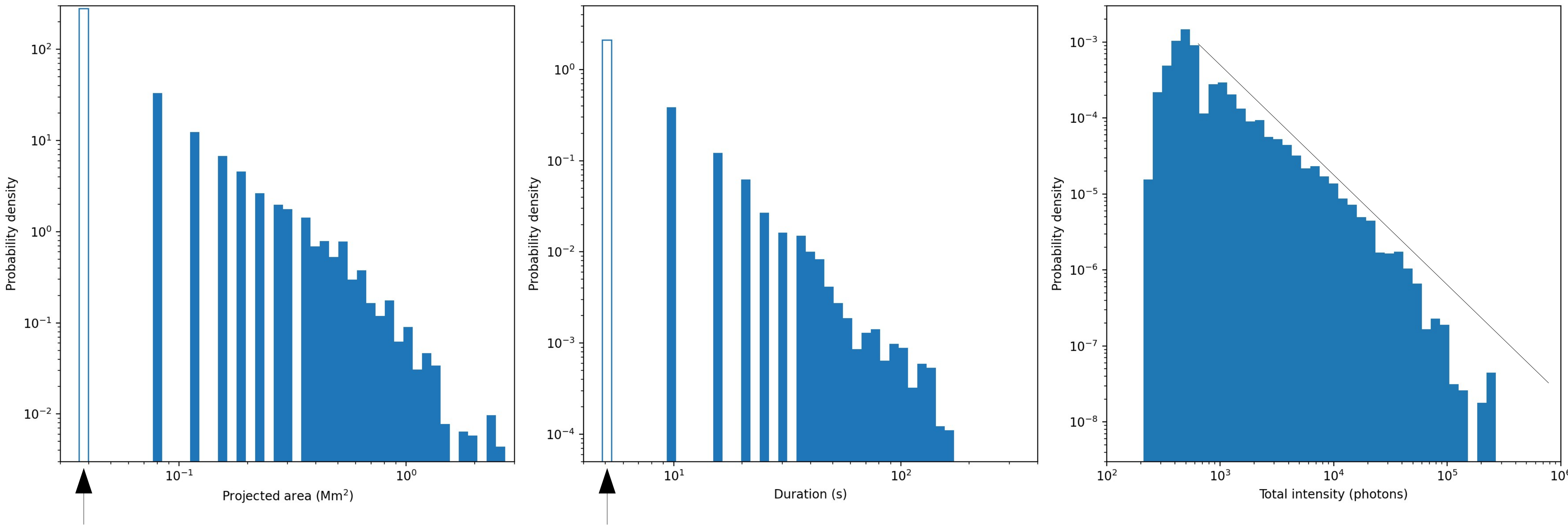

One single pixel (excluded)

Single exposure (excluded)

Probability density distribution is a power law down to smallest detectable structures!

Summary Solar Wind:

Fast solar wind from coronal holes
Fairly uniform but strong turbulence, „young“ SW

Slow solar wind from unknown regions in streamer belt
Highly variable, dynamically „old“
Active regions, interchange reconnection, S-web

(Interplanetary) Coronal Mass ejections **(I)CMEs**
Highly variable but very low turbulence

Magnetic field structured as **Parker spiral**

Stream interaction regions develop as fast wind catches up with slow wind. Shocks develop beyond ~2 AU.

Coronal heating solved? EUI discovery of „campfires“.

Part II

Suprathermal and Energetic Particles

Introduction

In 1896 Henri Bequerel and others discover non-chemical process capable of penetrating black paper and darkening photo plates. It also excites fluorescence. Uranium salt is used for this. Exciting discovery! New physics or chemistry!

Marie Curie discovers that uranium salt also ionizes air, strictly proportional to the amount of material. Therefore nonchemical process. Pitchblend is four times more effective, therefore, it must contain a new element. Discovery of polonium and radium. Invention of the word 'radioactivity'.

Died of aplastic anemia (radioactivity...)

Something can ionize air and penetrate paper.

Ionization is a good measure of radioactivity.

Introduction

On a balloon flight in 1912 Victor Hess discovers 'Höhenstrahlung' at large heights. The degree of ionization increases with height! Millikan interprets it as cosmic or extraterrestrial radiation.

Image credit: NY Times

Level of radiation must increase with height.

Why? Is there a source of radiation out there?

What is this source?

What are the properties of this radiation?

Why does ionization increase with height?

Measurements show count rate increases with height.

Air pressure decreases with height.

If Earth's radiation were ionizing, count rate should decrease with height because there is less air to ionize.

Can only be explained by ionizing agent coming in from outside the Earth ---> extraterrestrial origin!

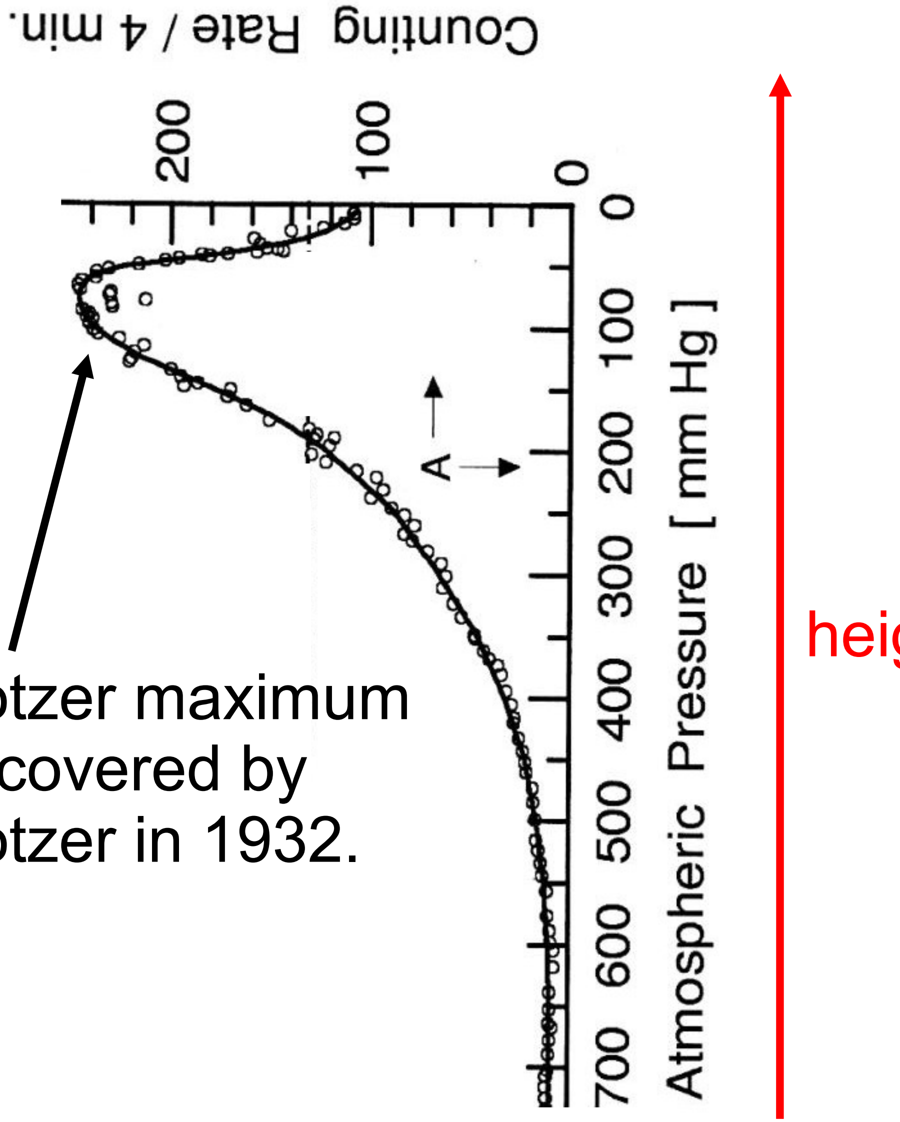

Pfotzer maximum discovered by Pfotzer in 1932.

(Grieder, 2002)

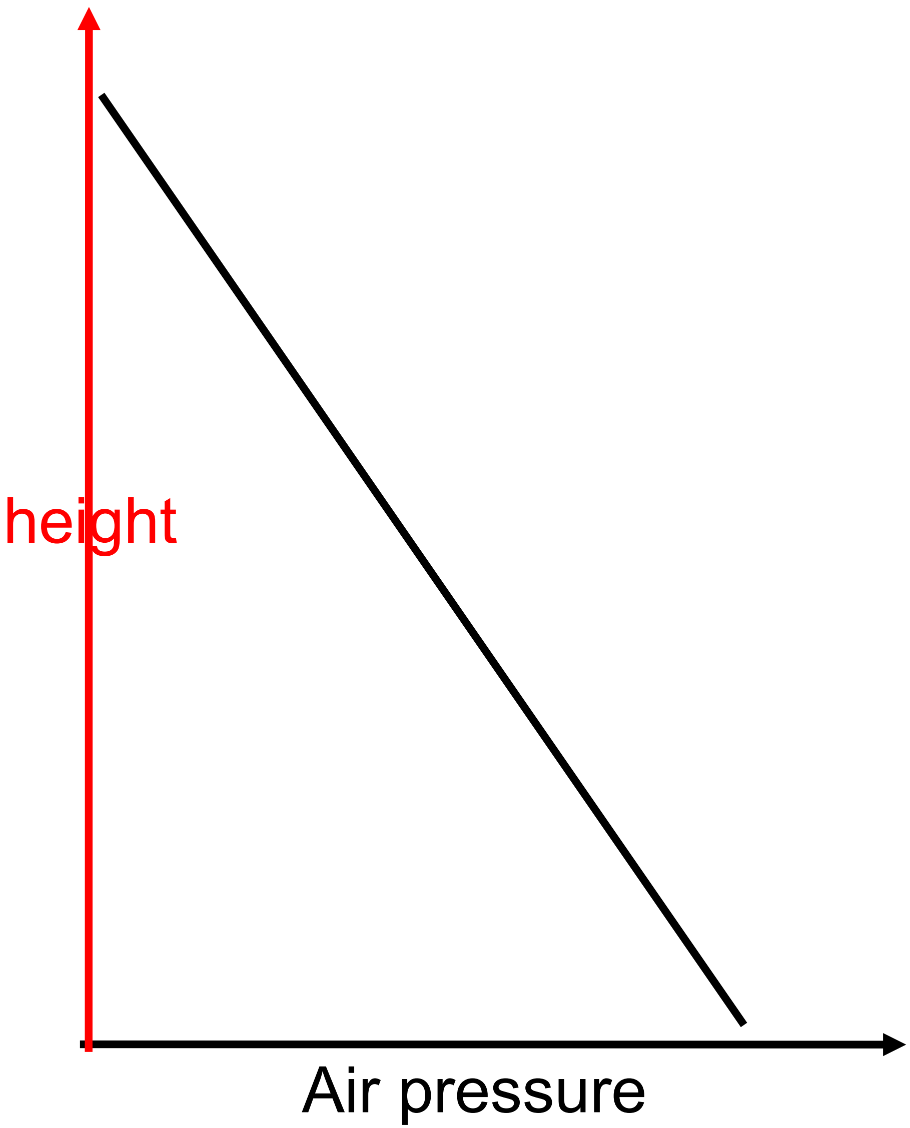

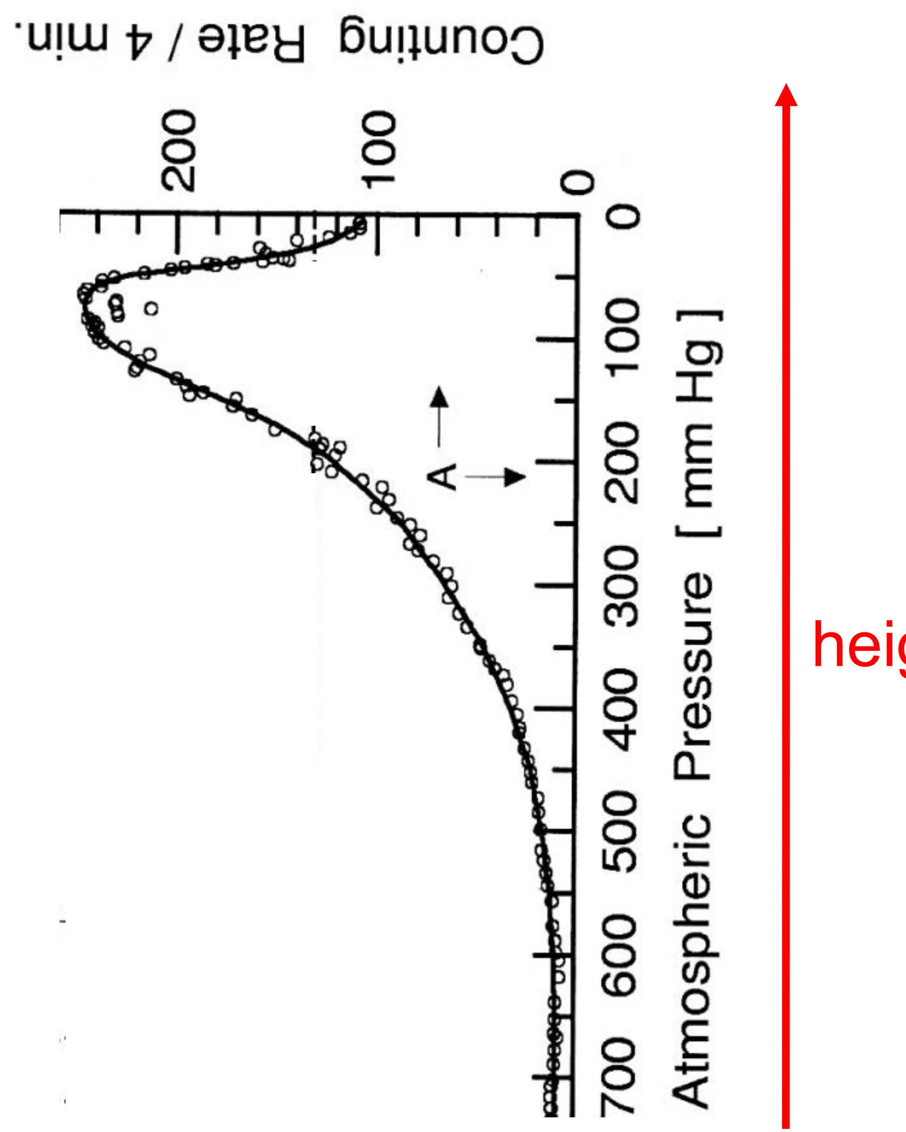

(Grieder, 2002)

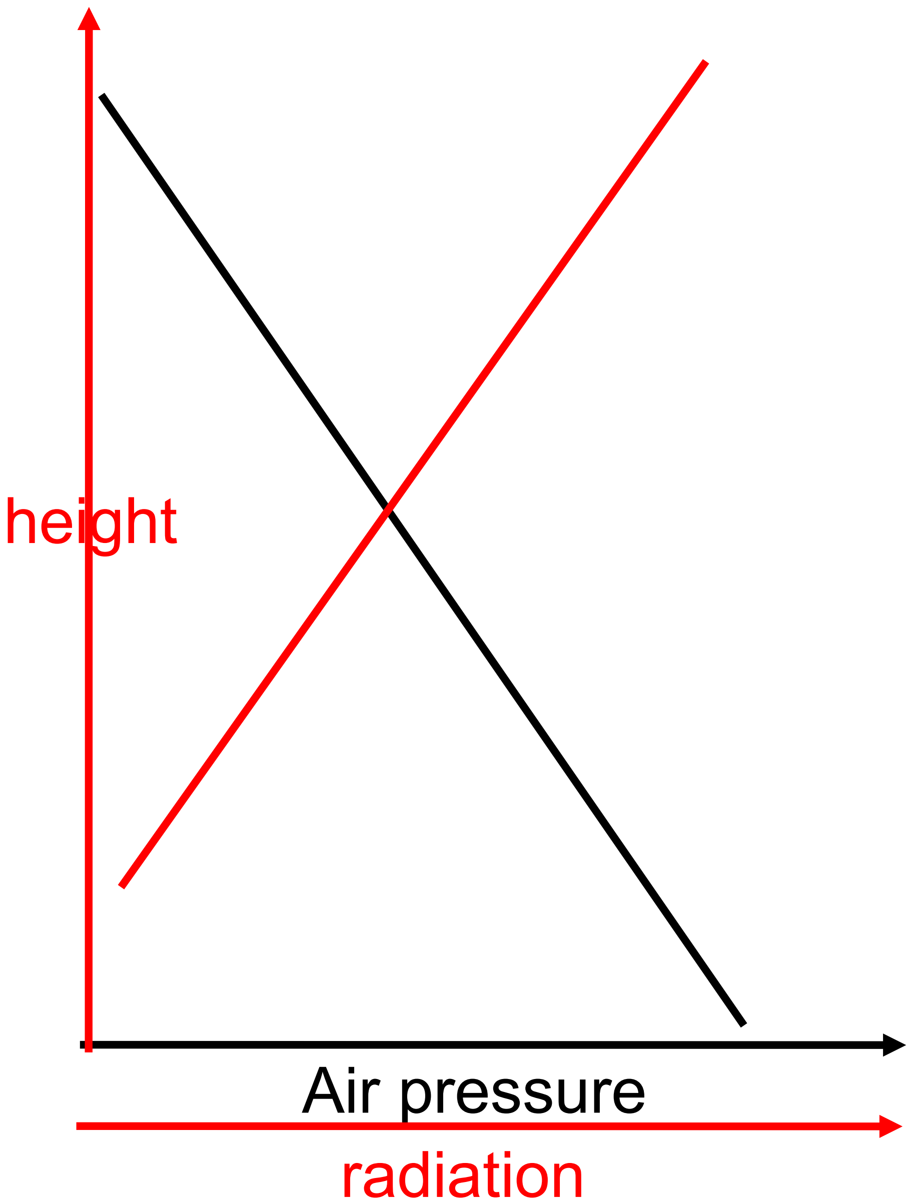

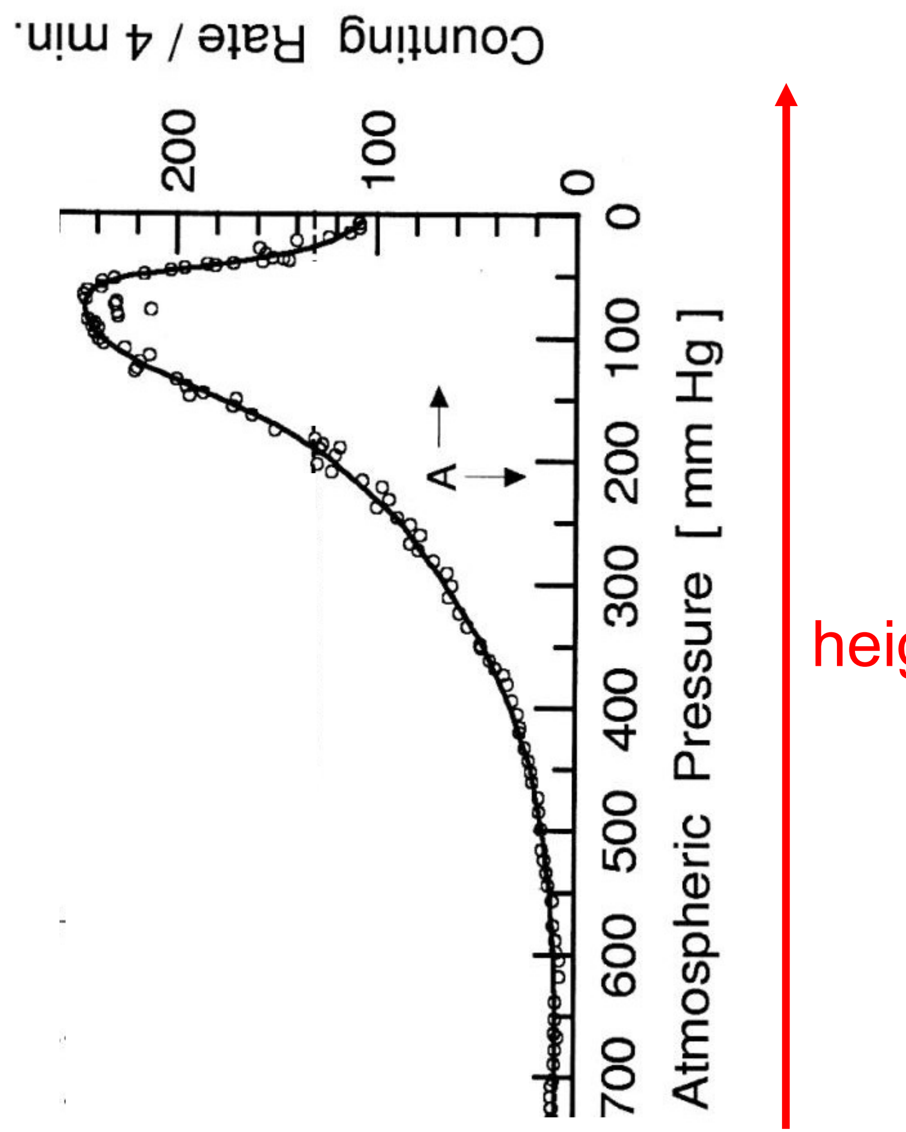

(Grieder, 2002)

Formation of Pfotzer Maximum

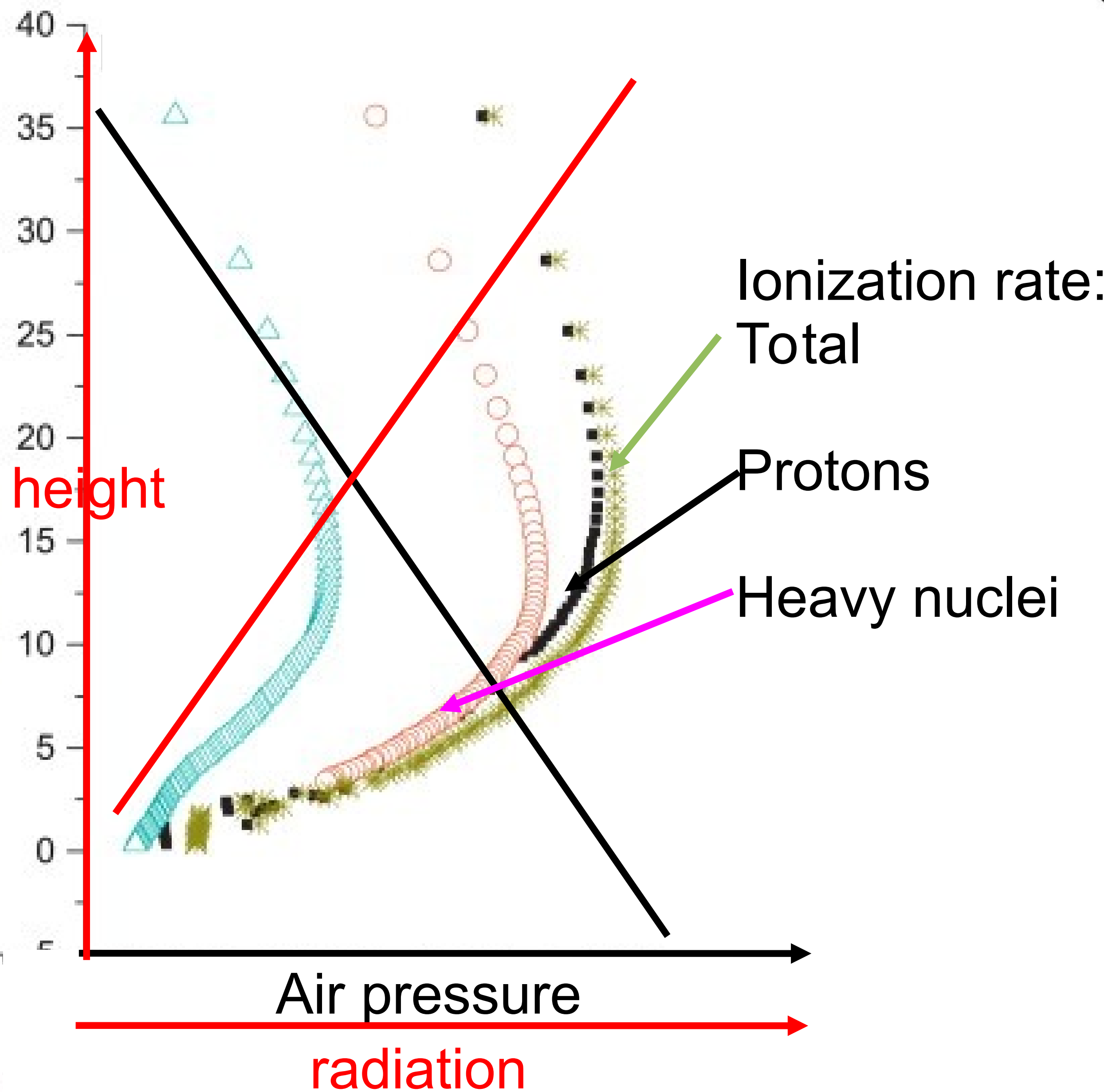

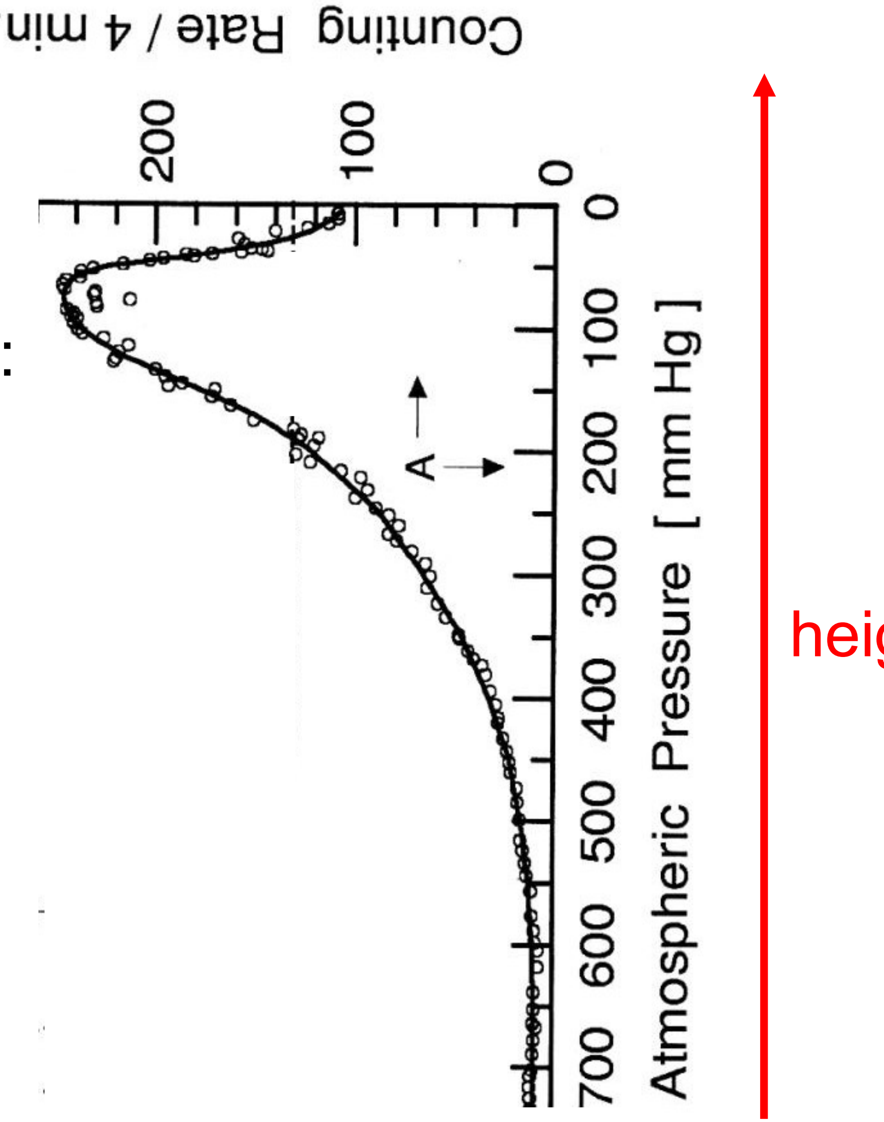

(Grieder, 2002)

Long-term average of the particle spectrum in the heliosphere

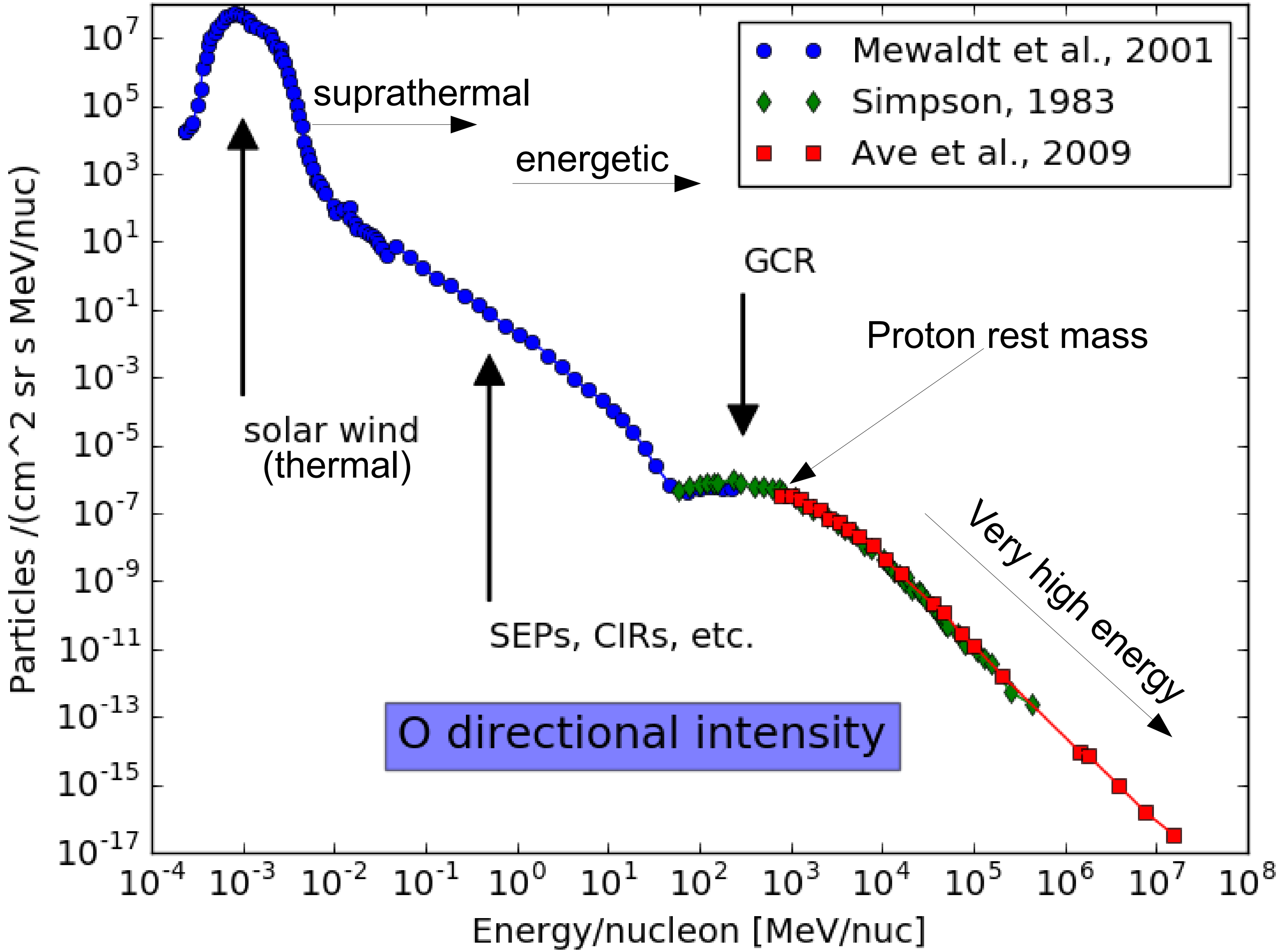

Energetic Particles in the Heliosphere

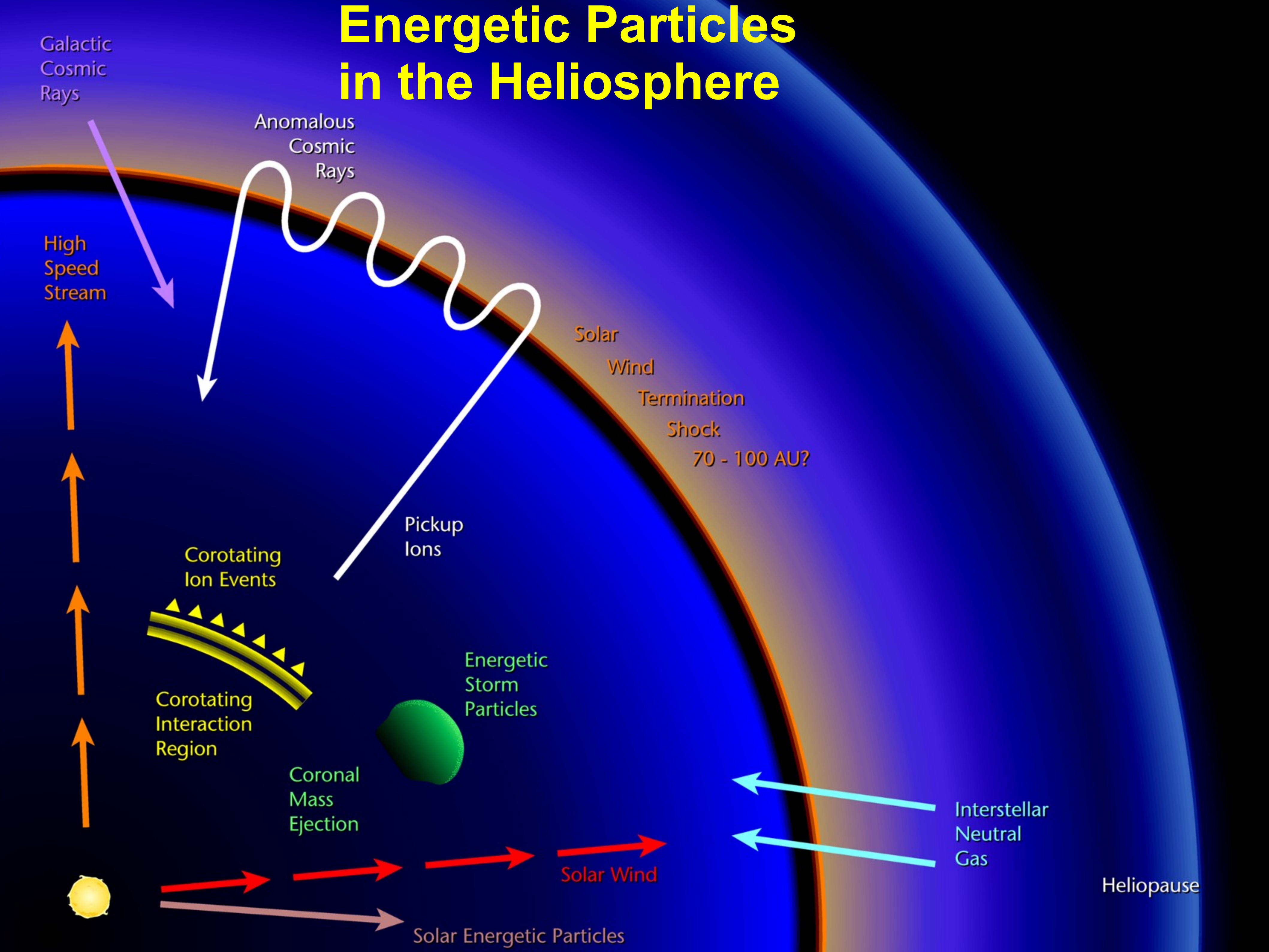

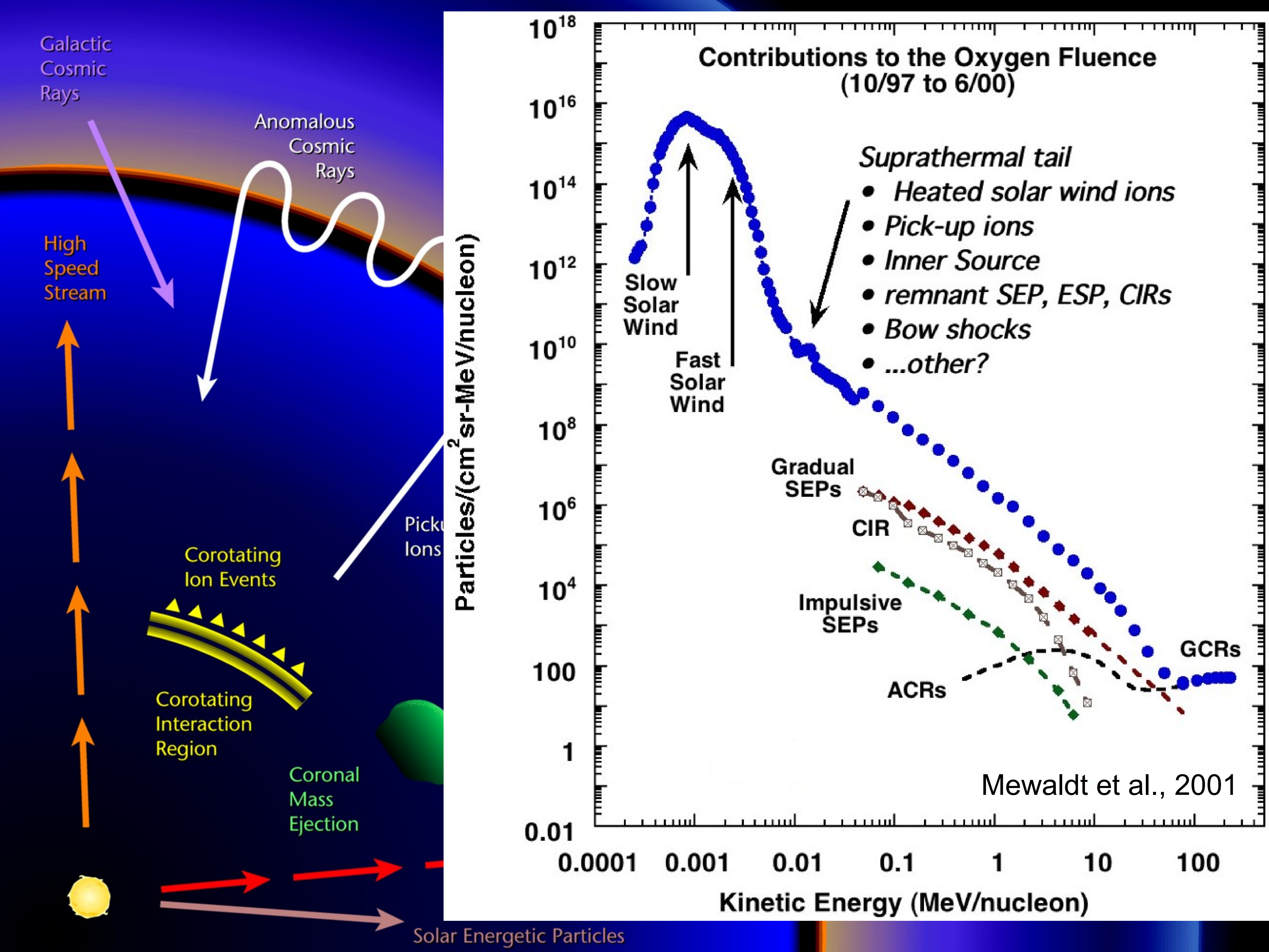
Galactic Cosmic Rays
Anomalous Cosmic Rays
High Speed Stream
Corotating Ion Events
Corotating Interaction Region
Coronal Mass Ejection
Ions
Solar Energetic Particles
Contributions to the Oxygen Fluence
(10/97 to 6/00)
Suprathermal tail
• Heated solar wind ions
• Pick-up ions
• Inner Source
• remnant SEP, ESP, CIRs
• Bow shocks
• ...other?
Slow Solar Wind
Fast Solar Wind
Gradual SEPs
CIR
Impulsive SEPs
ACRs
GCRs
Mewaldt et al., 2001
Particles/(cm^2 sr-MeV/nucleon)
Kinetic Energy (MeV/nucleon)
10^{18}
10^{16}
10^{14}
10^{12}
10^{10}
10^{8}
10^{6}
10^{4}
100
1
0.01
0.0001
0.001
0.01
0.1
1
10
100

Energetic particles in the Heliosphere

Solar wind thermal particles:
protons, E < 10 keV
electrons, ~2 eV

Slowly varying Cosmic Rays:
~ 1GeV < E < 10 PeV

Recurrent weak Co-rotating Interaction Region (CIR) events, ~ 27-day periodicity:
E < ~ 10 MeV

SEPs: protons, electrons, and a small fraction of heavy ions:
~20 keV < E < 2 GeV

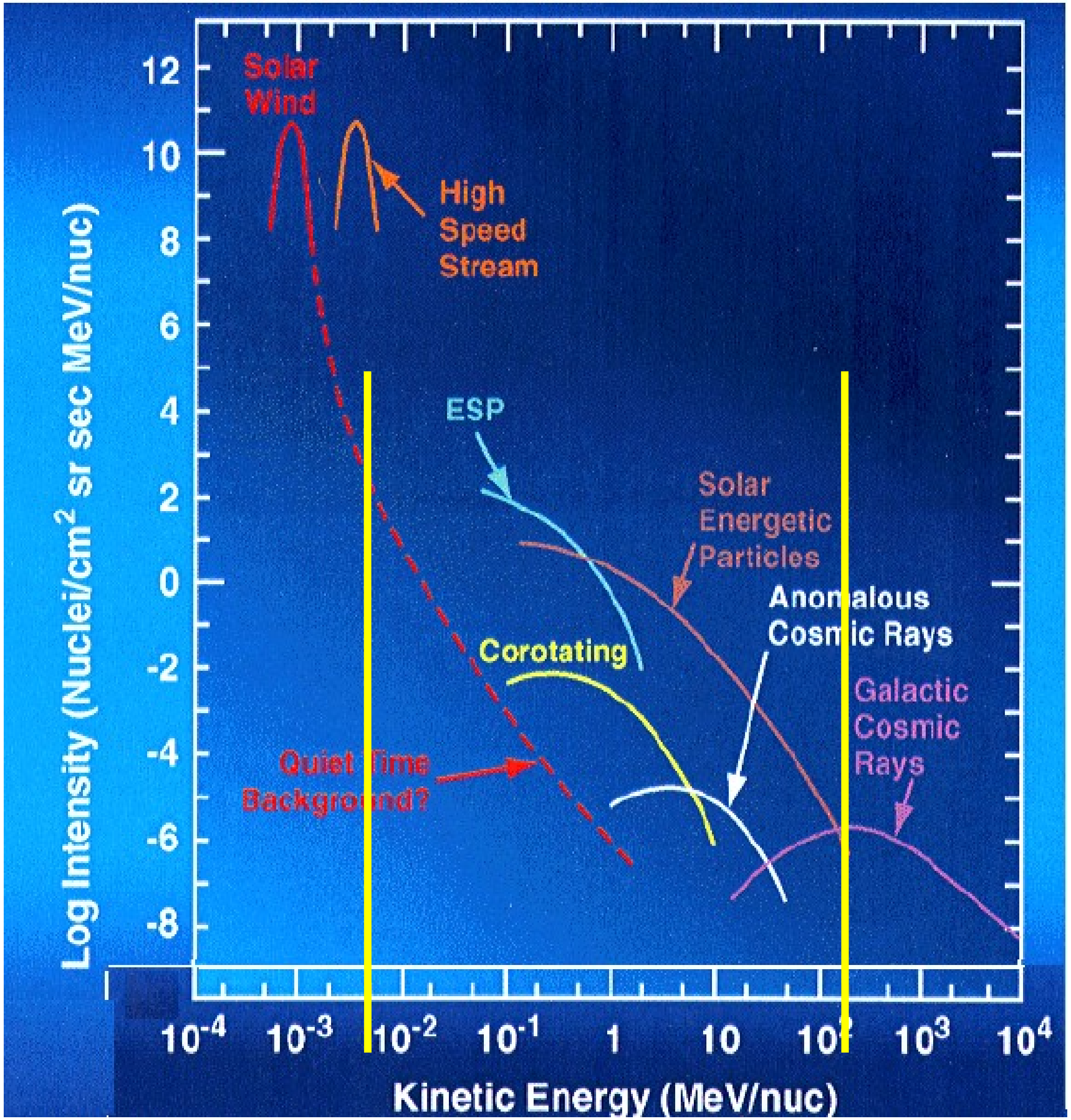

Some important points to remember

- Particles bound to B
- Gyro-radius, r_c
- Pitch angle α
- Gyrofrequency $\vec{\Omega} \doteq \frac{-q}{m\,\gamma}\vec{B}$
  where

$$\gamma \doteq \frac{1}{\sqrt{1 - v^2 / c^2}}$$

- Rigidity $c\,B\,r_c = \frac{p\,c}{q}$

$$r_c = \frac{|p_\perp|}{q\,B}$$

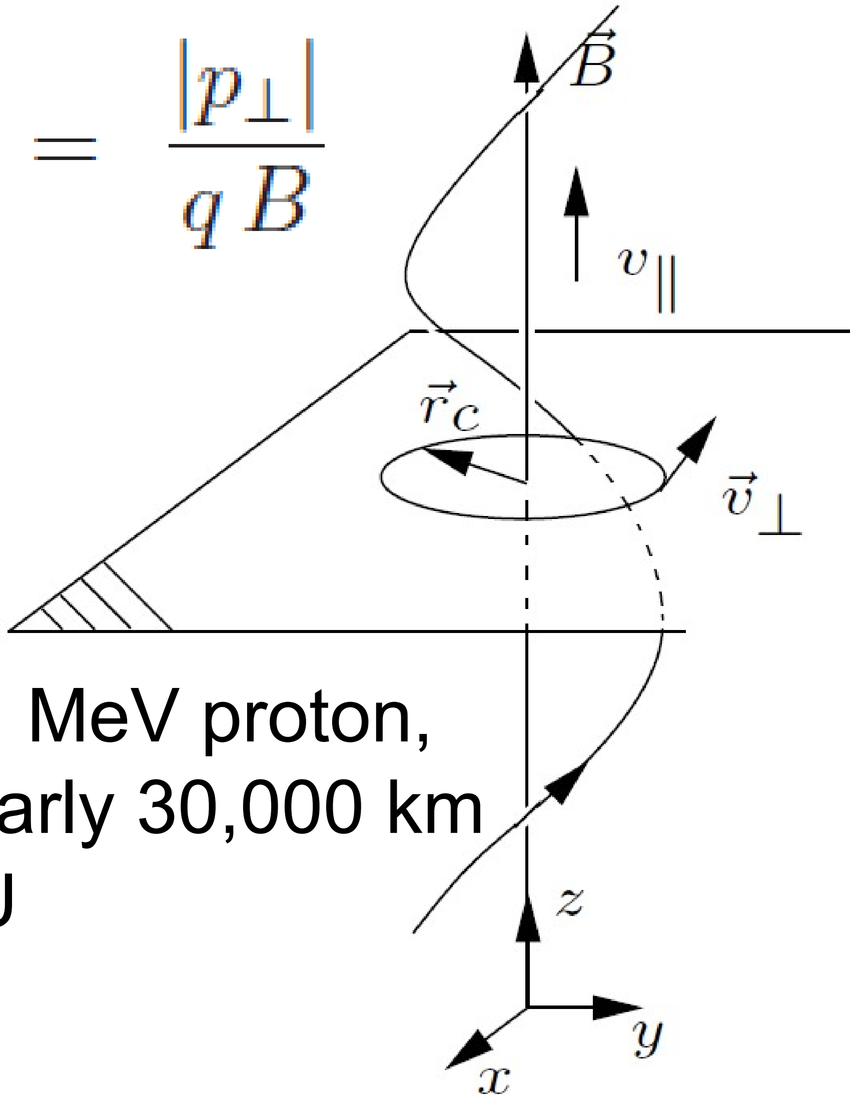

For a 1 MeV proton, r_c is nearly 30,000 km at 1 AU

Impulsive and Gradual Events

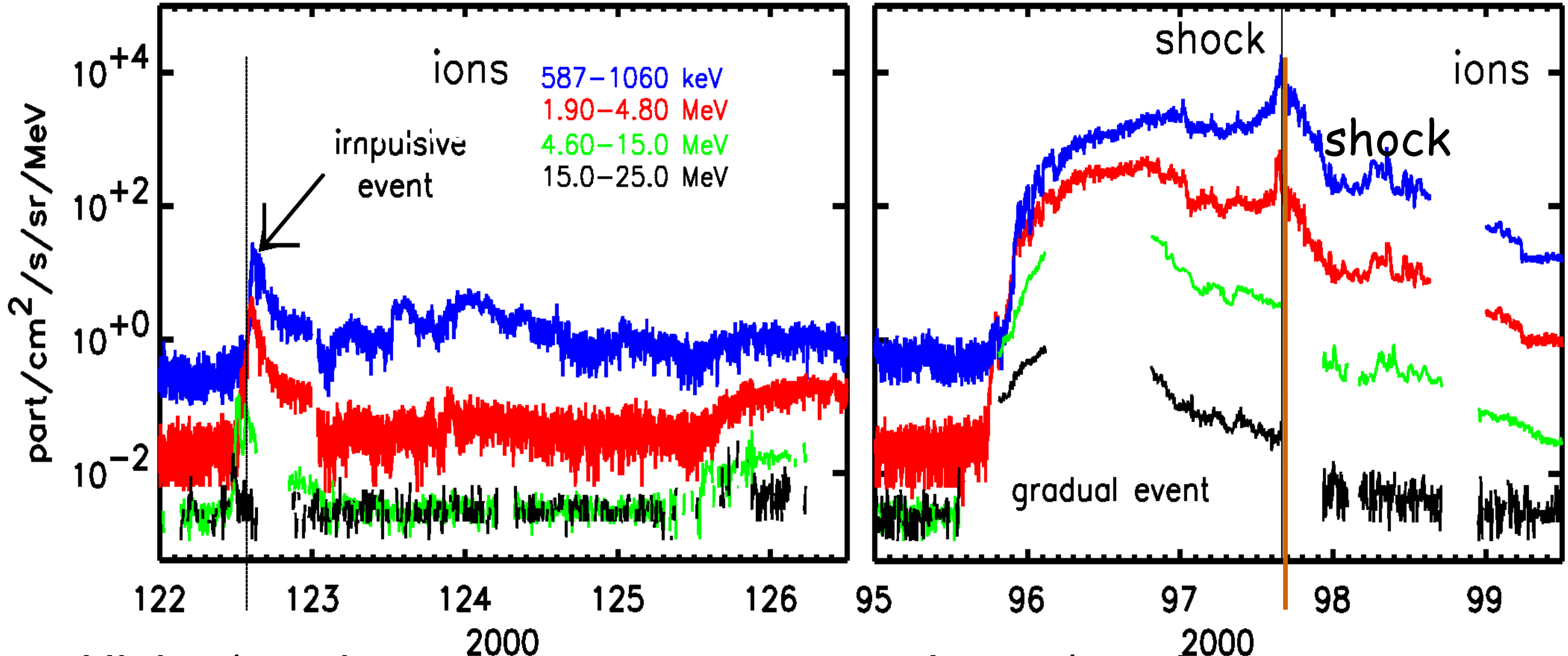

- High e/p ratio
- Mainly low-energy e & p
- Enhanced ^{3}He, α/p, and heavy ions
- High <Q>
- Narrow (~30° longitude)
- Type III radio bursts

- Low e/p ratio,
- variable composition and <Q>
- Rather wide (~100° longitude)
- Large flares and CMEs
- Accelerated by CME shocks

Impulsive and Gradual Events

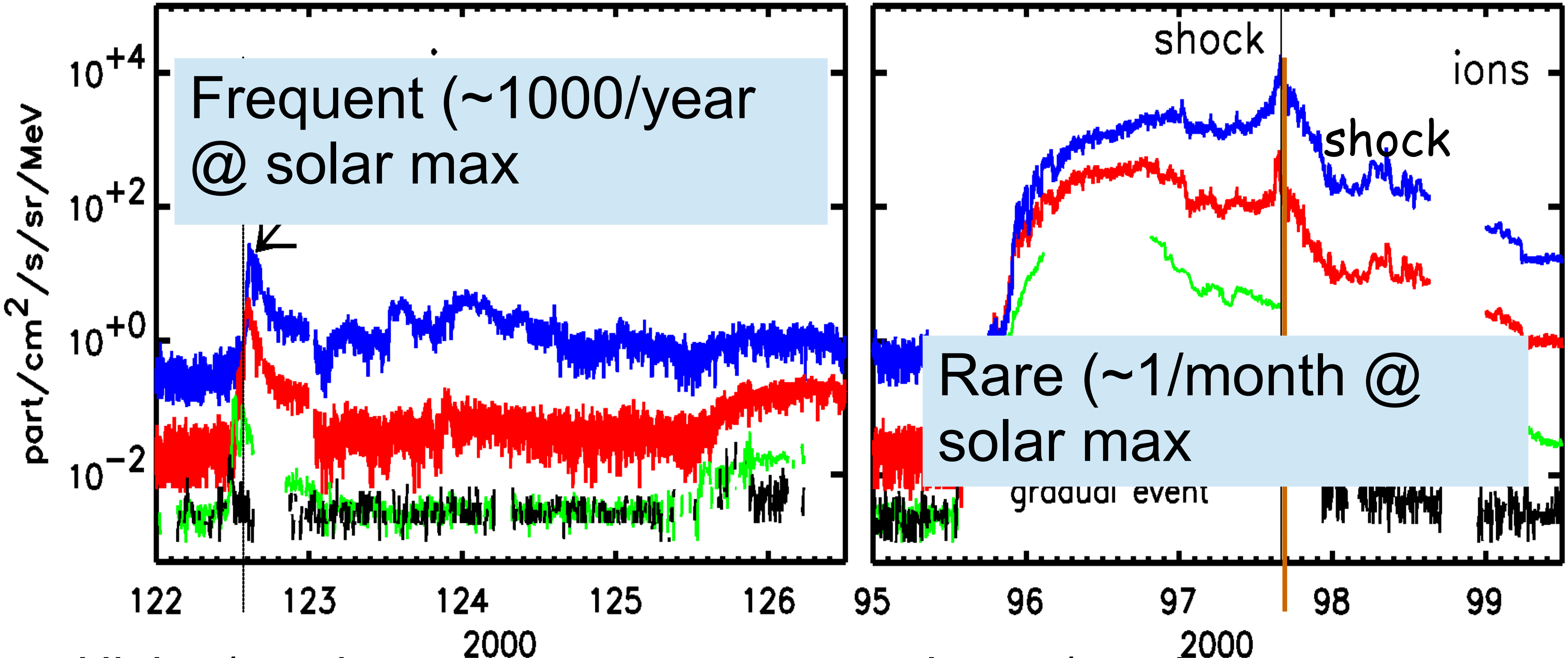

- High e/p ratio
- Mainly low-energy e & p
- Enhanced ^{3}He, α/p, and heavy ions
- High <Q>
- Narrow (~30° longitude)
- Type III radio bursts

- Low e/p ratio,
- variable composition and <Q>
- Rather wide (~100° longitude)
- Large flares and CMEs
- Accelerated by CME shocks

To be an energetic particle, you need to be:

- injected

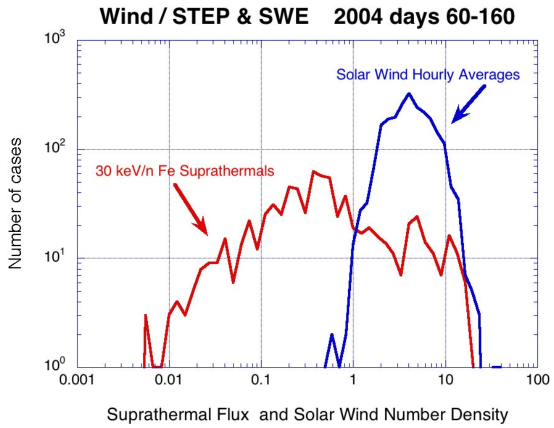

- accelerated

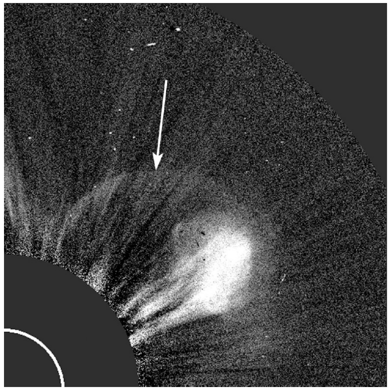

- transported

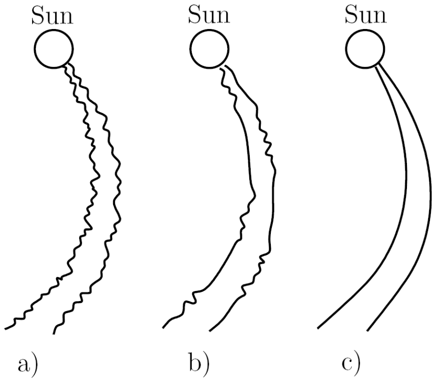

Role of suprathermal seed population?

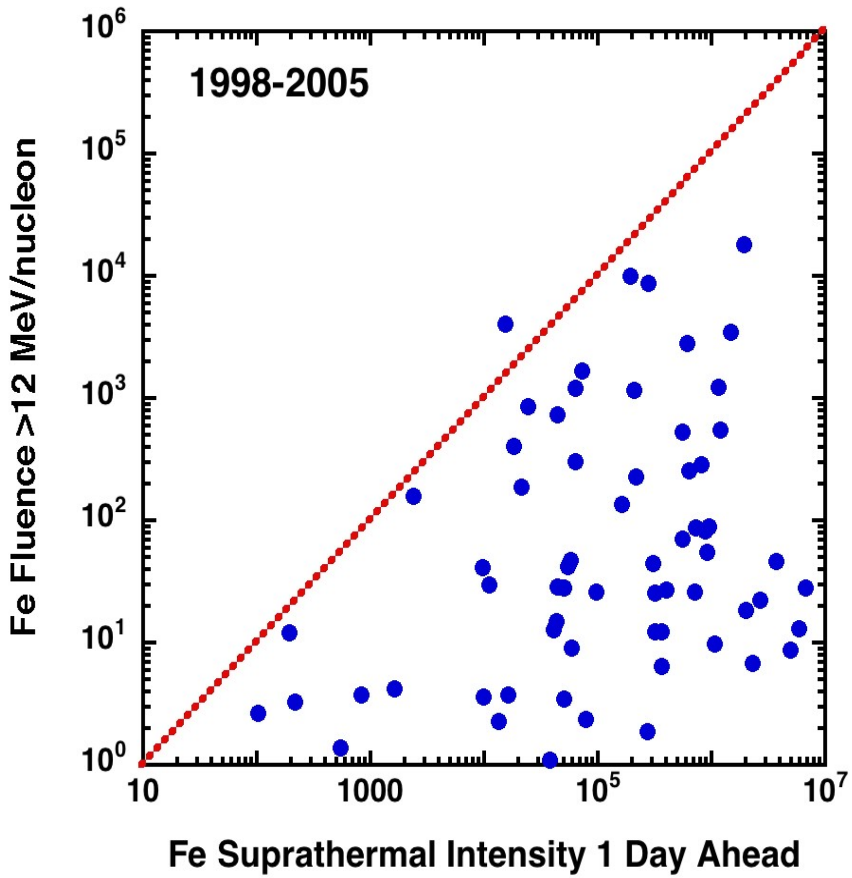

- Diffusive Shock Acceleration, but:
  - Origins of seed populations
  - Proton-amplified waves and turbulence
  - Acceleration efficiencies of CME shocks
  - Shock geometry & variations
- CME shock acceleration efficiencies highly variable

→ **Need near Sun data to resolve different effects and mechanisms**

How does the suprathermal particle population through which a shock moves influence the resulting intensity of energetic particles that are accelerated?

Immense variability in suprathermal heavy ion flux

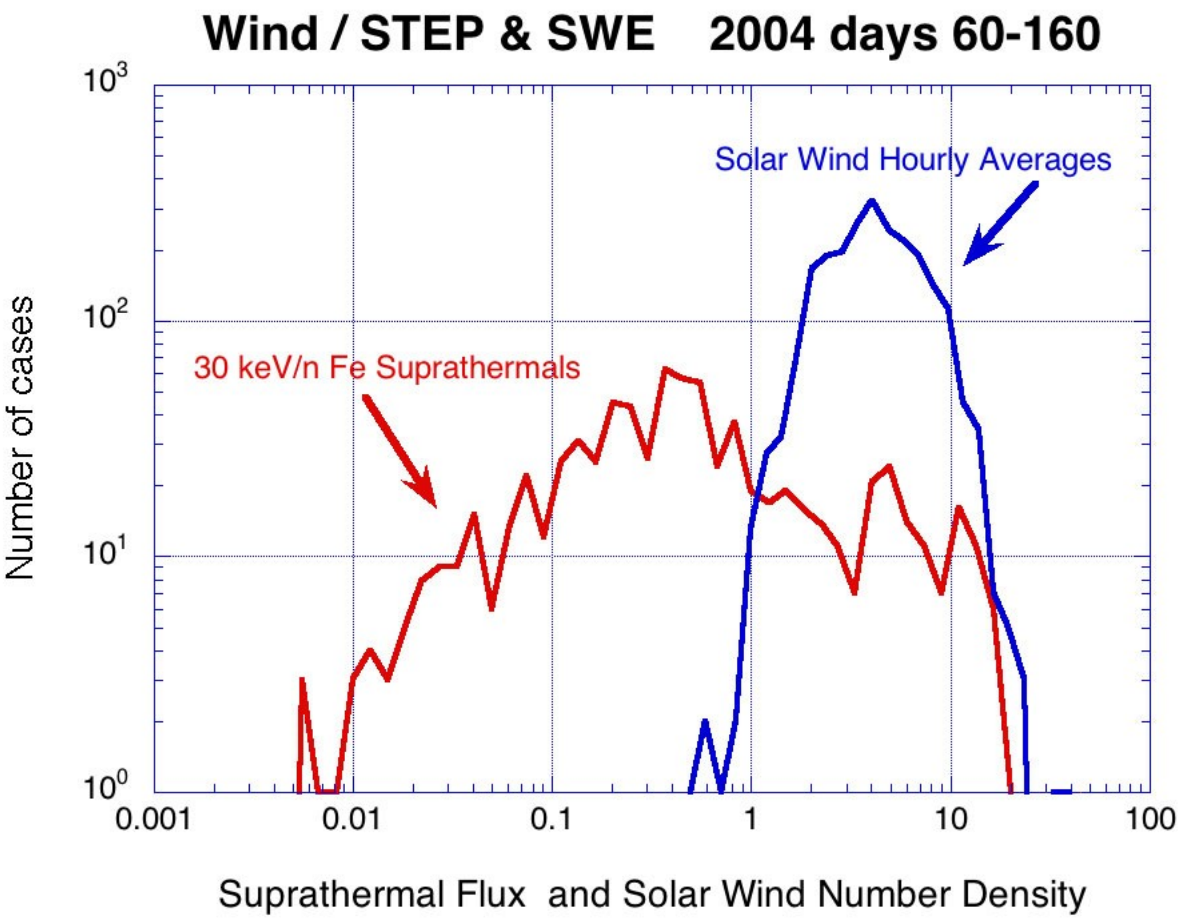

Peak intensities in shock events vary over a range of ~10^4

- not explained by CME speed
- not explained by shock acceleration models
- not explained by solar wind number density which does not change nearly as much

(Mason et al., 2005)

Suprathermal particles present most of the time

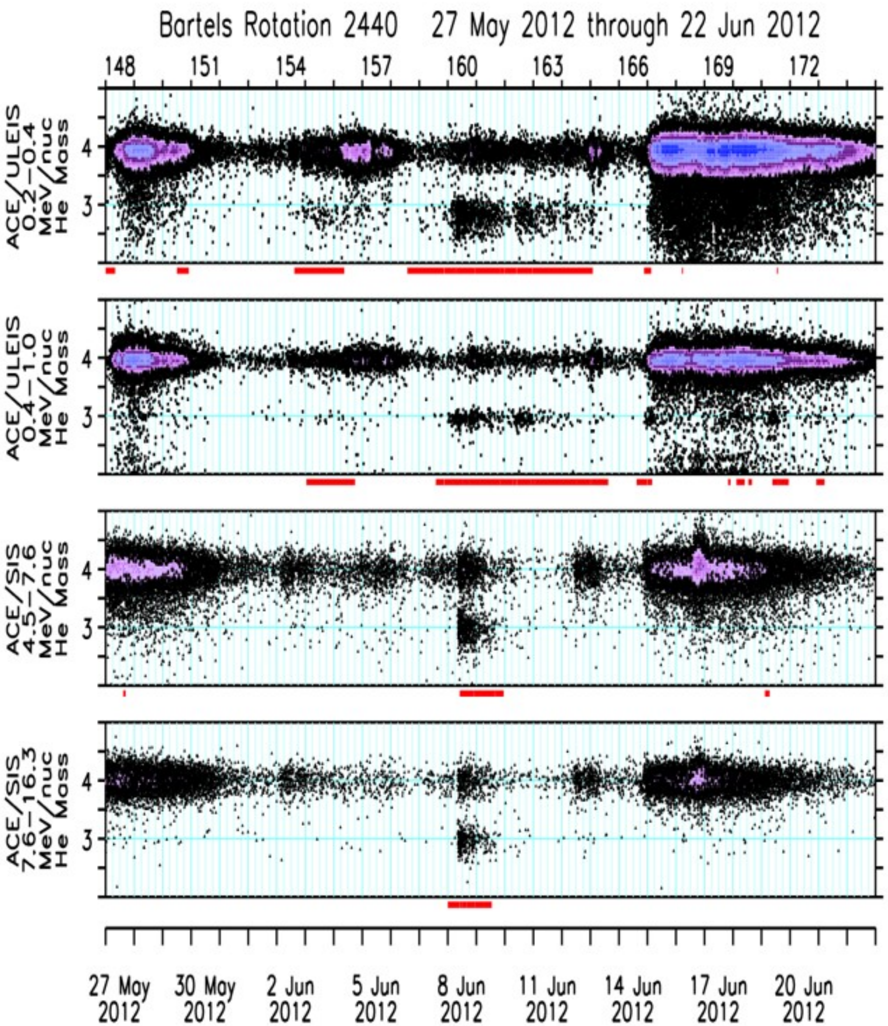

Flare suprathermals

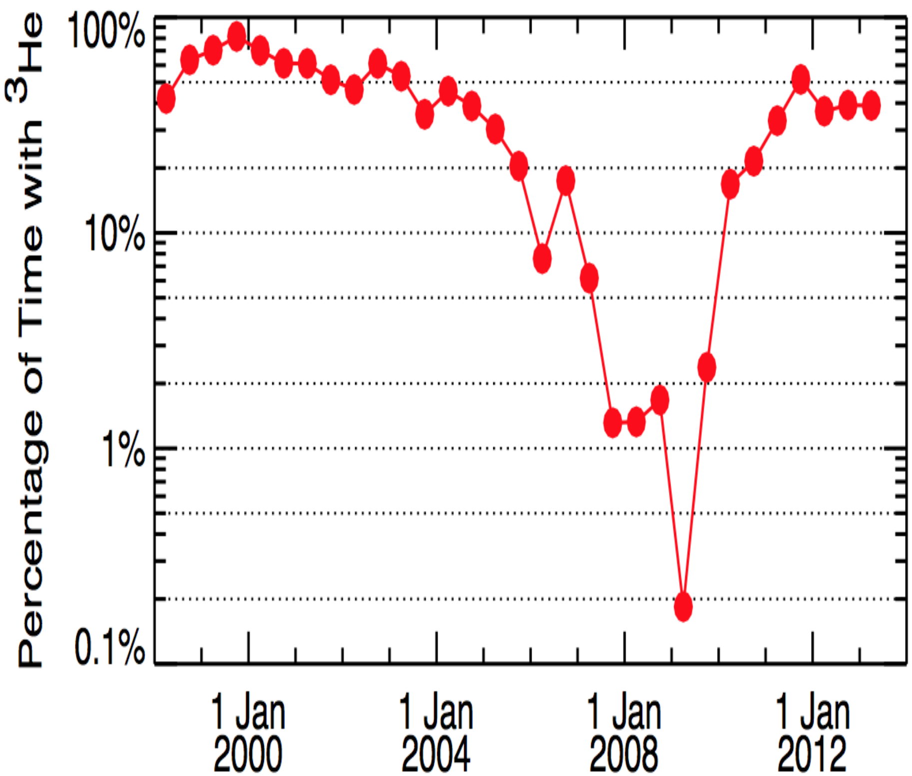

Figure 2. Average percentage of time that ^{3}He was detected at ACE during each 6-month period from the start of 1998 through mid-2013. All four of the energy intervals illustrated in Fig. 1 were used in identifying times when ^{3}He was present.

(Wiedenbeck et al., 2014)

Old Picture:

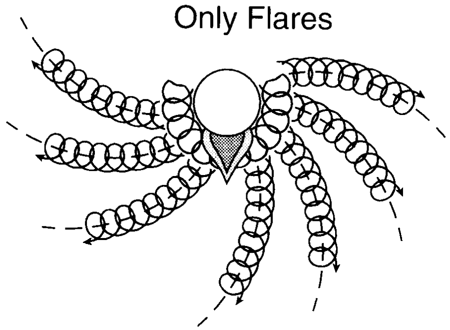

But flares don't rule (alone)!

CME-driven shocks play an important role in accelerating particles.

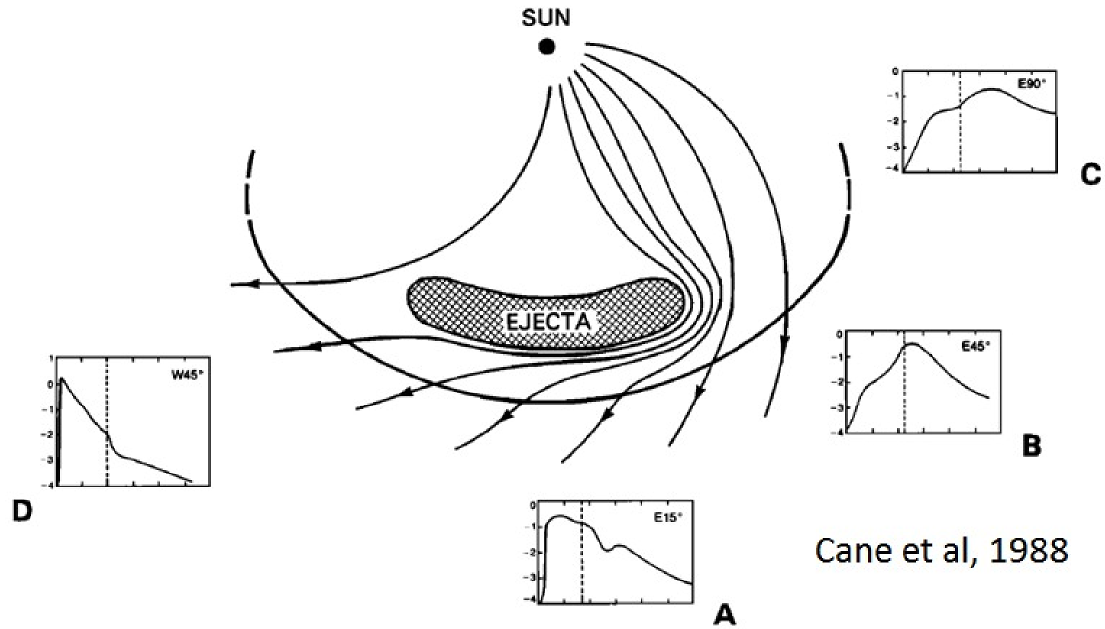

Cane et al, 1988

Old new

~~New~~ **Picture:**

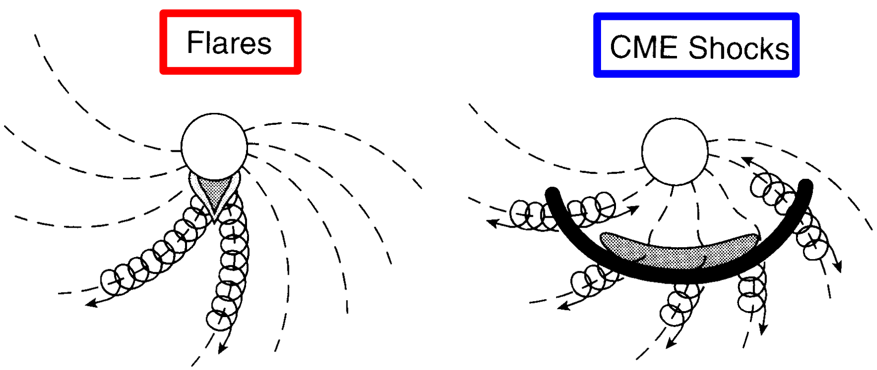

New Picture:

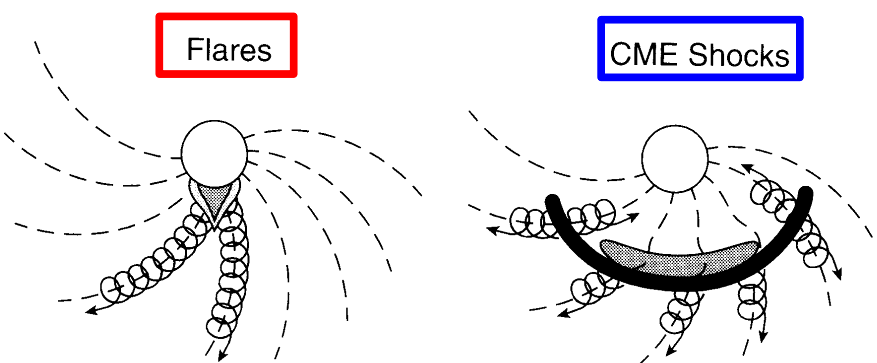

Life is more complicated:
Flares can contribute to shock-accelerated particles. Exact role is current research topic.

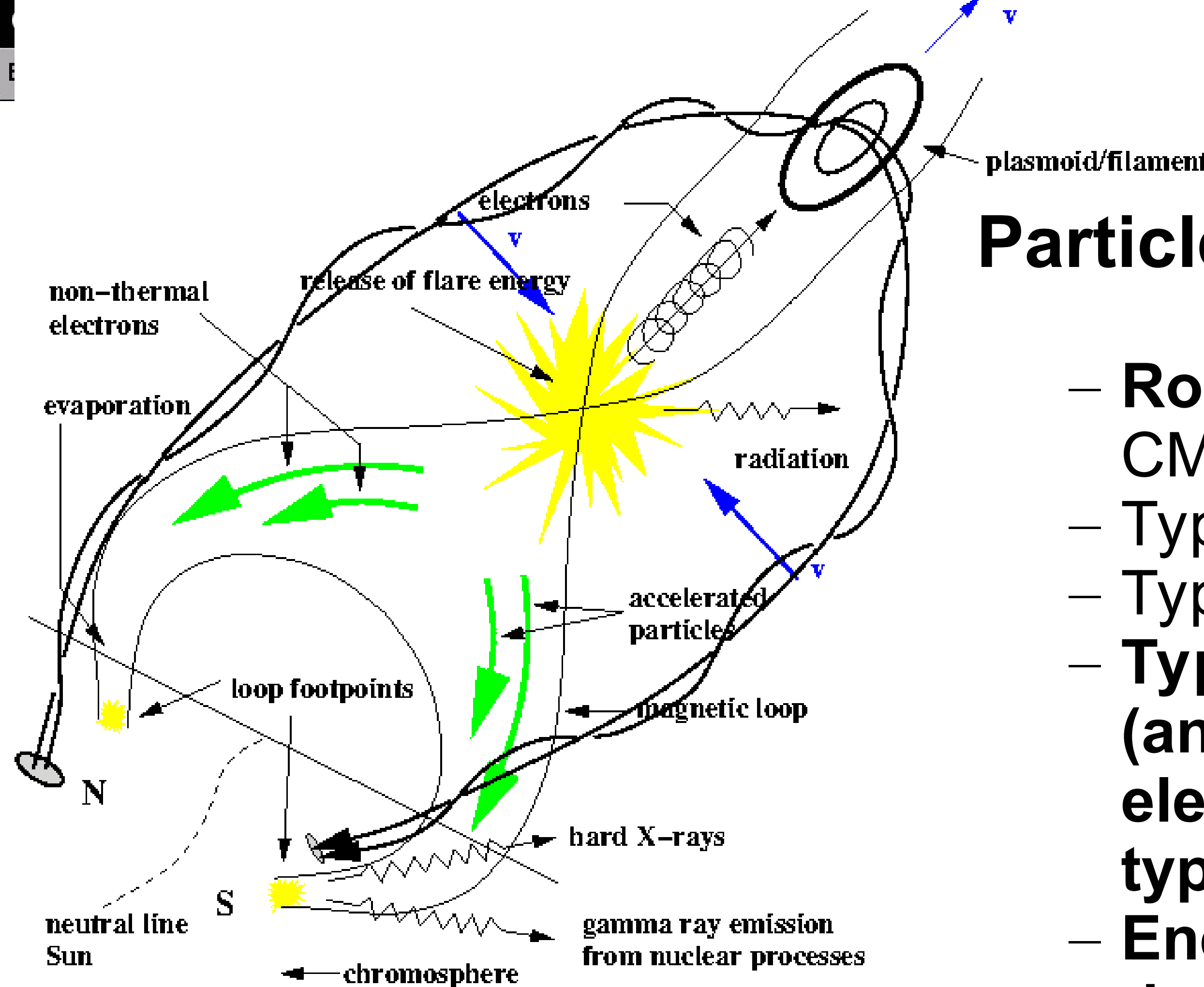

Particle acceleration in flares:

- **Rough** equipartition of flare and CME energy
- Typical duration 10 – 100 s
- Typical energy 10^{23} J
- **Typically between 1% - 10% (and up to 100%) of all electrons are accelerated to typically 100 keV**
- **Energetically these electrons dominate the plasma**
- Ions are also accelerated (and produce gamma rays)
- Occasionally, particles are accelerated to relativistic energies (GLEs).

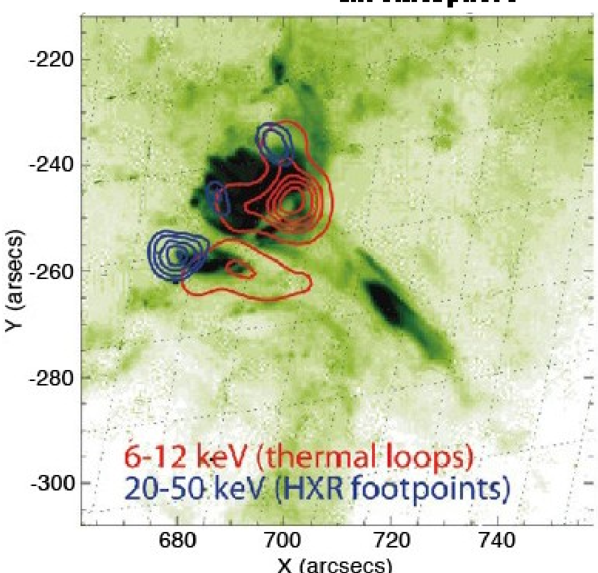

Shock Acceleration - A more organized way of accelerating particles?

a.) diffusive shock-acceleration
b.) shock-drift acceleration

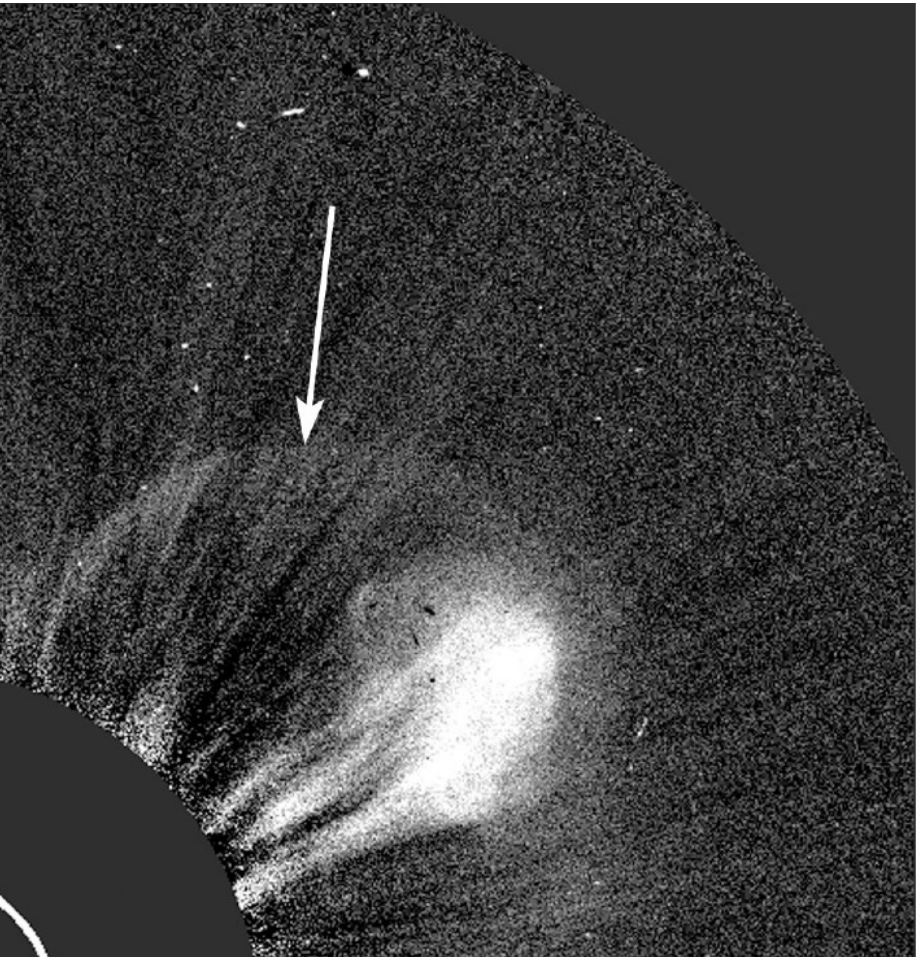

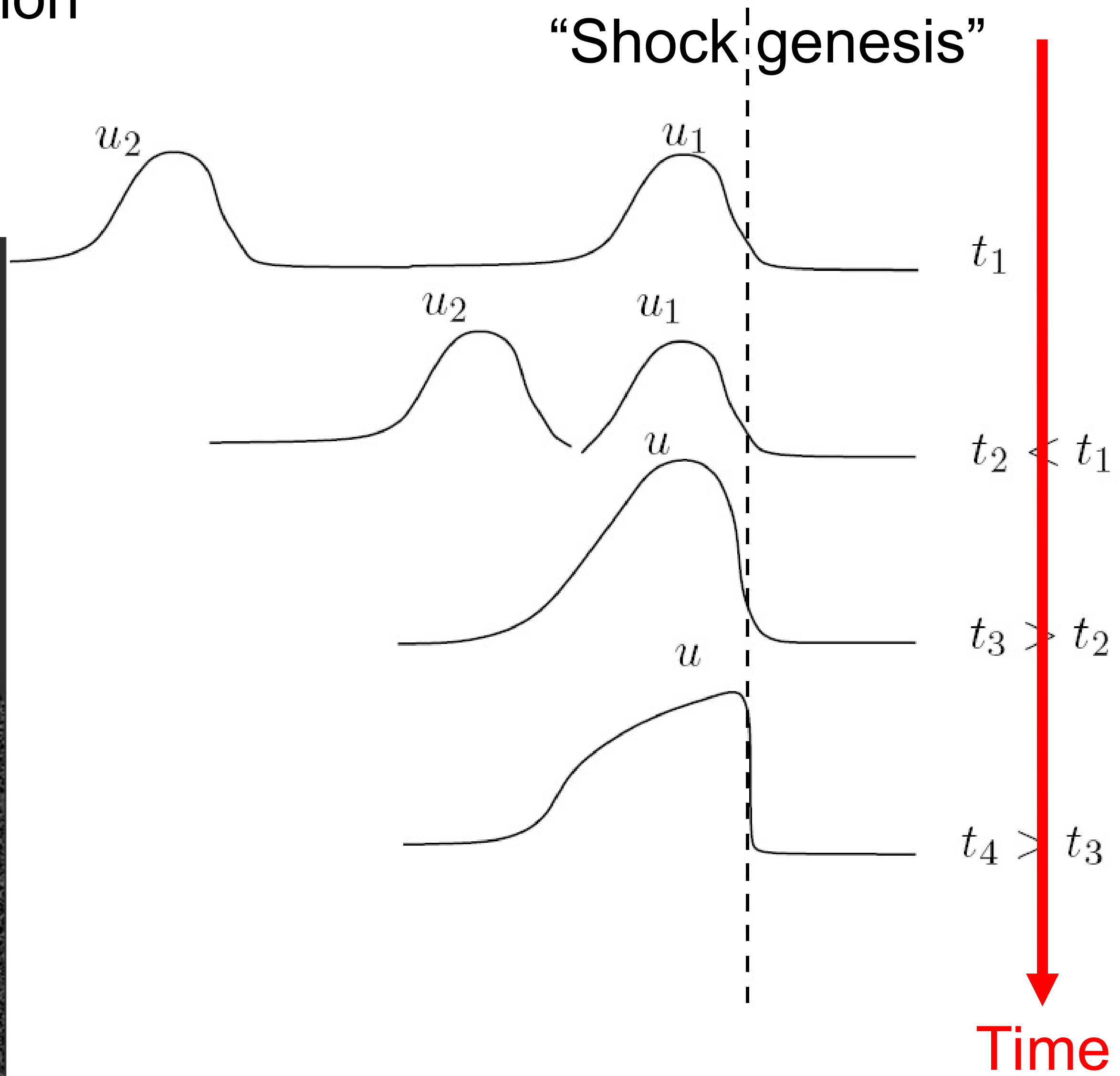

Shock or diffusive (Fermi 2) acceleration

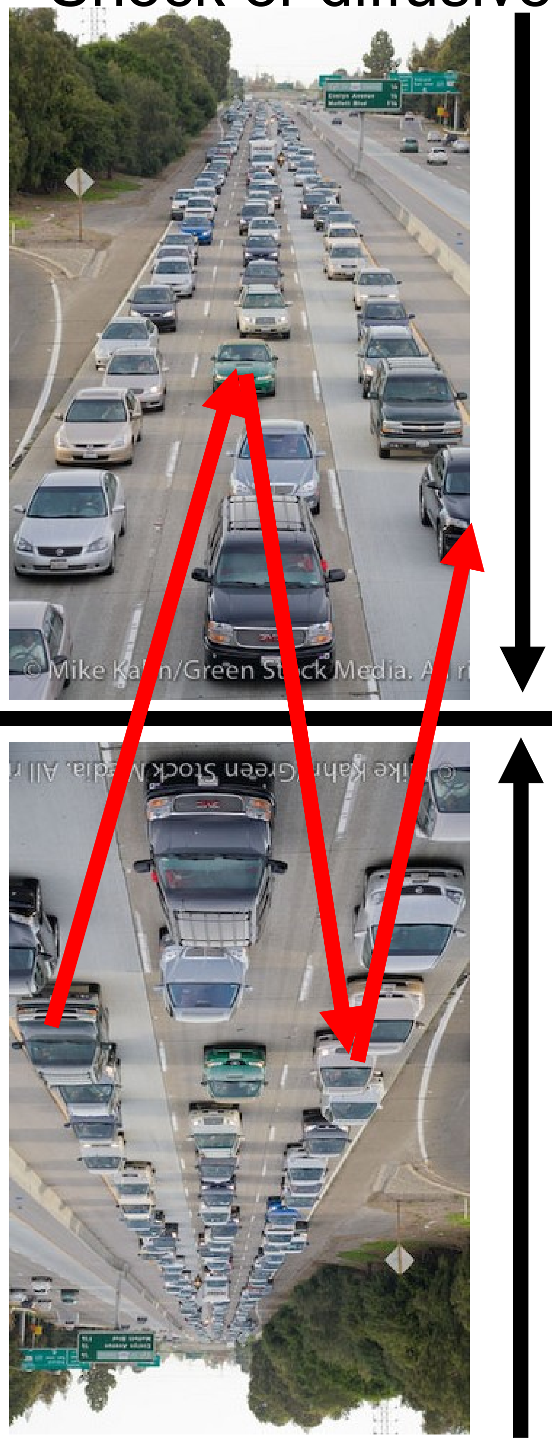

Turbulent structures moving towards you

stepwise acceleration via turbulent motions

Some particles gain energy in every reflection (Fermi acceleration)

Shock (in fact, any location with converging turbulence)

This scenario ultimately leads to the observed power-law distribution in energy. If the shock is large enough, it can explain large events.

Turbulent structures moving towards you

Once accelerated, particles get away, but continue to be scattered, a process called **transport**

Three different scenarios:

a) diffusive

b) focused - transport

c) scatter free

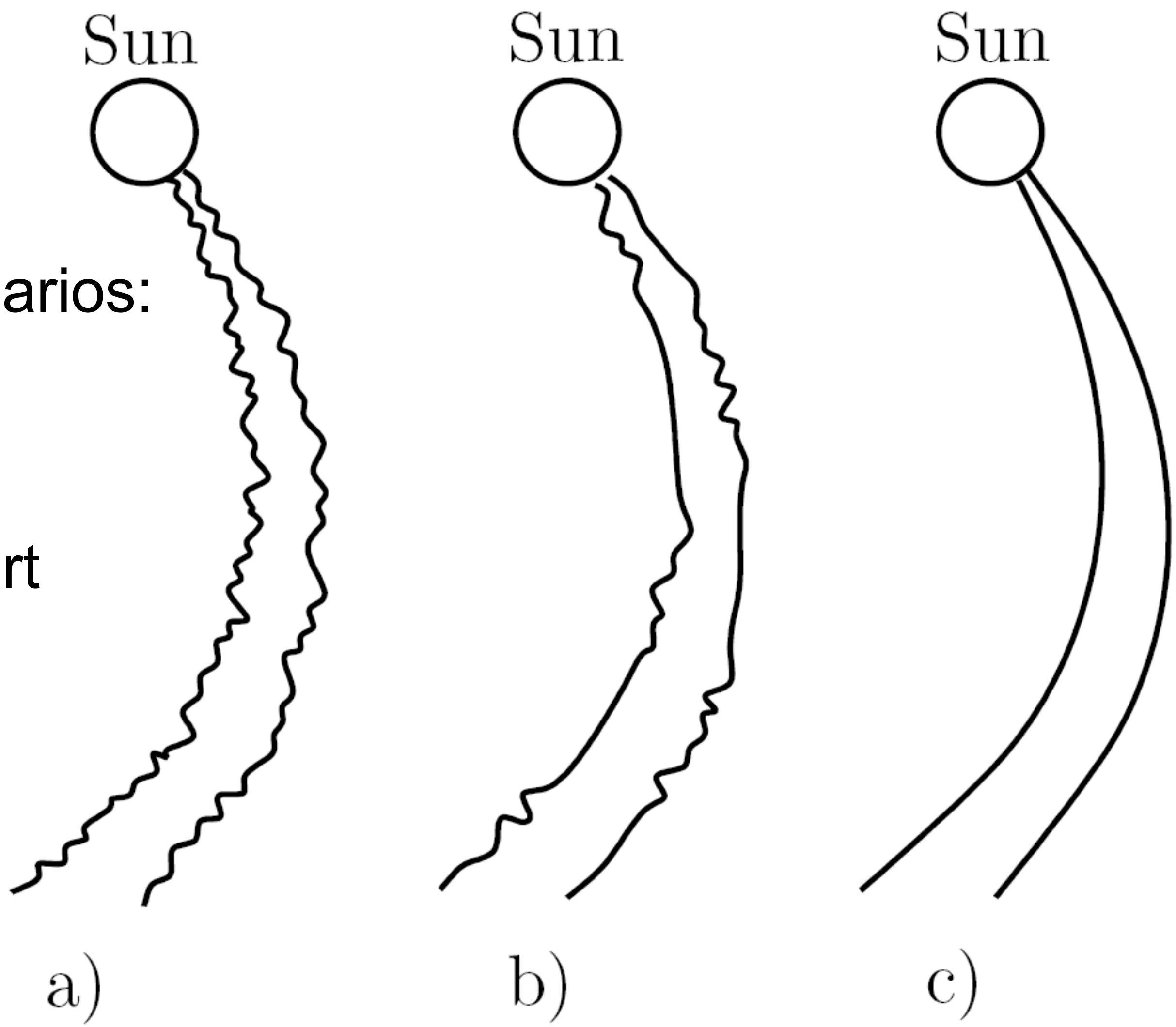

Timing studies are best done with scatter-free events. They can be recognized by beam-like pitch-angle distributions.

The particle transport equation

$$
\begin{aligned}
\frac{\partial F(t, \mu, r, p)}{\partial t} = & -\cos\psi \frac{\partial}{\partial r} \\
& \times \left\{ \left[v\mu + \left(1 - \mu^2 \frac{v^2}{c^2}\right) v_{\rm sw} \sec\psi \right] F(t, \mu, r, p) \right\} && \text{Streaming + Convection} \\
& - \frac{\partial}{\partial \mu} \left\{ \left[\frac{v}{2L(r)} \left(1 + \mu \frac{v_{\rm sw}}{v} \sec\psi - \mu \frac{v_{\rm sw} v}{c^2} \sec\psi \right) \right. \right. && \text{Focusing} \\
& \left. \left. + v_{\rm sw} \left(\cos\psi \frac{d}{dr} \sec\psi\right) \mu \right] (1 - \mu^2) F(t, \mu, r, p) \right\} && \text{Differential convection} \\
& + \frac{\partial}{\partial \mu} \left\{ D_{\mu\mu} \frac{\partial}{\partial \mu} \left[\left(1 - \mu \frac{v_{\rm sw} v}{c^2} \sec\psi \right) F(t, \mu, r, p) \right] \right\} && \text{Pitch-angle scattering} \\
& + \frac{\partial}{\partial p} \left\{ p v_{\rm sw} \left[\frac{\sec\psi}{2L(r)} (1 - \mu^2) + \cos\psi \frac{d}{dr} (\sec\psi) \mu^2 \right] \right. && \text{Adiabatic deceleration} \\
& \left. \times F(t, \mu, r, p) \right\} + G(t, \mu, r, p) \, , \qquad (1) && \text{Source term}
\end{aligned}
$$

Pristine shock acceleration at CIRs?

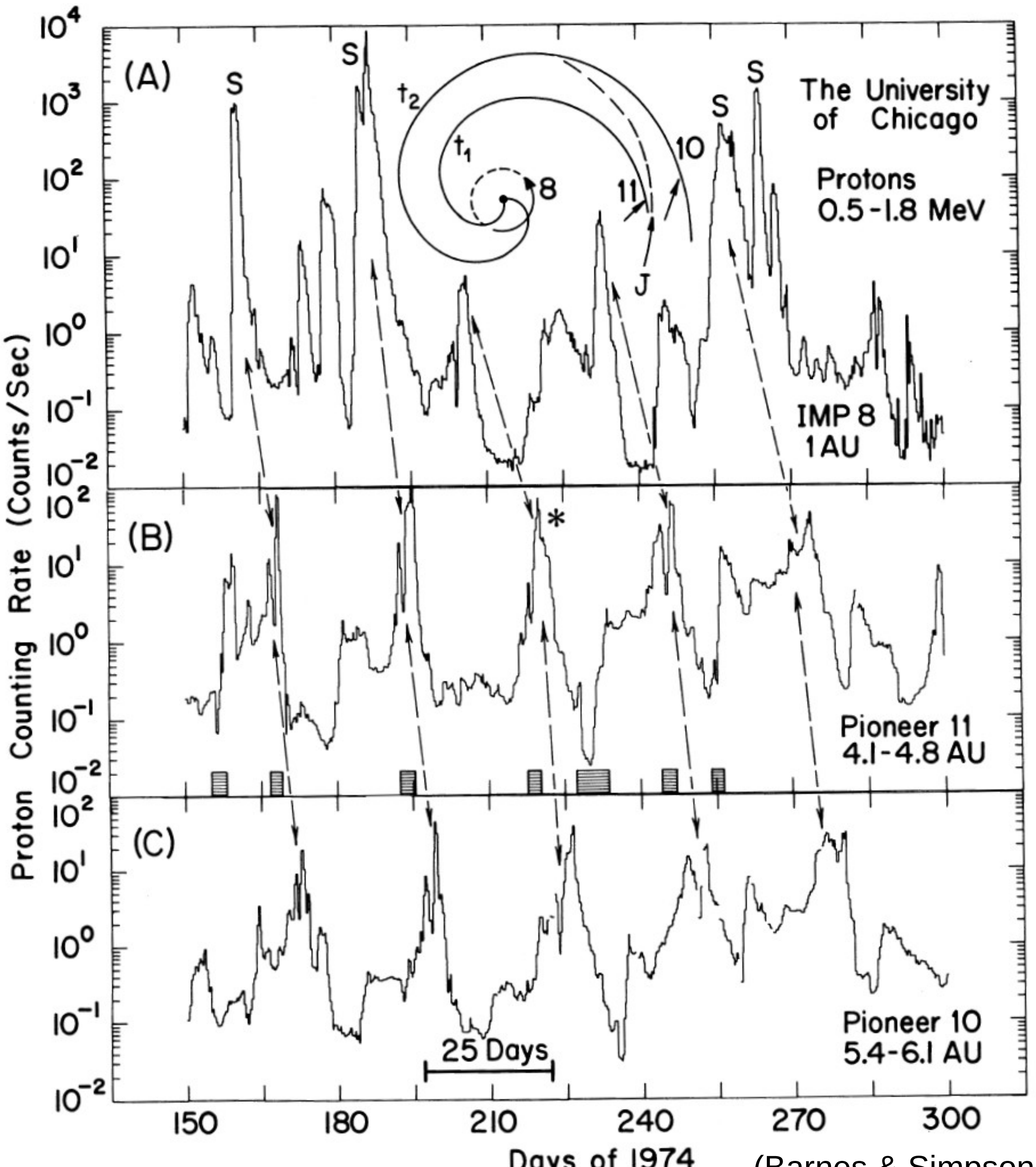

(Barnes & Simpson, 1979)

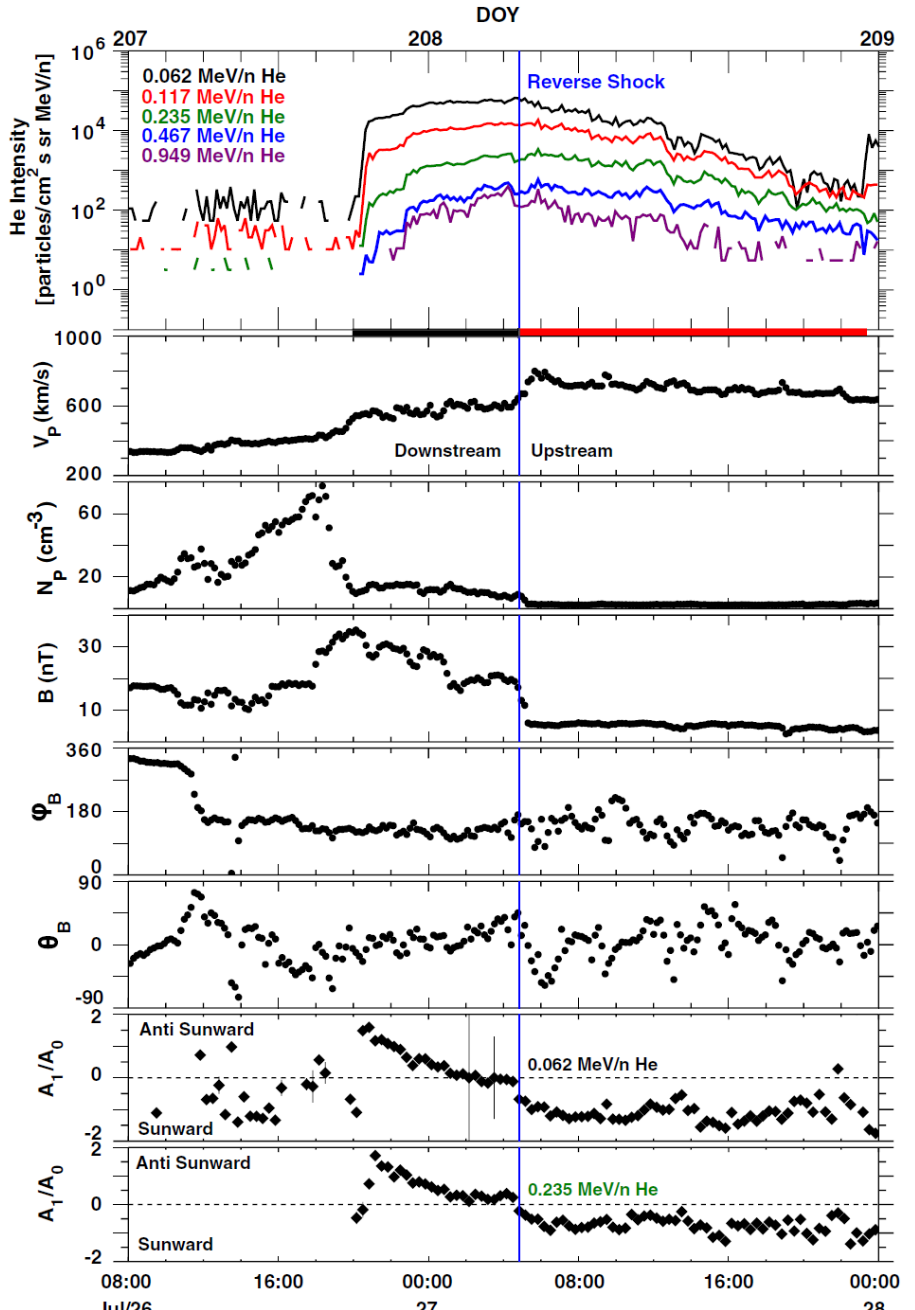

(Ebert et al., 2012)

Suprathermal He^{++} at CIRs

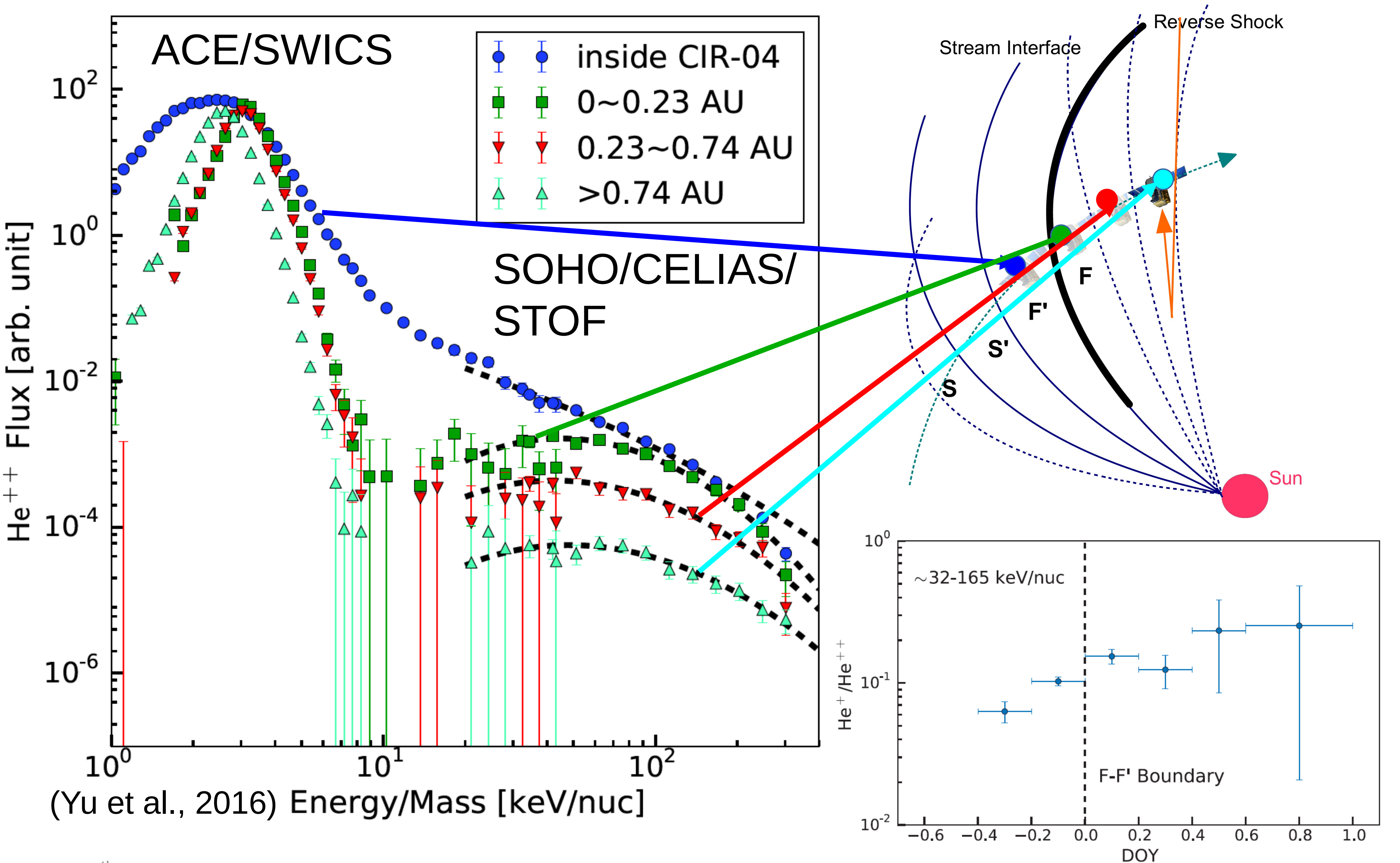

(Yu et al., 2016)

Not unexpectedly, we observe similar behavior at CME-driven, transient shocks.

$$\frac{1}{v_{\text{ion}}}\,[\text{s/Mm}]$$

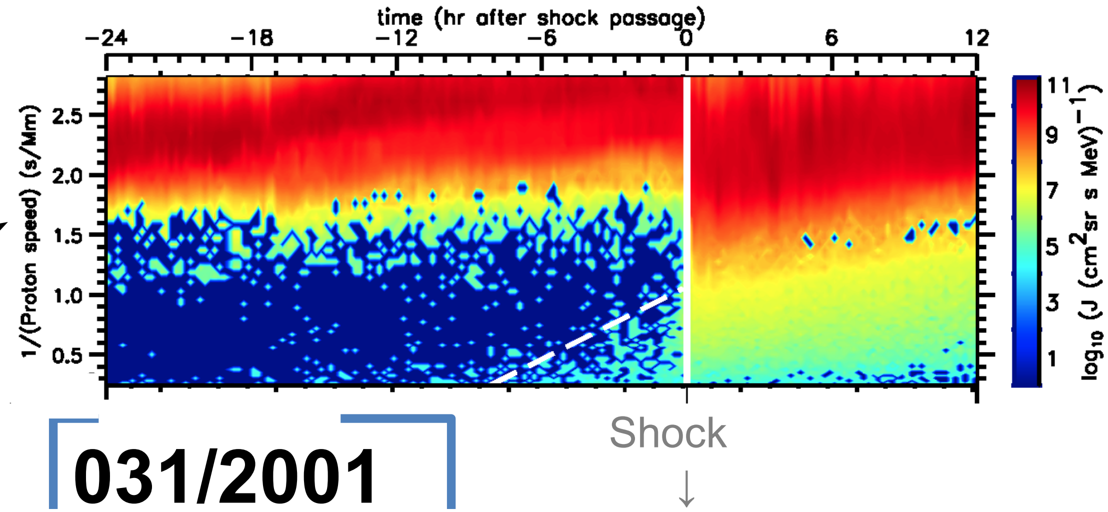

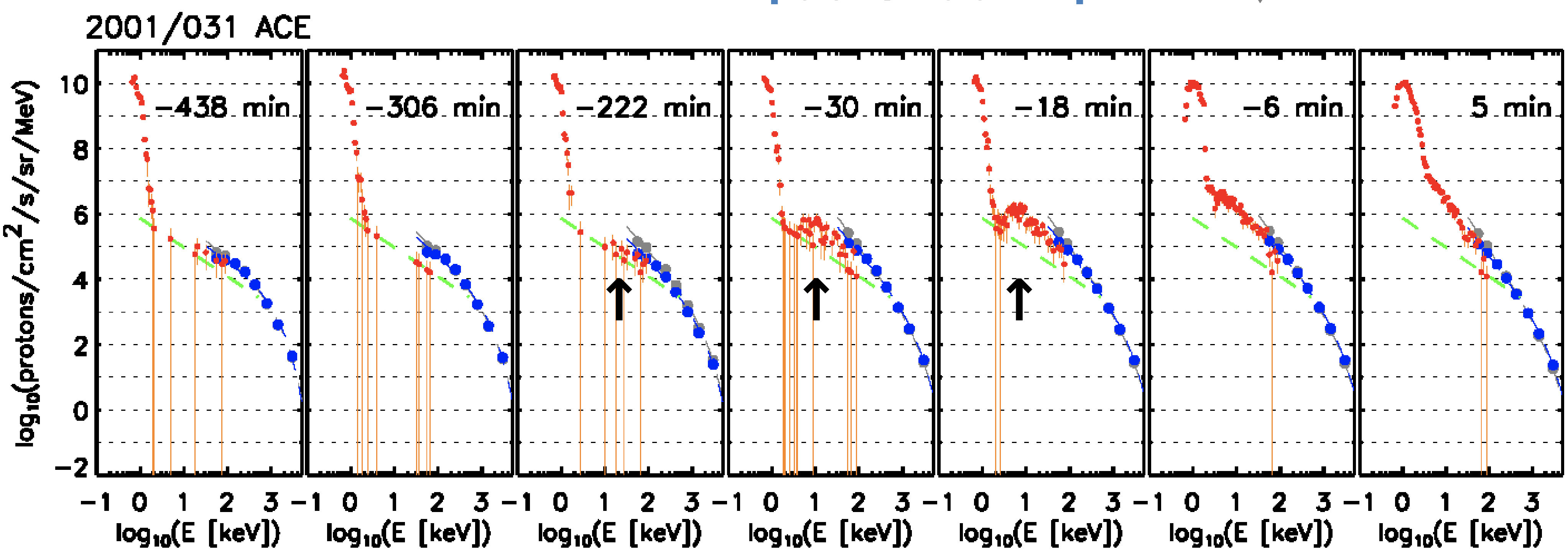

(Lario, et al.)

Substantial pressure in energetic particles

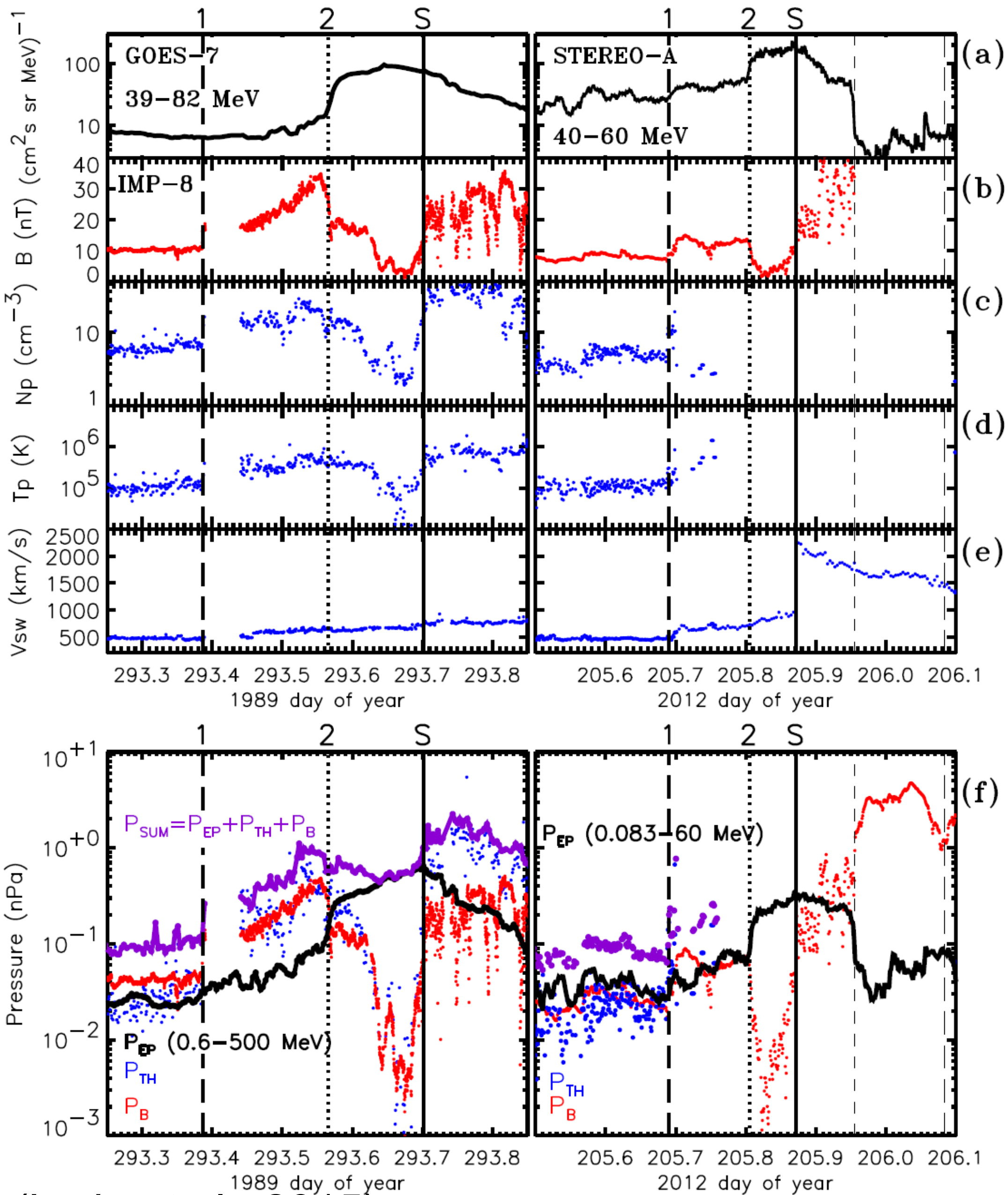

(Lario et al., 2015)

Lario et al., 2015, studied periods of elevated energetic particle intensities in which pressure of > 83 keV protons is larger than thermal or magnetic pressure.

Such periods are not rare.

Energetic particles often matter for shock dynamics.

Energetic particle pressure should be accounted for when computing shock parameters.

Illustration of the effect of transport on particles

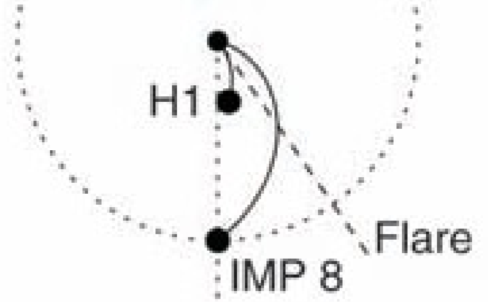

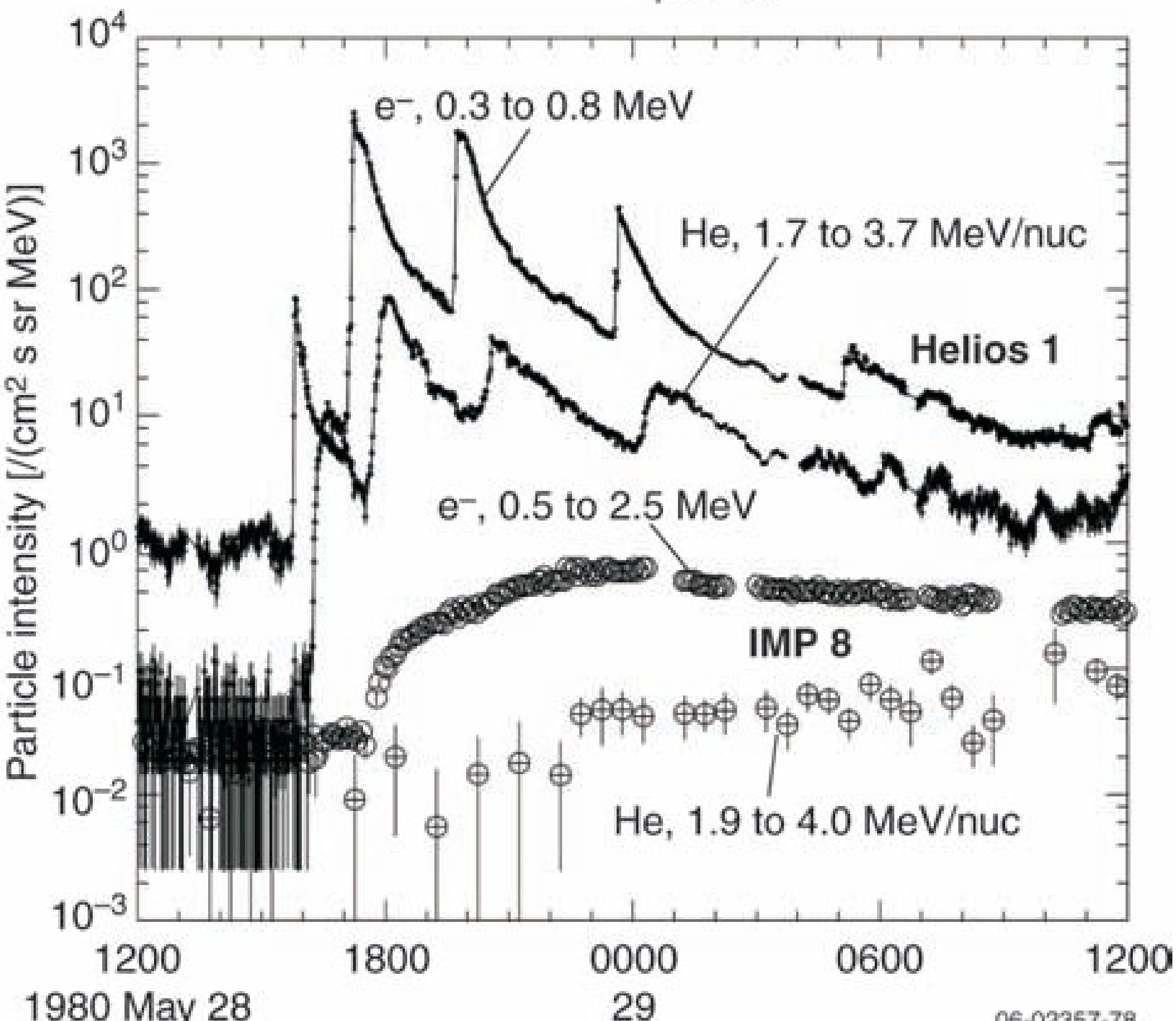

Kallenrode & Wibberenz, 1991

Solar Orbiter & SP+ can disentangle transport effects from injection effects.

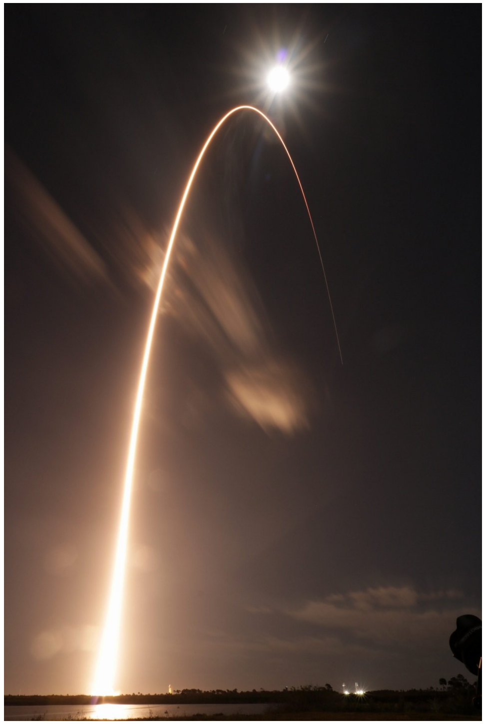

The first wide-spread energetic particle event observed by Solar Orbiter on 2020 November 29

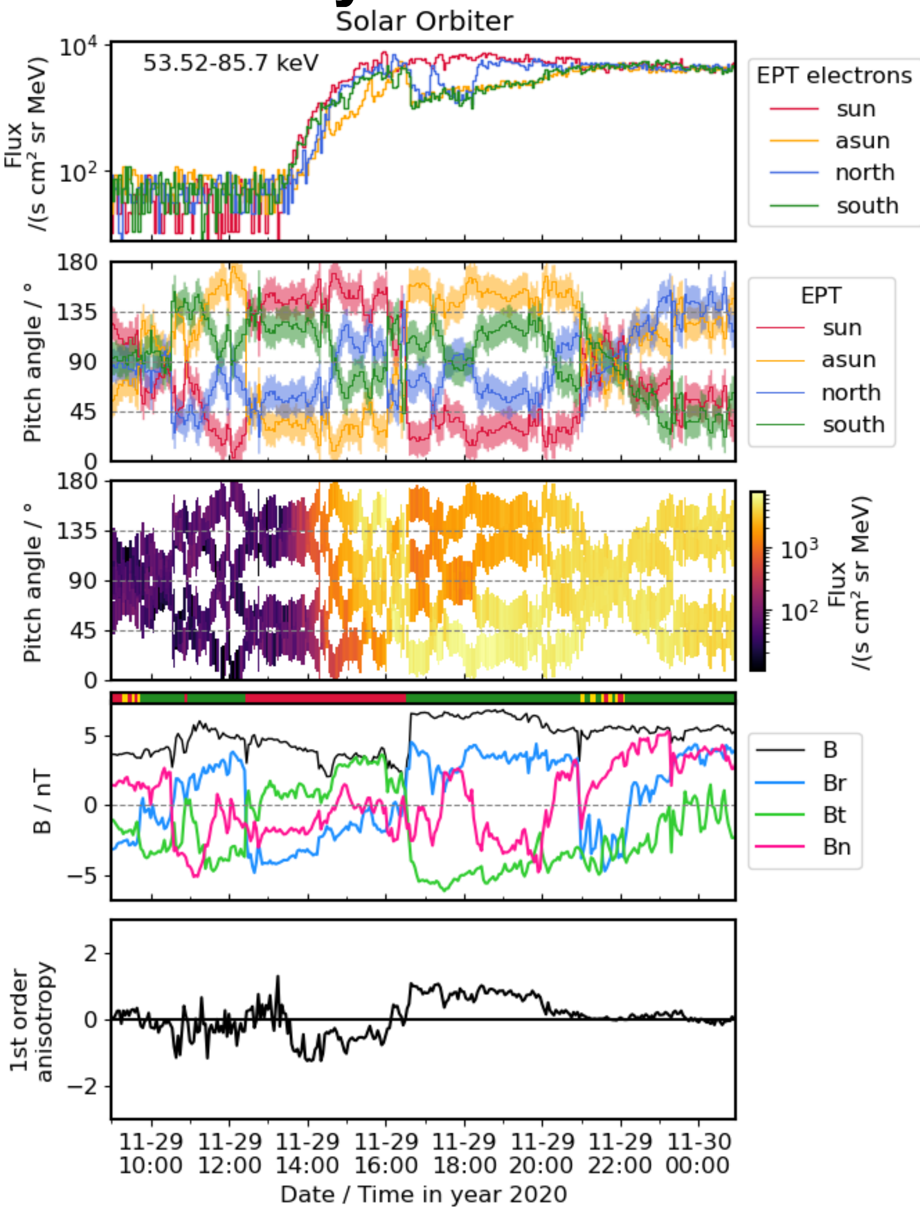

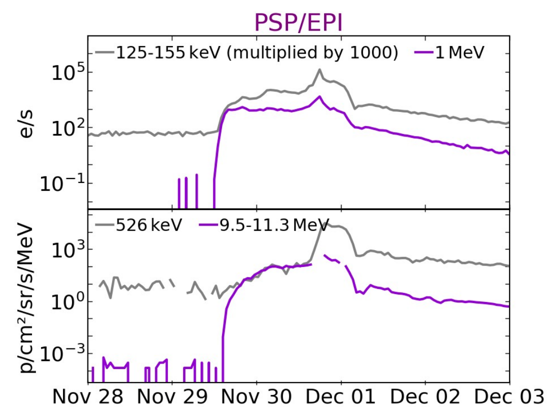

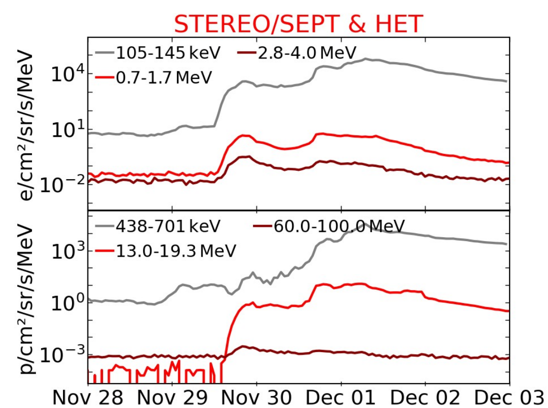

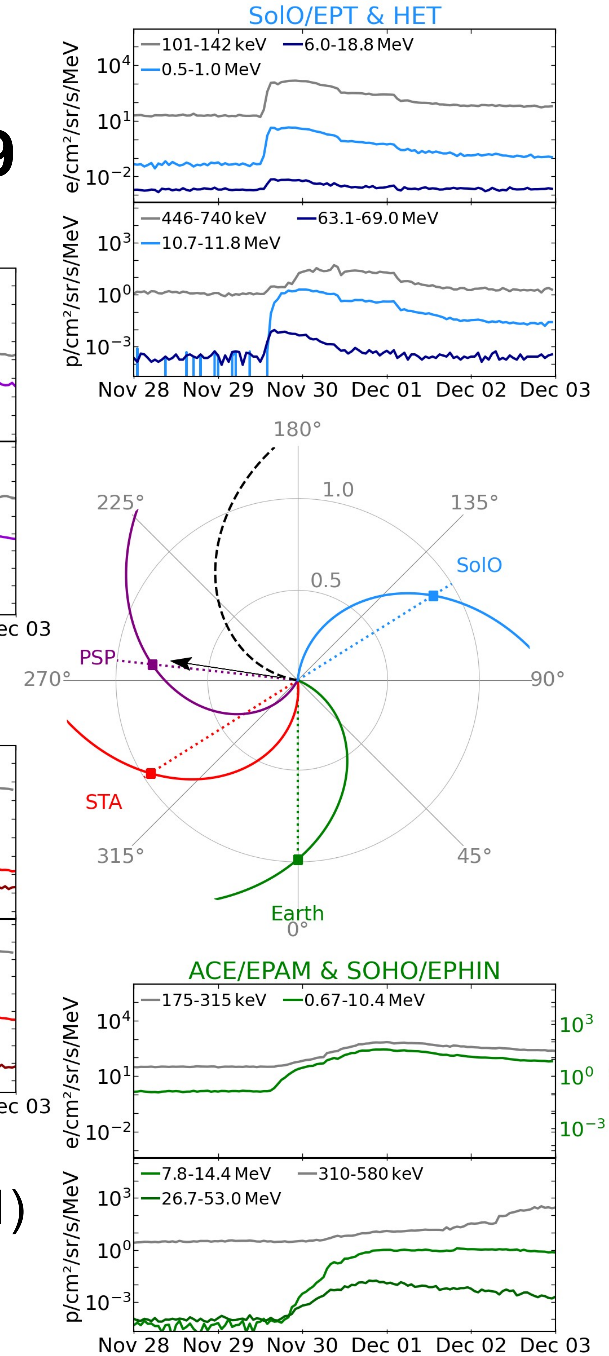

(Kollhoff et al., 2021)

The first wide-spread energetic particle event observed by Solar Orbiter on 2020 November 29

Anisotropic onset at wide separations!

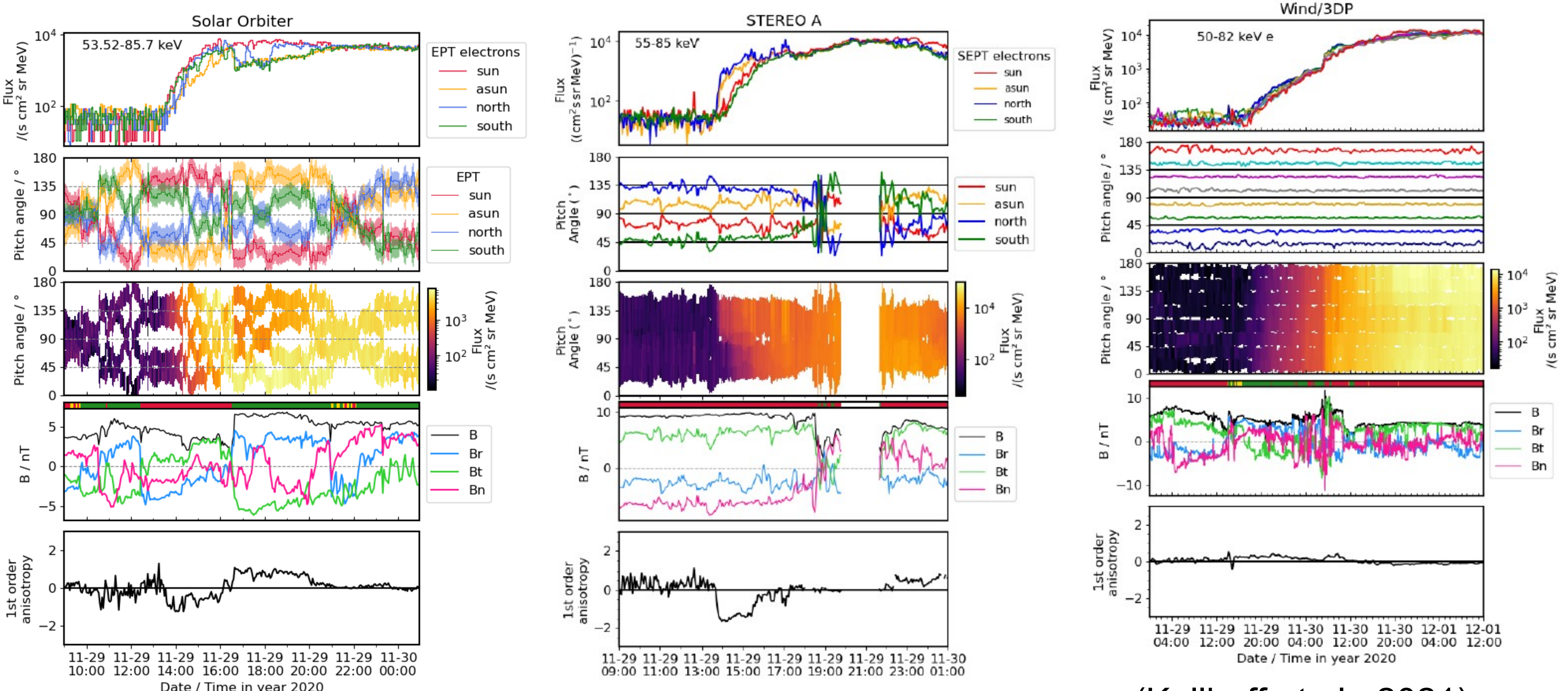

(Kollhoff et al., 2021)

The first wide-spread energetic particle event observed by Solar Orbiter on 2020 November 29

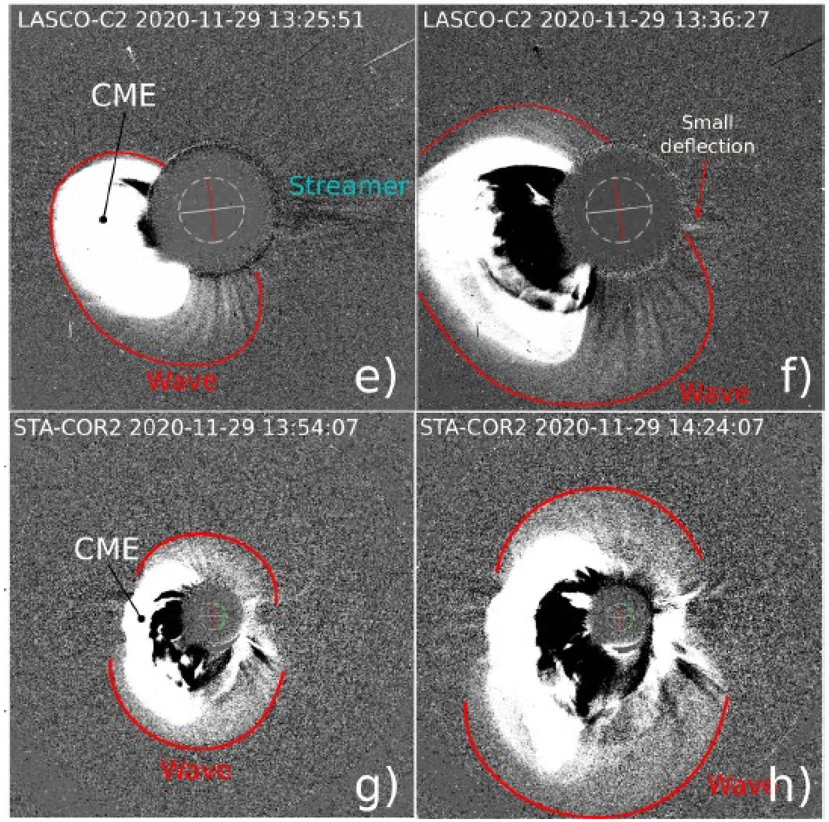

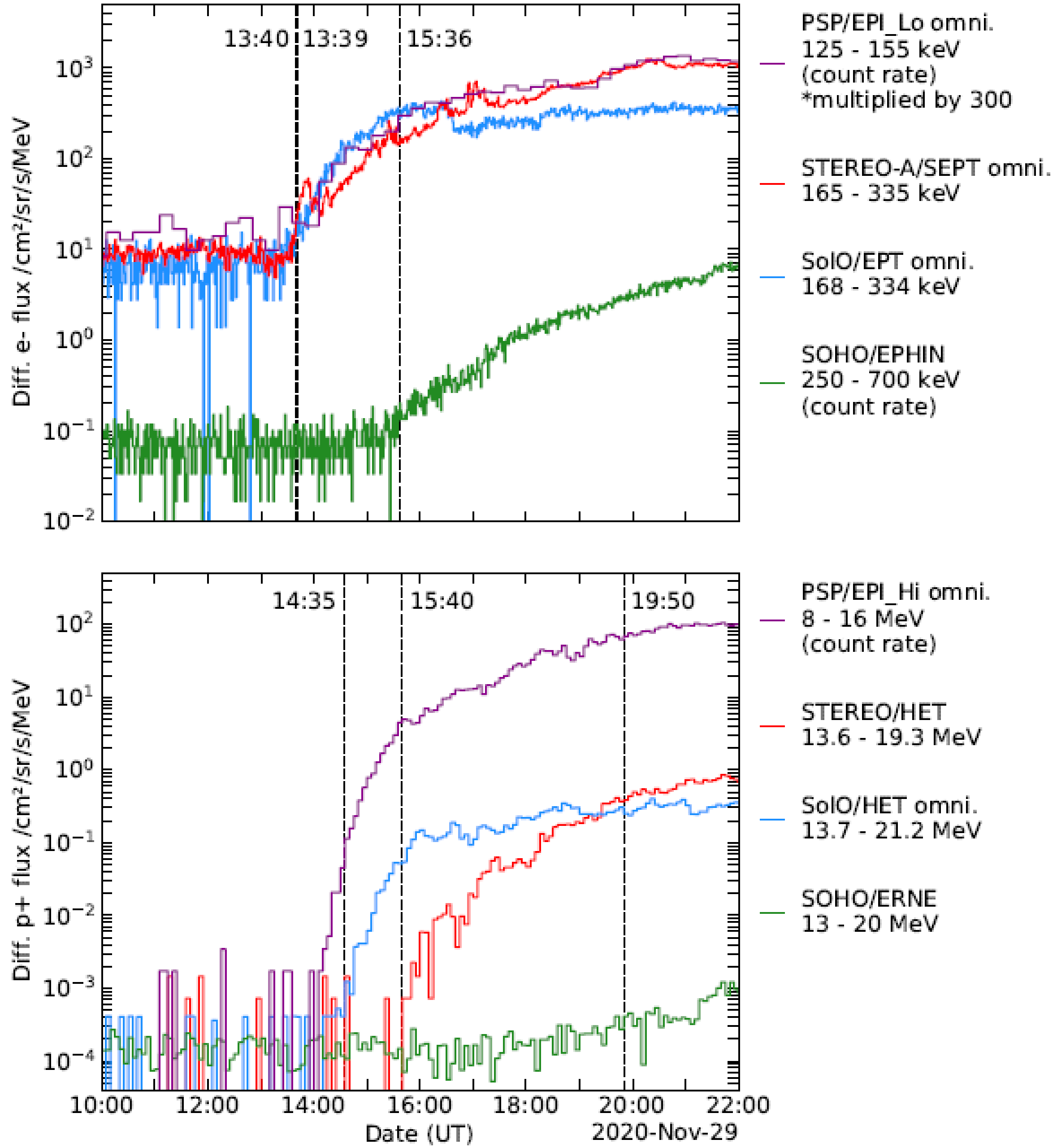

Onset timing and anisotropies inconsistent with triggering by EUV wave.

(Kollhoff e

EPD on Solar Orbiter covers a wide range of energies (energy/nuc)

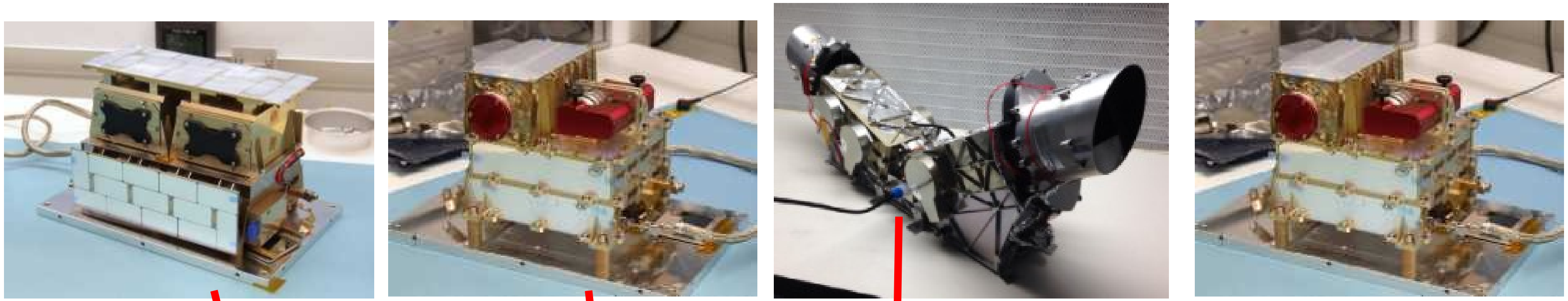

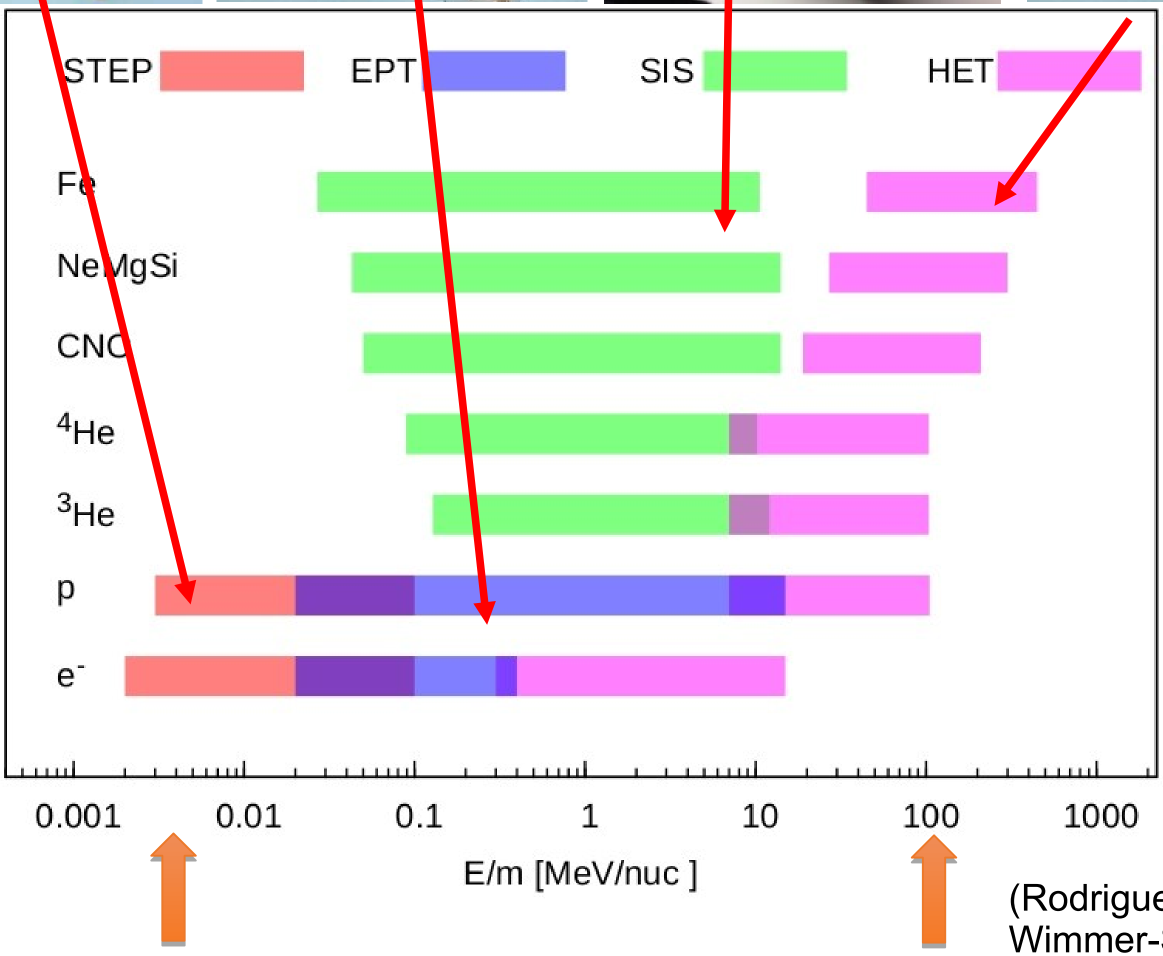

(Rodriguez-Pacheco et al., 2020,
Wimmer-Schweingruber et al., 2021)

EPD on Solar Orbiter has different viewing directions to provide adequate pitch-angle distributions.

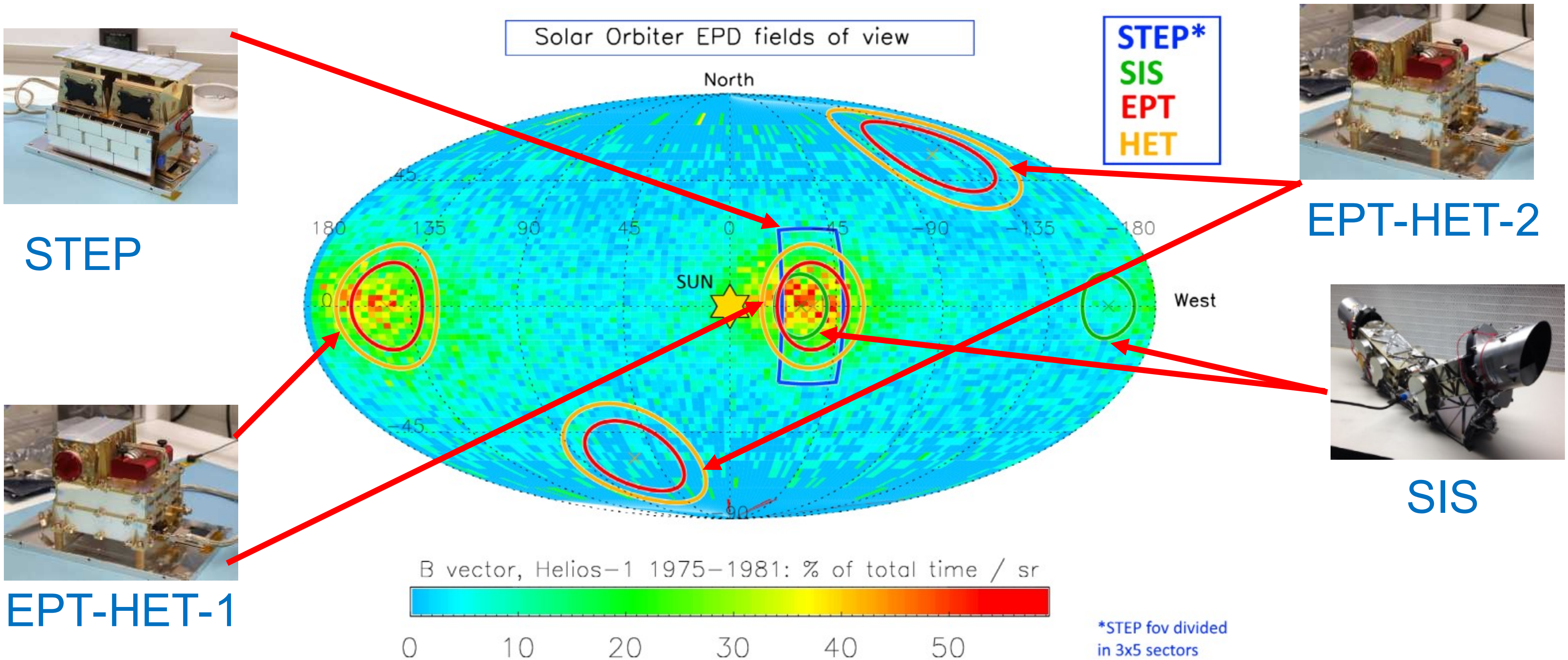

(Rodriguez-Pacheco et al., 2020, Wimmer-Schweingruber et al., 2021)

Measuring suprathermal ions

(Rodriguez-Pacheco et al., 2020)

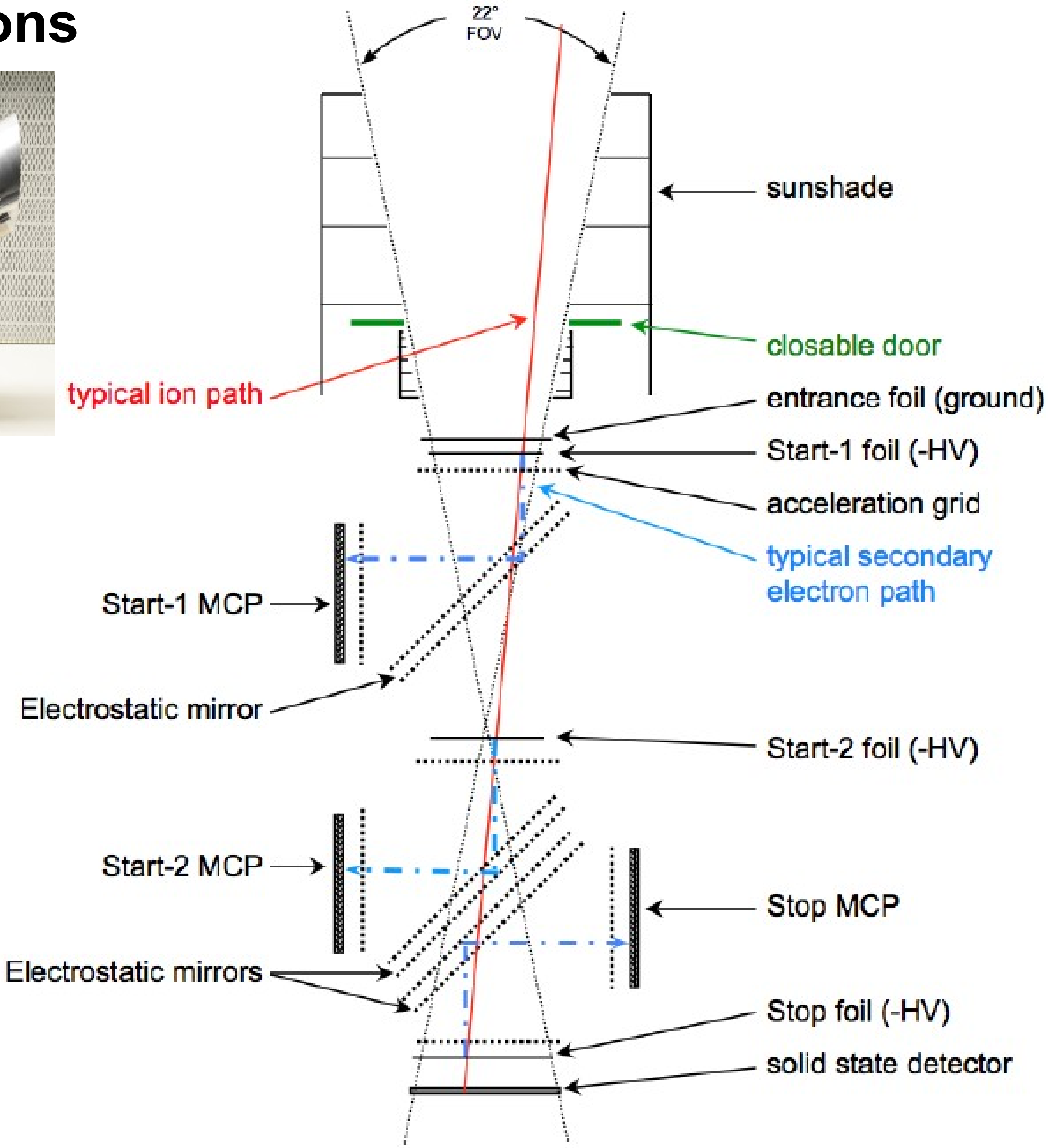

SIS on Solar Orbiter
Measures:
- multiple ToF
- total energy

Excellent ToF resolution allows isotope separation!

Elemental and isotopic resolution of SIS

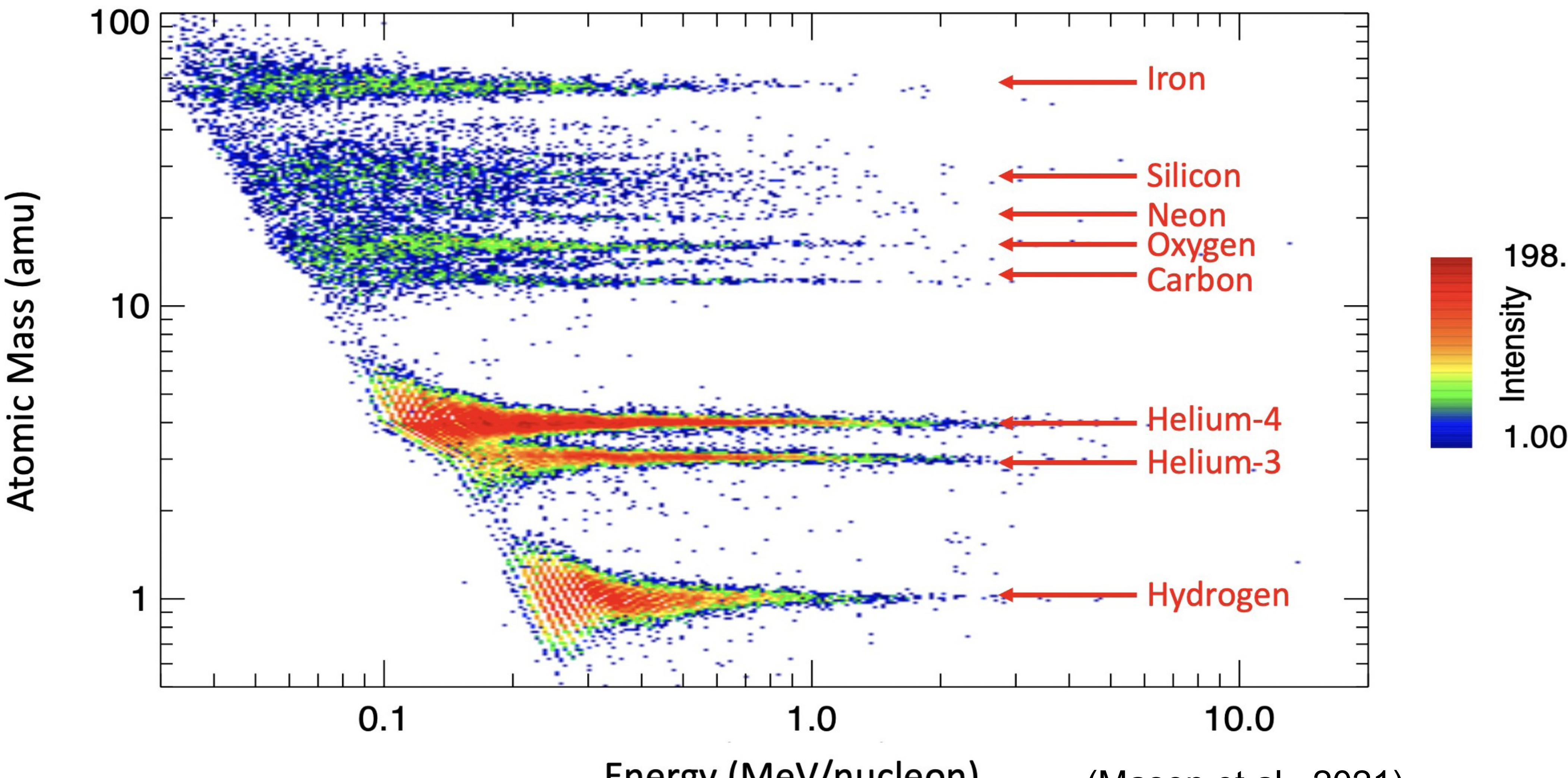

(Mason et al., 2021)

Measuring high-energy ions & electrons: The High-Energy Telescope (HET)

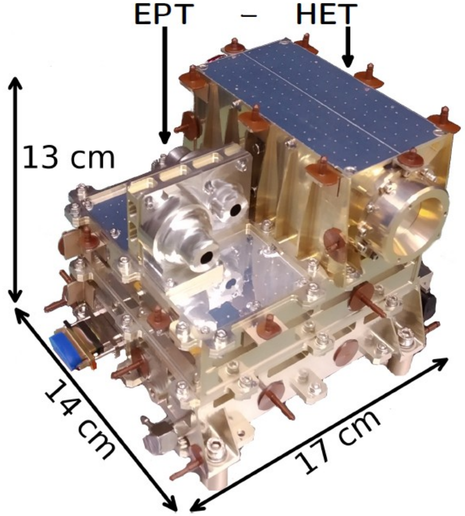

Multiple dE/dx vs. total E measurement allows element and isotope resolution

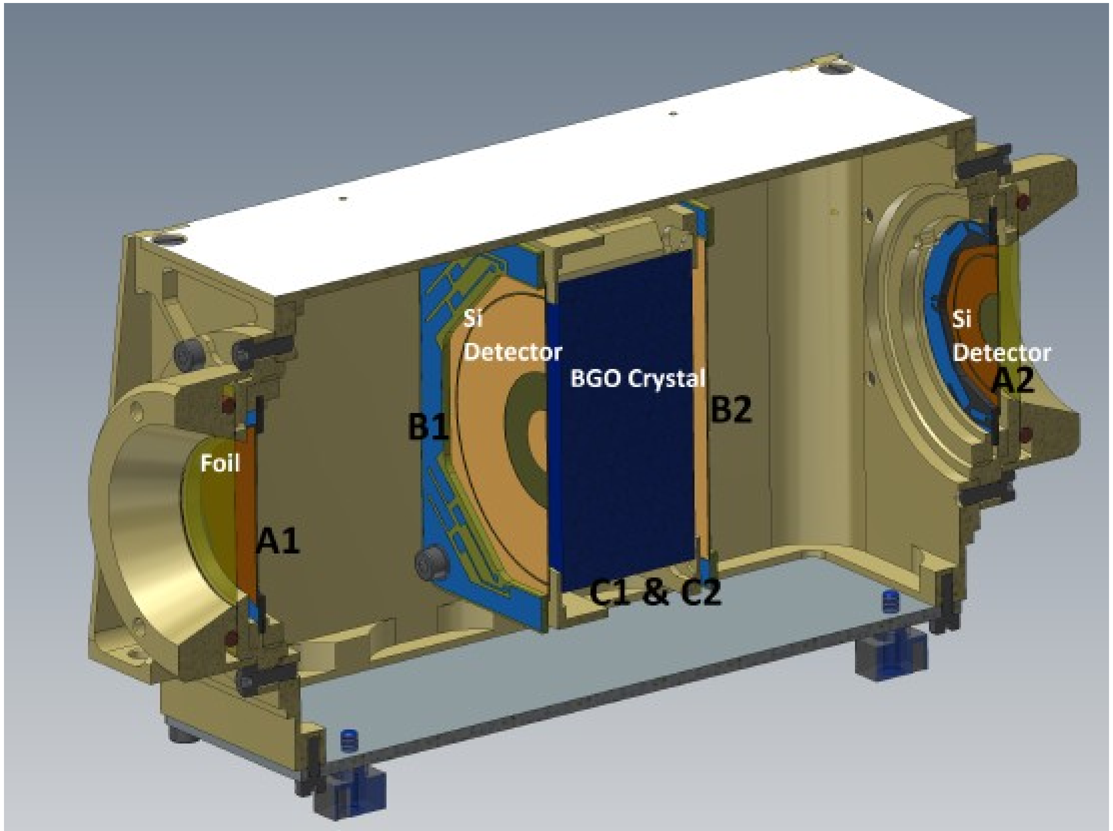

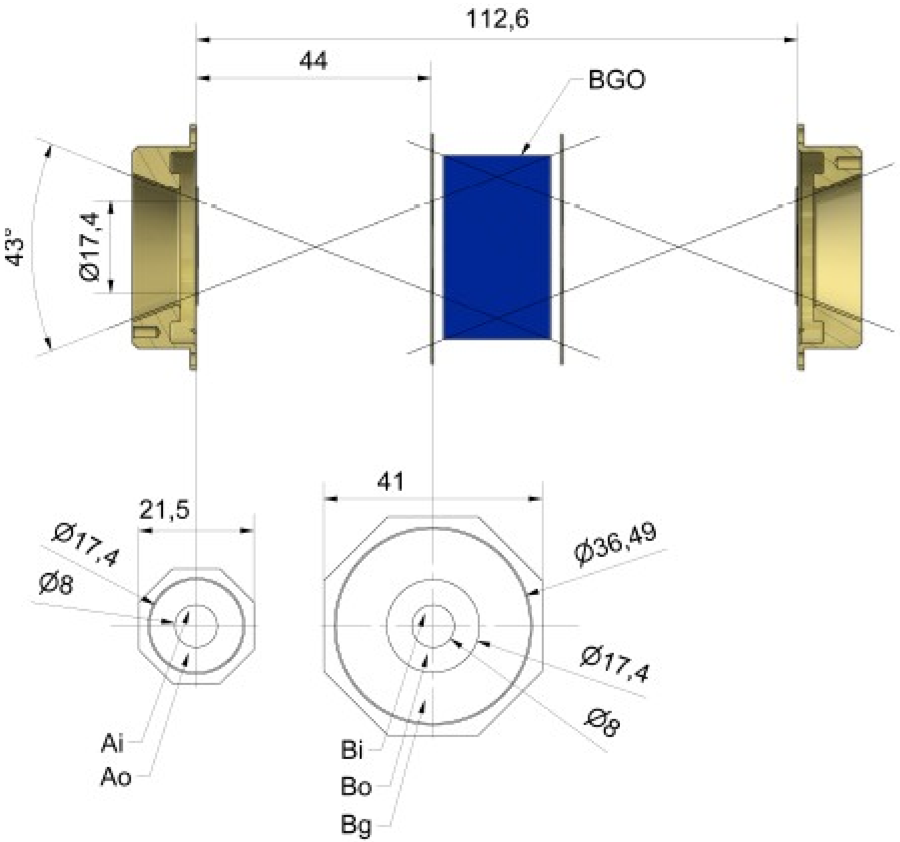

(Rodriguez-Pacheco et al., 2020)

Interaction of charged radiation with matter

- „Ionizing radiation“:
  - Collisions with electrons

- Other interactions (not necessarily ionizing):
  - Collisions with nuclei
  - Nuclear reactions
  - Excitation of phonons

Reactions need to be described by cross sections, but some analytic approximations are sometimes helpful. The most important is the one by Bethe, Bloch, Lindhard, and Schjott.

Interaction of charged radiation with matter

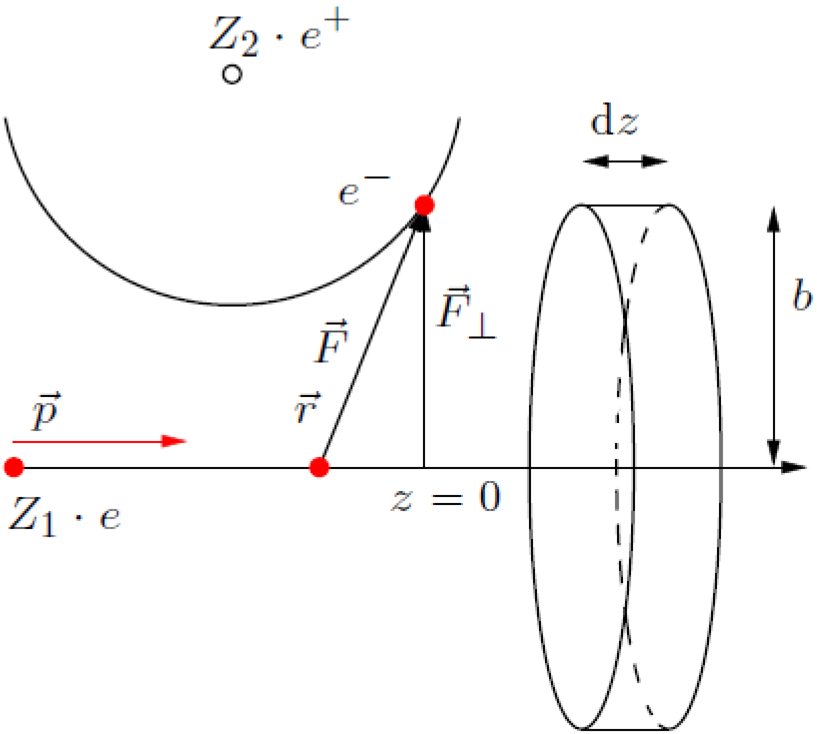

Force on electron is

$$\vec{F} = \frac{Z_1 e^2}{4\pi\varepsilon_0(z^2+b^2)}\frac{\vec{r}}{r}.$$

Momentum transfer is:

$$\Delta p = \int_{-\infty}^{+\infty} F\mathrm{d}t = \int_{-\infty}^{+\infty} F_\perp \mathrm{d}t$$
$$= \frac{1}{v}\int_{-\infty}^{+\infty} F_\perp \mathrm{d}z = \frac{e}{v}\int_{-\infty}^{+\infty} E_\perp \mathrm{d}z.$$

Use Gauß' law $\int_A \vec{E}\cdot\mathrm{d}\vec{A} = 2\pi b\int E_\perp \mathrm{d}z = Q/\varepsilon_0 = Z_1 e/\varepsilon_0.$

and obtain momentum and energy transfer.

$$\Delta p = \frac{1}{2\pi\varepsilon_0}\cdot\frac{Z_1 e^2}{vb},$$

$$\Delta\epsilon = \frac{\Delta p^2}{2m_e} = \frac{1}{8\pi^2\varepsilon_0^2 m_e}\cdot\left(\frac{Z_1 e^2}{vb}\right)^2.$$

Ionizing energy loss of charged particles in matter: Bethe-Bloch

$$\frac{\mathrm{d}E}{\mathrm{d}x} = -\frac{Z_1^2 e^4 n_e}{4\pi \cdot \varepsilon_0^2 v^2 m_e} \cdot \left[\ln\left(\frac{2 m_e v^2}{\langle E_B \rangle}\right) - \ln(1-\beta^2) - \beta^2\right],$$ where $\beta = v/c$.

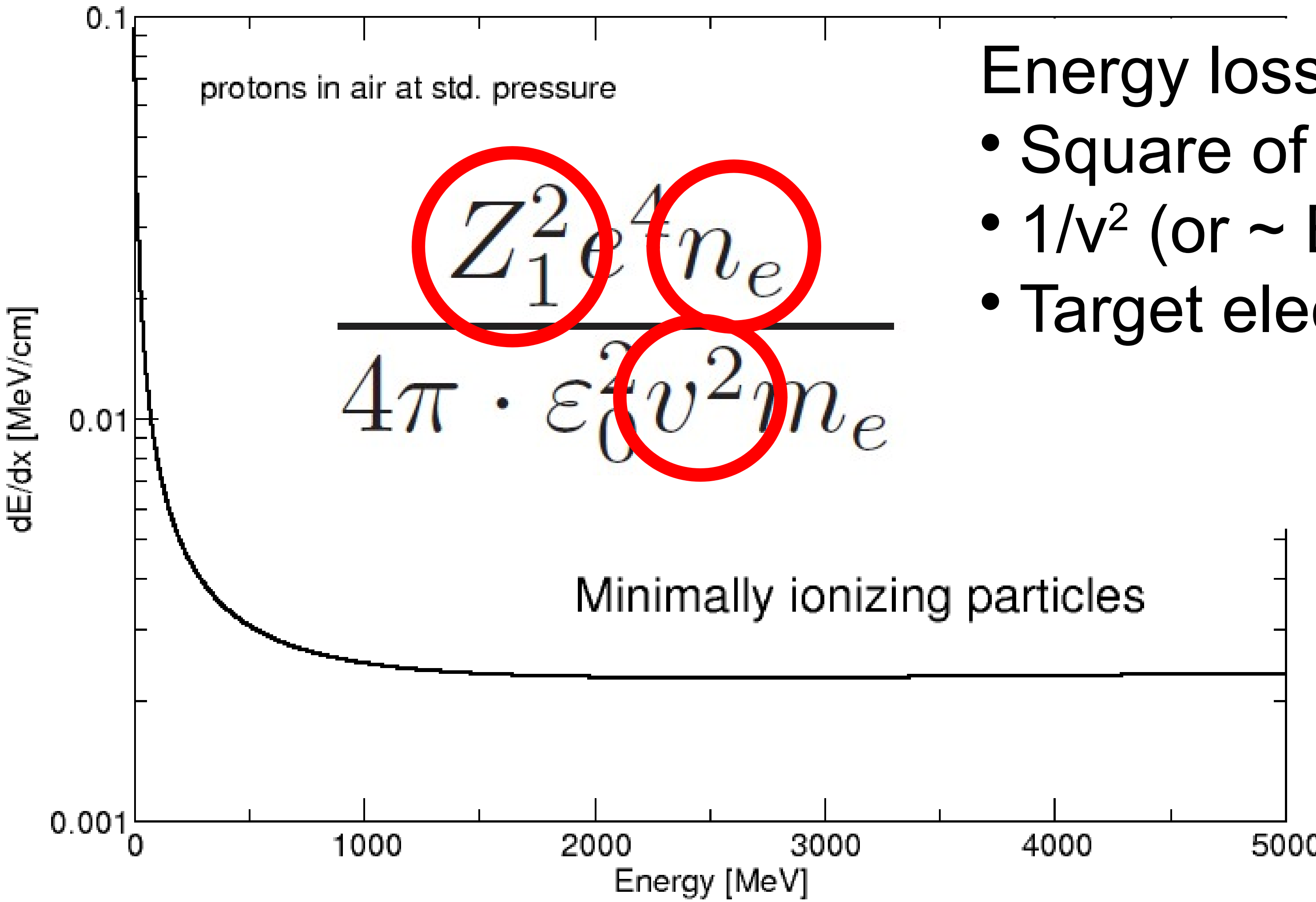

$$\frac{Z_1^2 e^4 n_e}{4\pi \cdot \varepsilon_0^2 v^2 m_e}$$

Energy loss goes with:

- Square of projectile charge
- $1/v^2$ (or ~ E/m) of projectile
- Target electron density

Ionizing energy loss of charged particles in matter: Bethe-Bloch

$$\frac{\mathrm{d}E}{\mathrm{d}x} = -\frac{Z_1^2 e^4 n_e}{4\pi \cdot \varepsilon_0^2 v^2 m_e} \cdot \left[\ln\left(\frac{2 m_e v^2}{\langle E_B \rangle}\right) - \ln(1-\beta^2) - \beta^2\right],$$ where $\beta = v/c$.

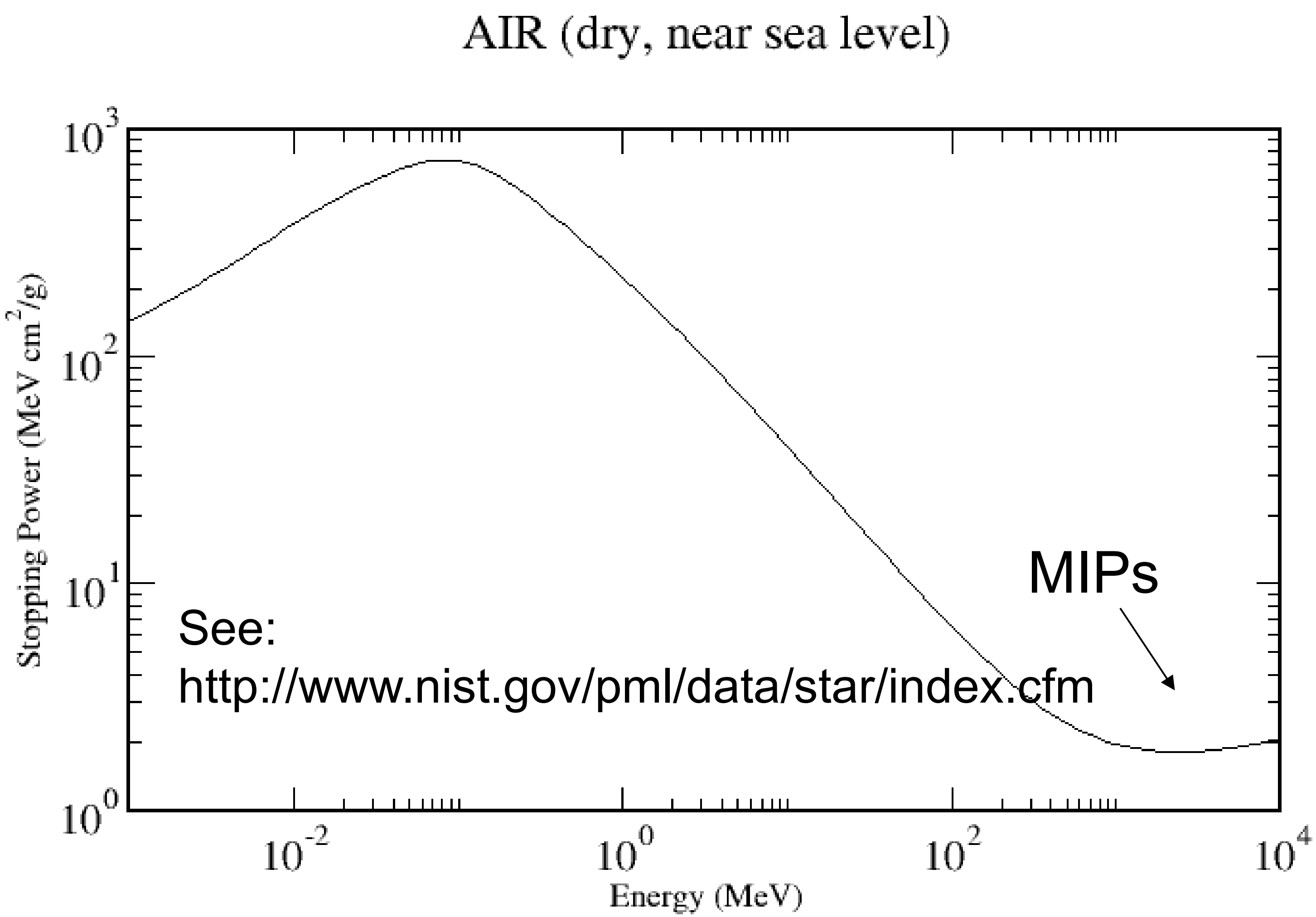

See: http://www.nist.gov/pml/data/star/index.cfm

You can calculate the stopping power at NIST for all sorts of combinations of projectile and target materials.

Energy loss of charged particles in matter

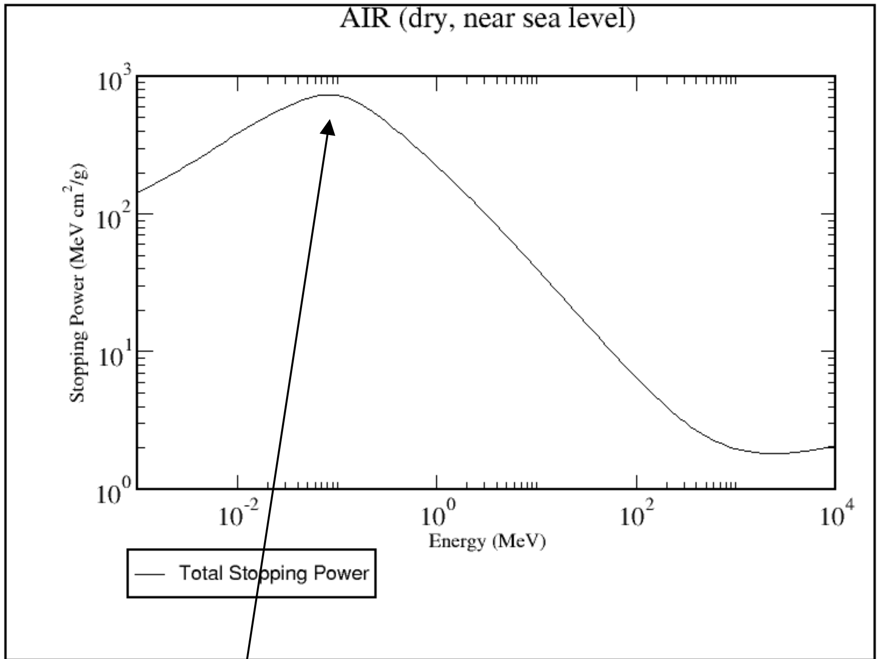

So energy loss is given as MeV/(g/cm^2).

What does that mean?

Multiply by density, ^ = g/cm3 to obtain

dE/dx in units of MeV/cm.

Air: 1kg/m^3 = 1mg/cm^3

So 10^3 MeV/(g/cm^2) = 1 MeV/cm. Compare this to binding energy of N_2 molecules of 15.6 eV. In fact, ions will also loose energy to nuclei, so 37 eV is the correct number to be used for $\langle E_B \rangle$.

Ionizing radiation ionizes air!

Energy loss of charged particles in matter: Deposition profile – The Bragg Peak

$$\frac{\mathrm{d}E}{\mathrm{d}x} = -\frac{Z_1^2 e^4 n_e}{4\pi \cdot \varepsilon_0^2 v^2 m_e} \cdot \left[\ln\left(\frac{2 m_e v^2}{\langle E_B \rangle}\right) - \ln(1-\beta^2) - \beta^2\right],$$ where $\beta = v/c$.

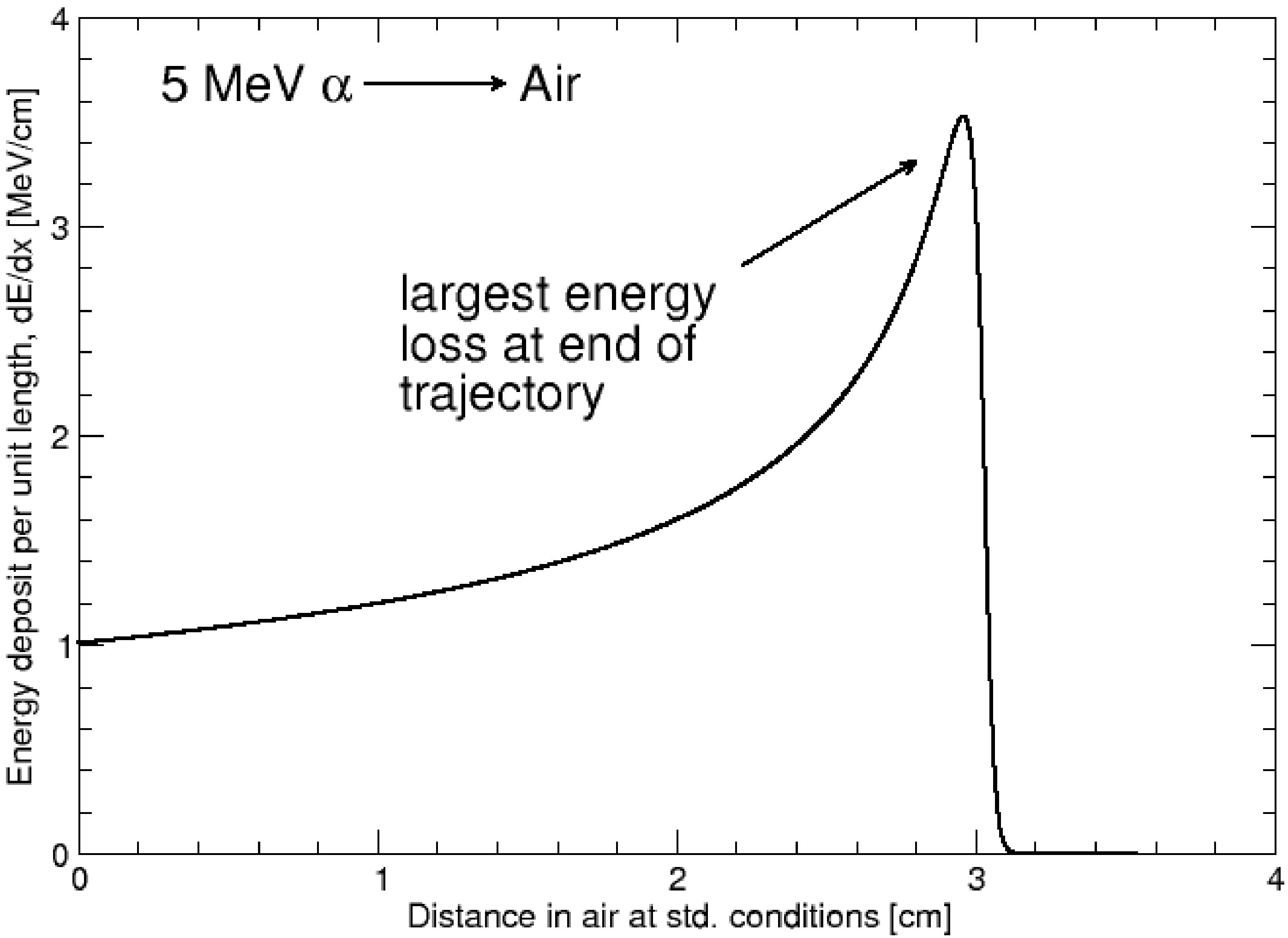

Because a particle looses more energy when it has less energy, it looses most of its energy at the end of its trajectory.

5 MeV ¬⅄ particle only penetrates few cm of air.

Elemental and isotopic resolution of HET

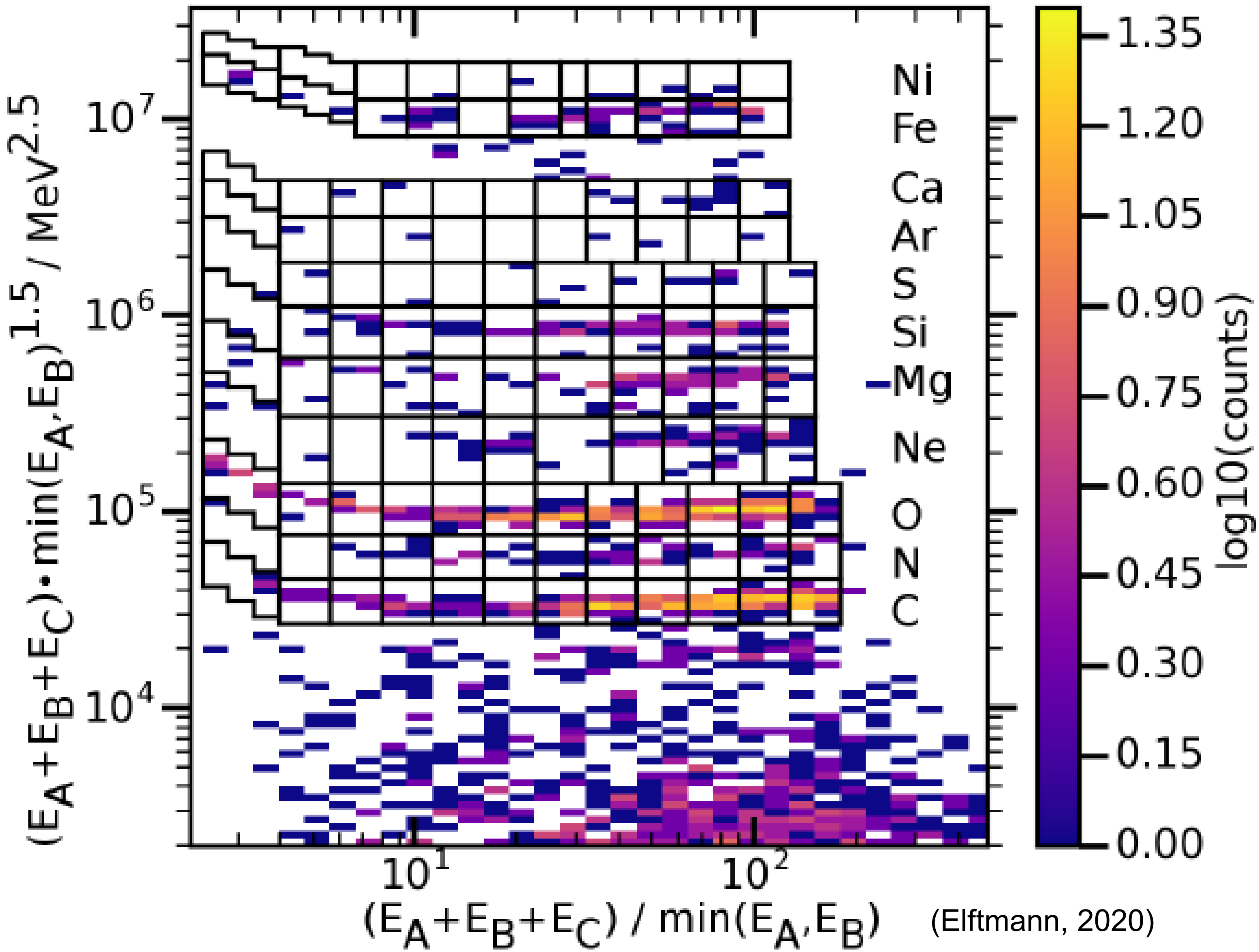

(Elftmann, 2020)

Elemental and isotopic resolution of SIS & HET

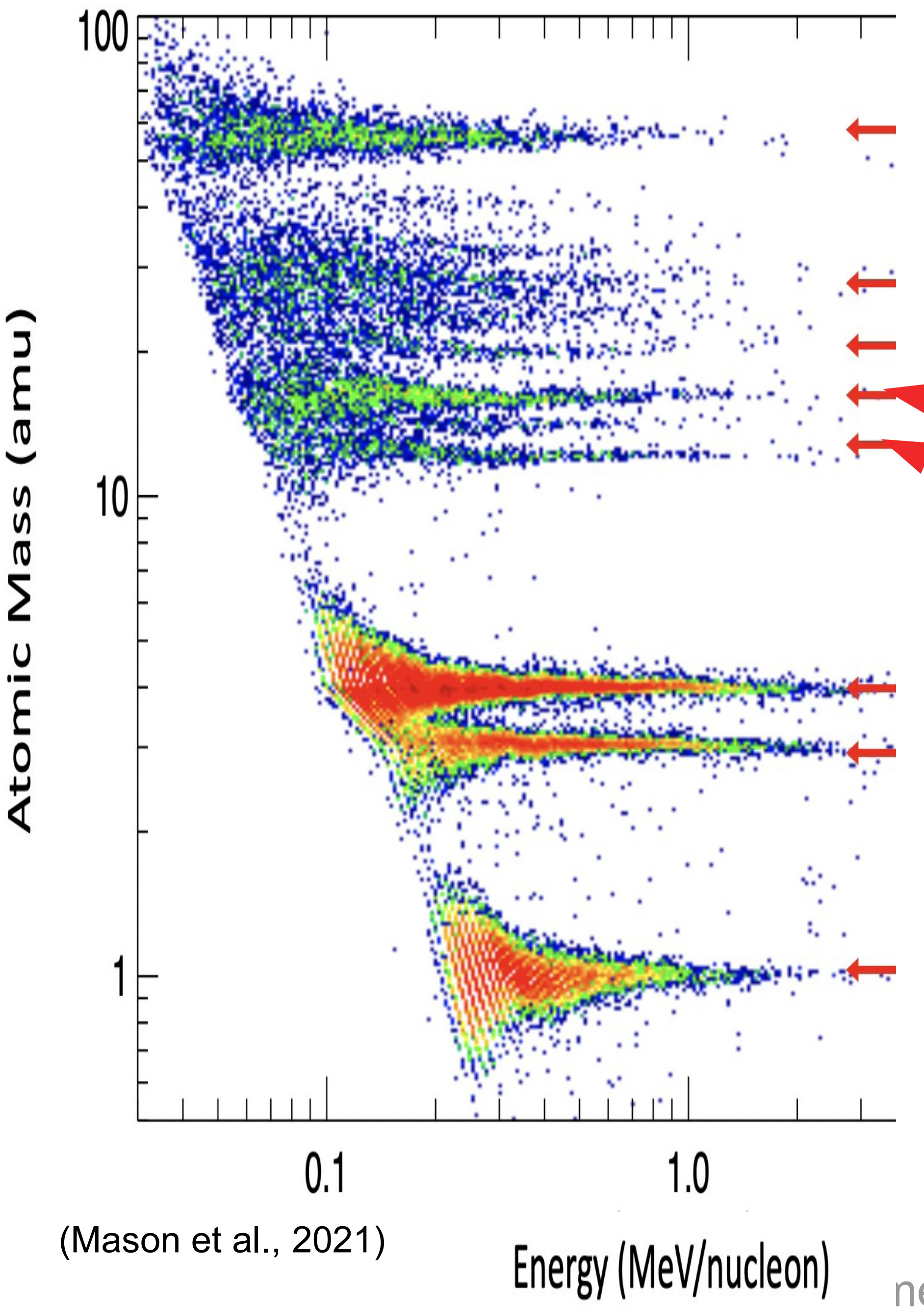

(Mason et al., 2021)

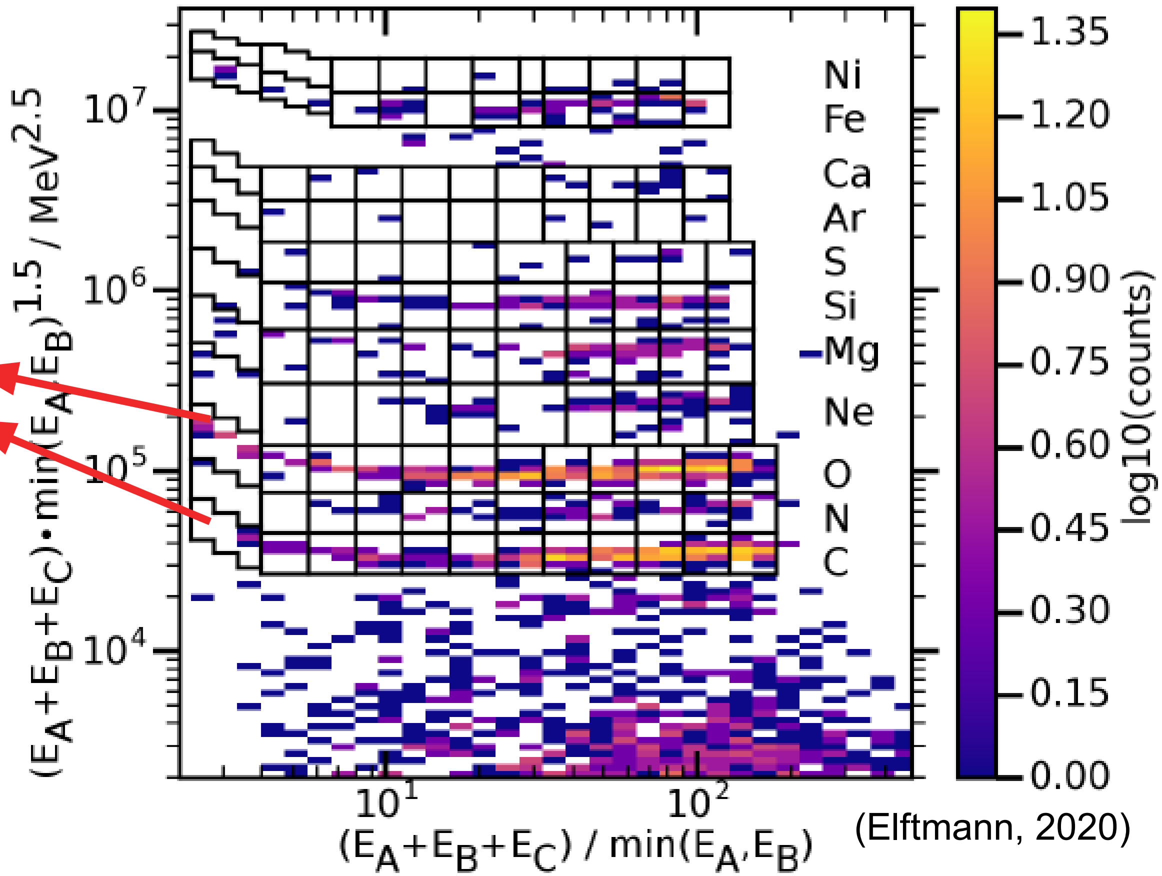

(Elftmann, 2020)

Combined spectra from SIS and HET show good agreement

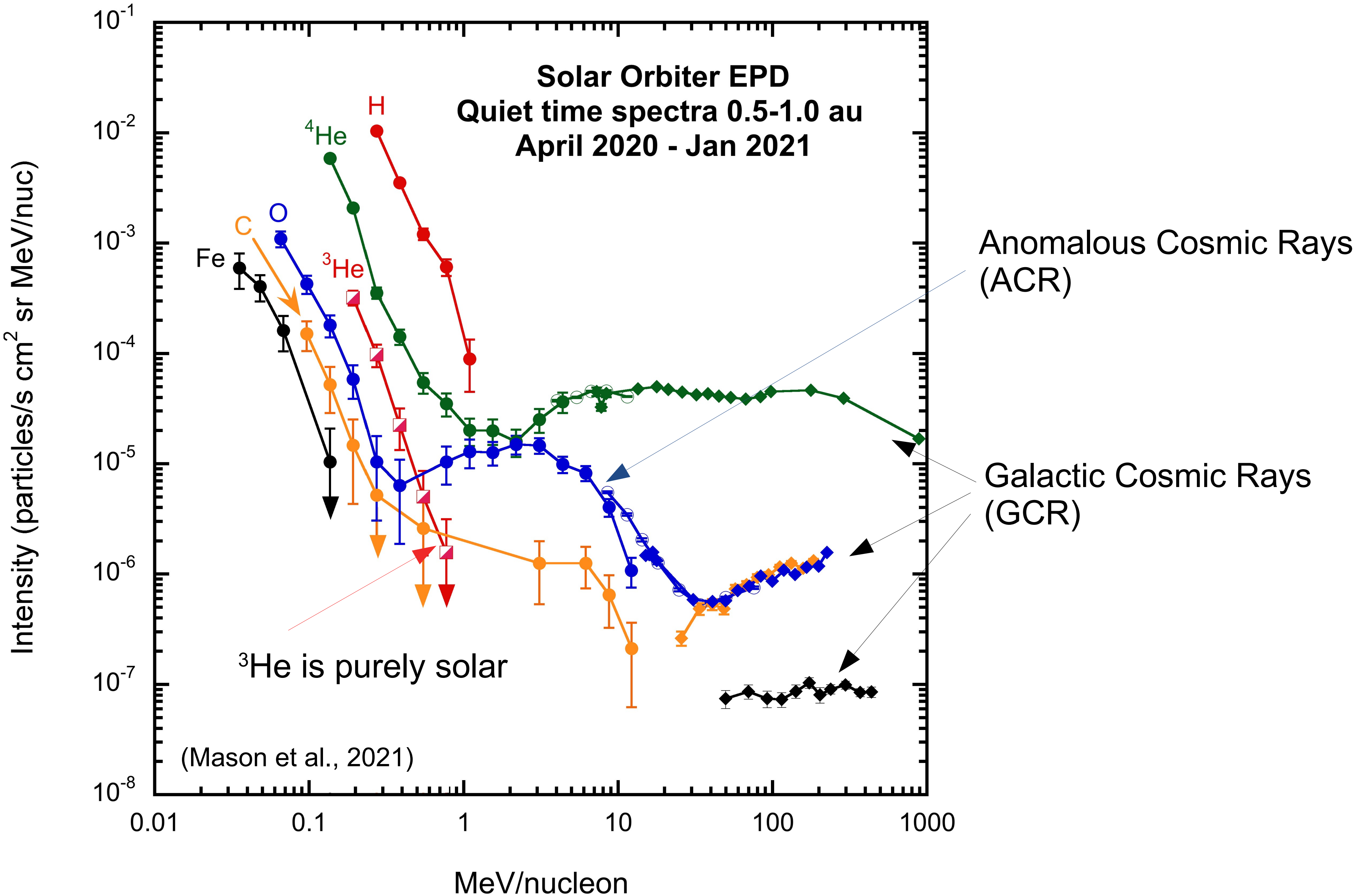

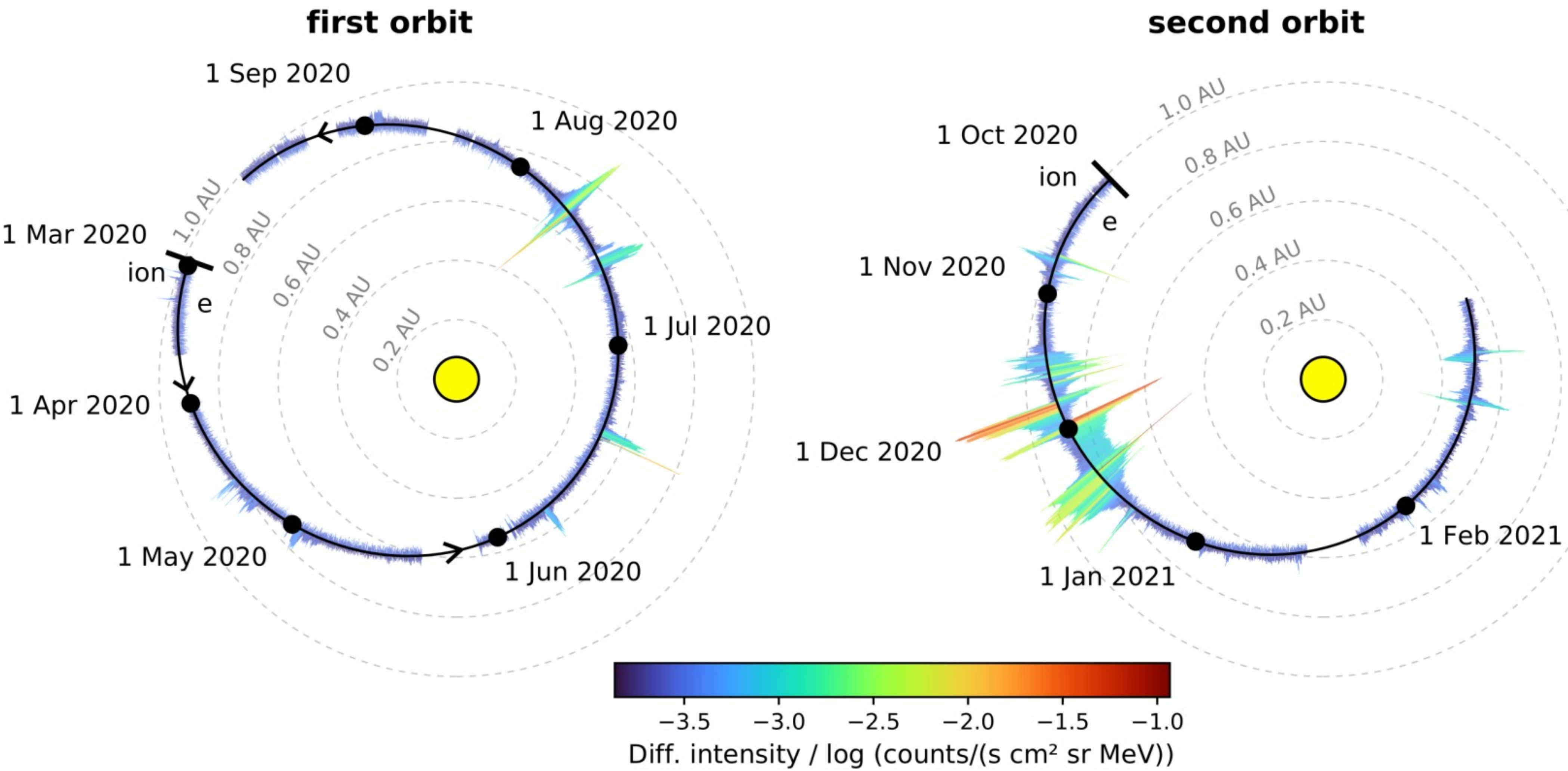
first orbit
second orbit
1 Sep 2020
1 Aug 2020
1 Mar 2020
ion
e
1 Jul 2020
1 Apr 2020
1 May 2020
1 Jun 2020
1.0 AU
0.8 AU
0.6 AU
0.4 AU
0.2 AU
1 Oct 2020
1 Nov 2020
1 Dec 2020
1 Jan 2021
1 Feb 2021
−3.5
−3.0
−2.5
−2.0
−1.5
−1.0
Diff. intensity / log (counts/(s cm² sr MeV))

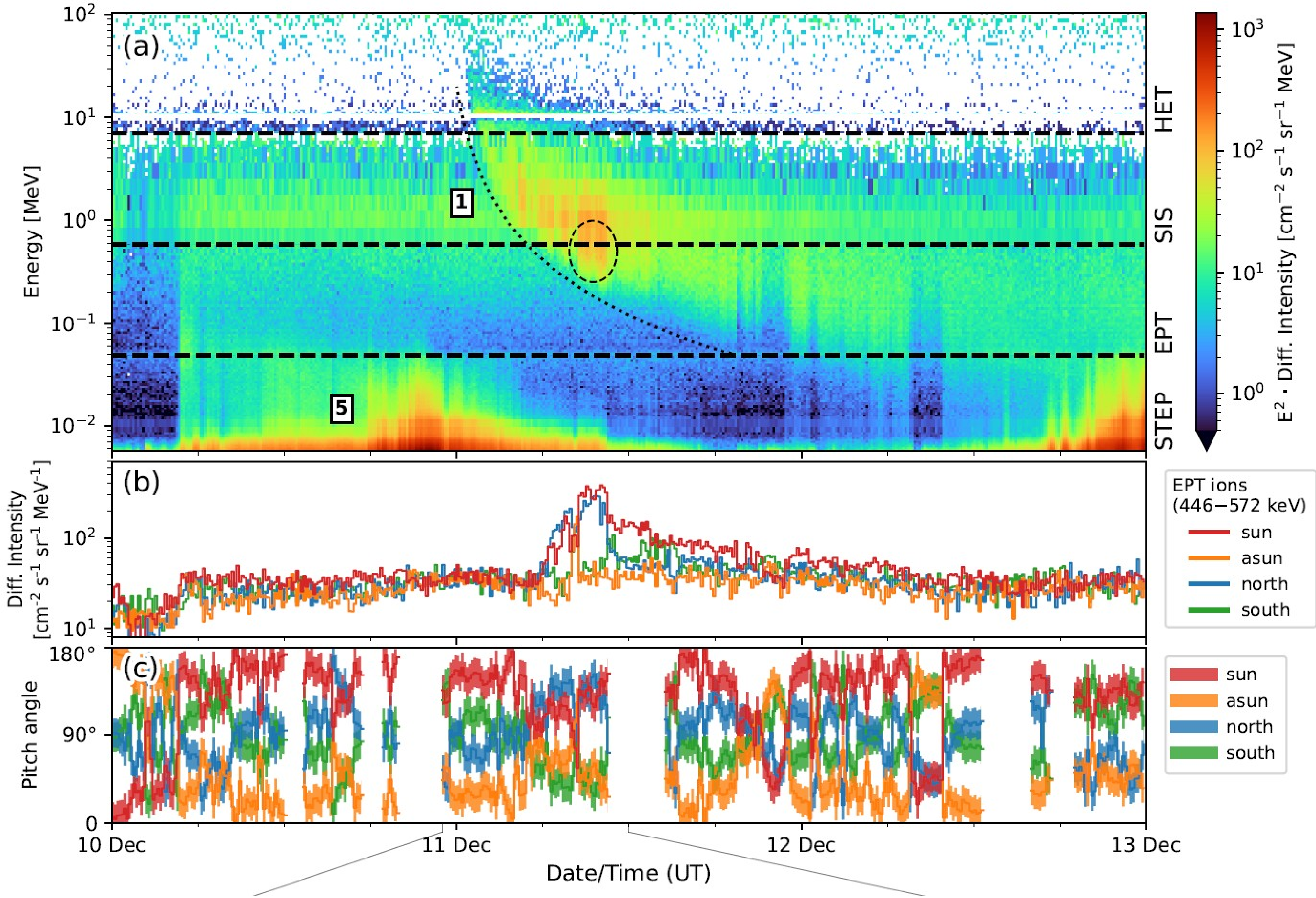
(a)
(b)
(c)
Energy [MeV]
10^2
10^1
10^0
10^{-1}
10^{-2}
1
5
HET
SIS
EPT
STEP
10^3
10^2
10^1
10^0
$E^2 \cdot$ Diff. Intensity [cm^{-2} s^{-1} sr^{-1} MeV]
Diff. Intensity [cm^{-2} s^{-1} sr^{-1} MeV^{-1}]
10^2
10^1
EPT ions (446−572 keV)
sun
asun
north
south
Pitch angle
180°
90°
0
sun
asun
north
south
10 Dec
11 Dec
12 Dec
13 Dec
Date/Time (UT)

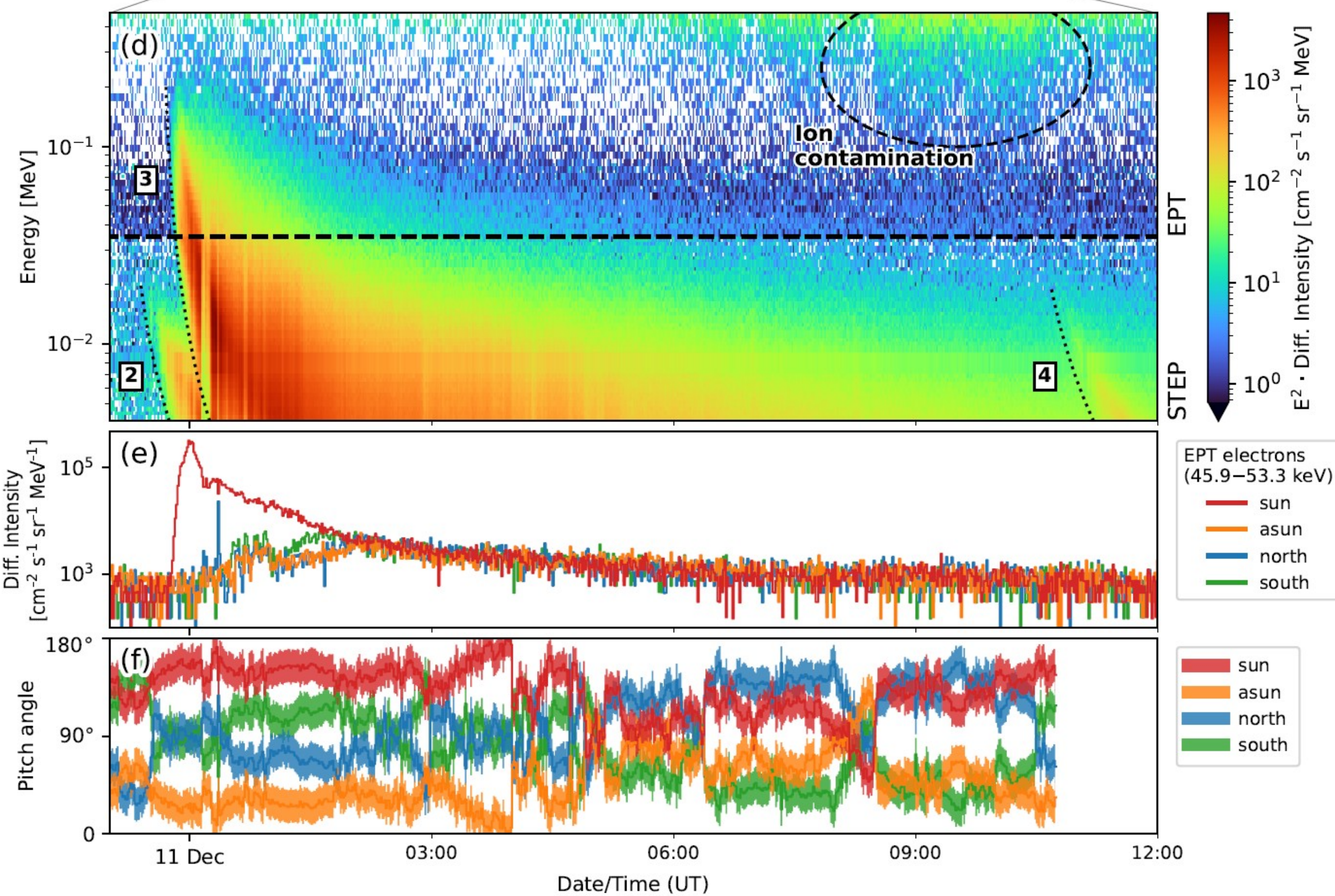
(d)
Ion contamination
3
2
4
EPT
STEP
Energy [MeV]
E² · Diff. Intensity [cm⁻² s⁻¹ sr⁻¹ MeV]
(e)
Diff. Intensity [cm⁻² s⁻¹ sr⁻¹ MeV⁻¹]
EPT electrons (45.9−53.3 keV)
sun
asun
north
south
(f)
Pitch angle
sun
asun
north
south
11 Dec
03:00
06:00
09:00
12:00
Date/Time (UT)

Electron pitch-angle distribution for the December 2020 event.

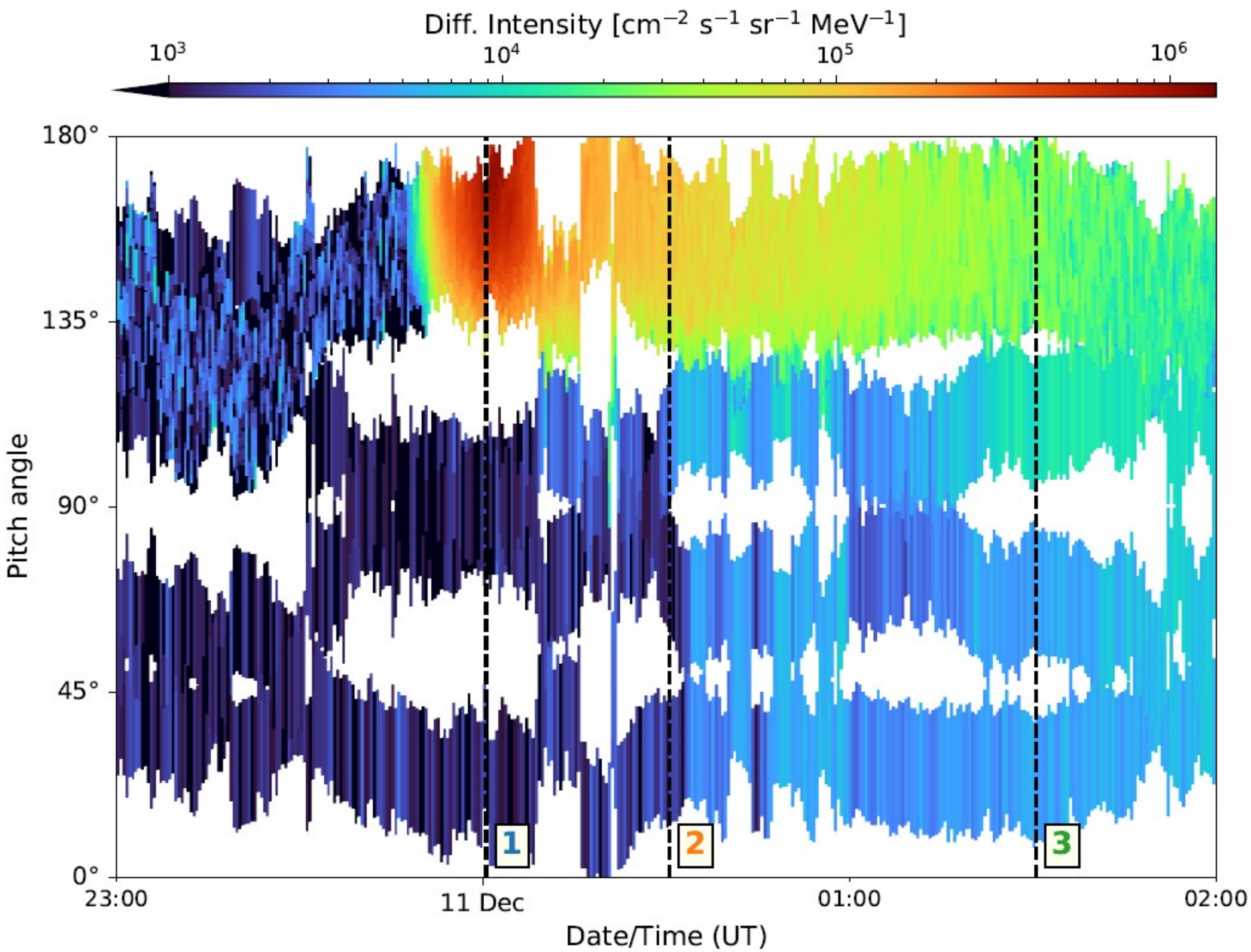

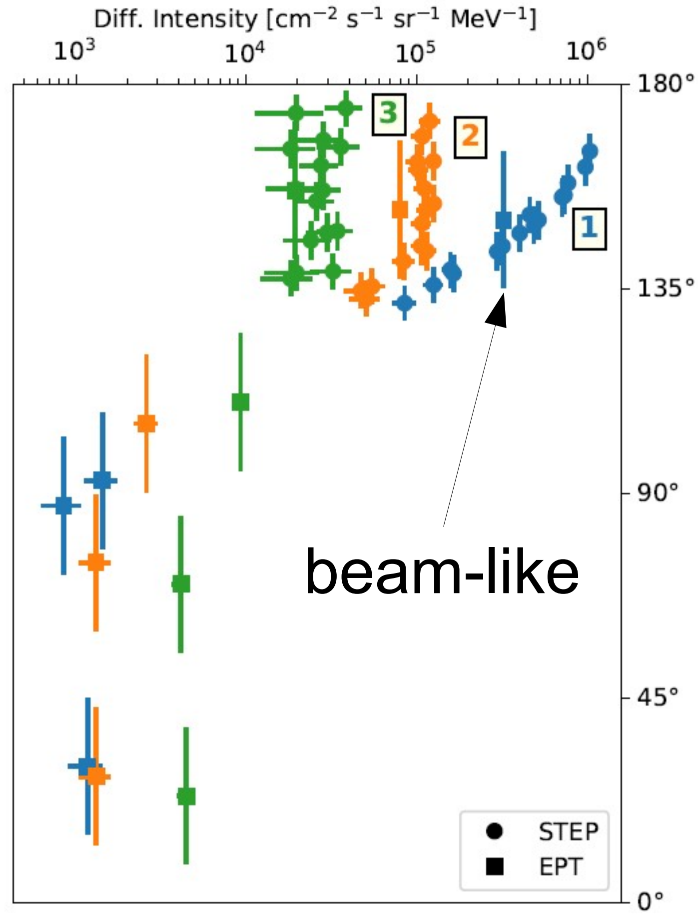

SupraThermal Electrons & Protons (STEP)

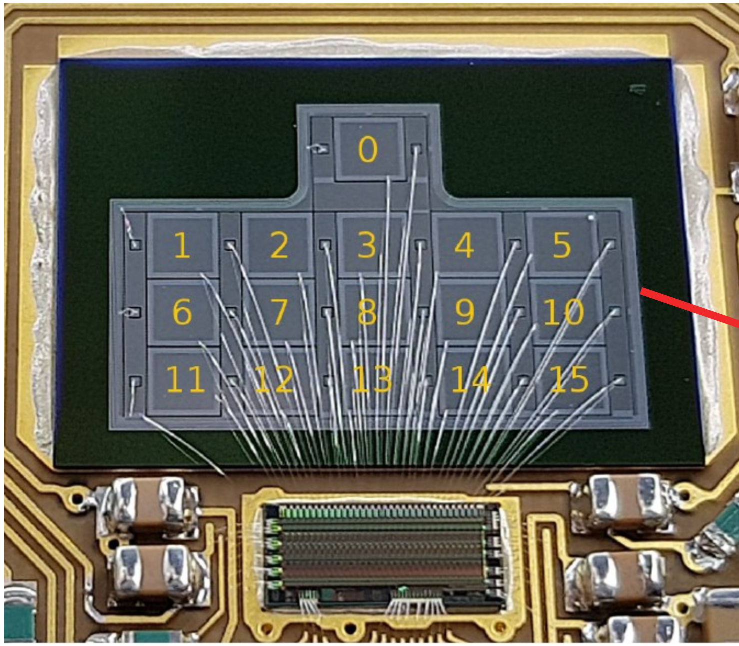

Integral channel:
Measures electrons & ions

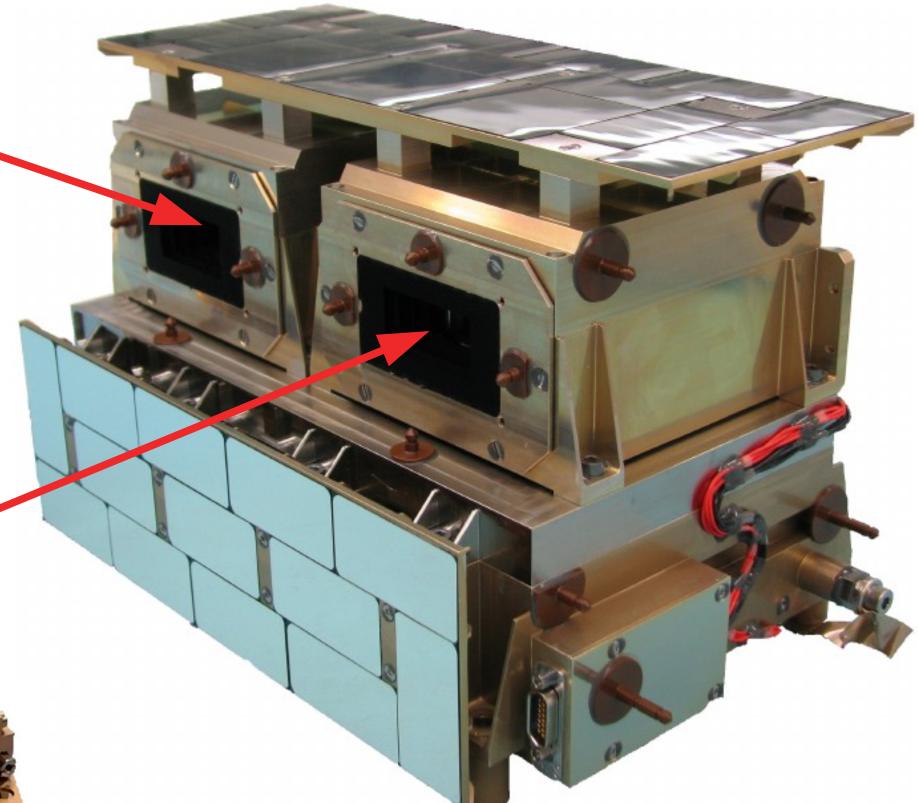

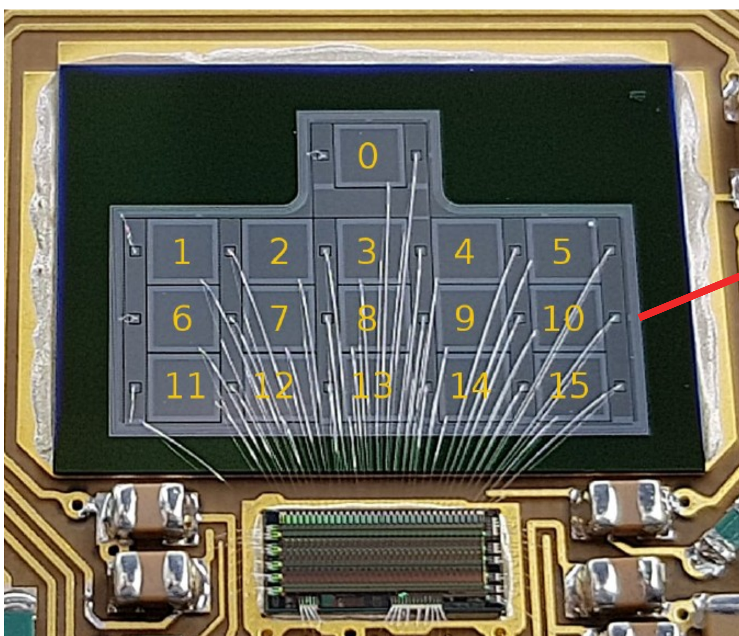

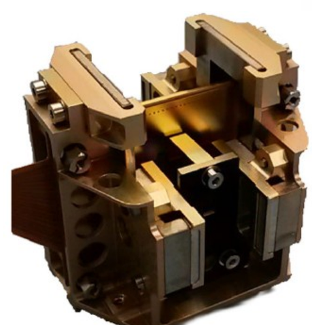

Magnet channel:
Deflects electrons,
measures ions

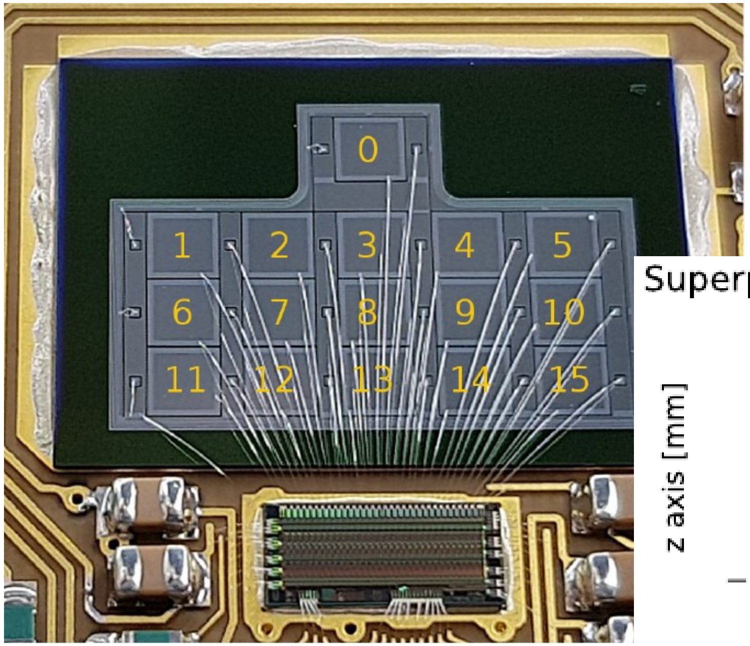

Integral channel:
Measures electrons & ions

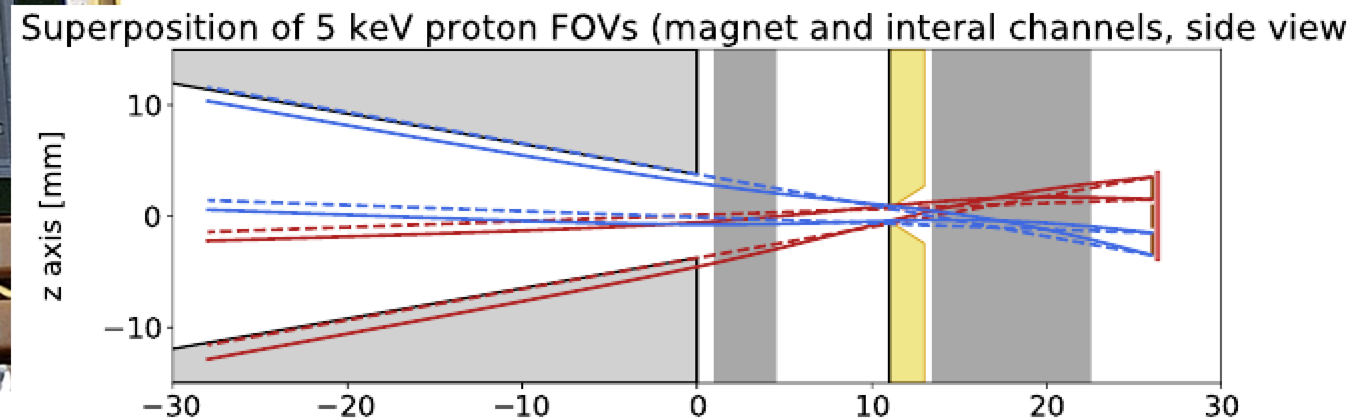

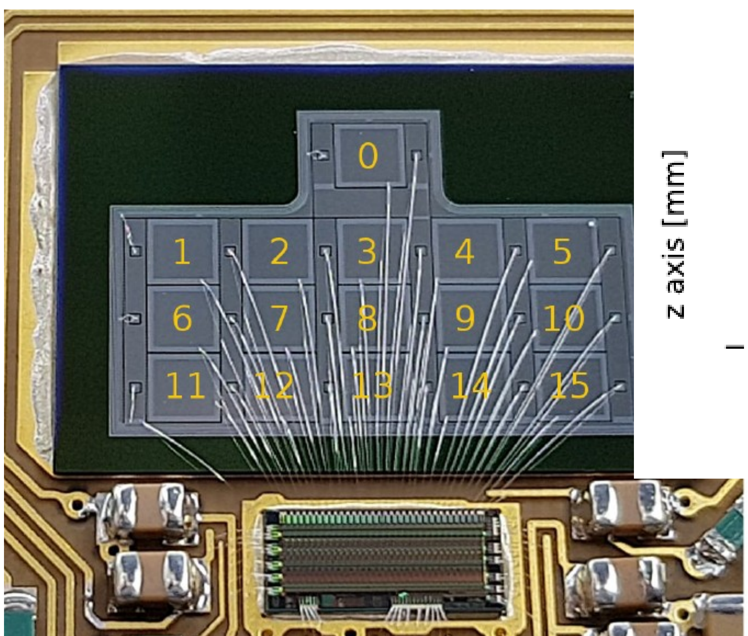

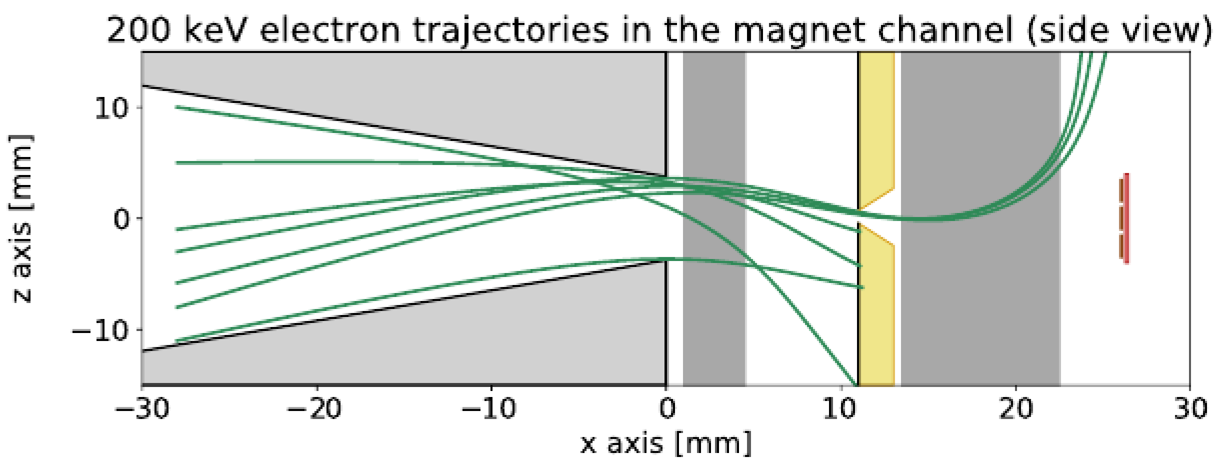

Magnet channel:
Deflects electrons, measures ions

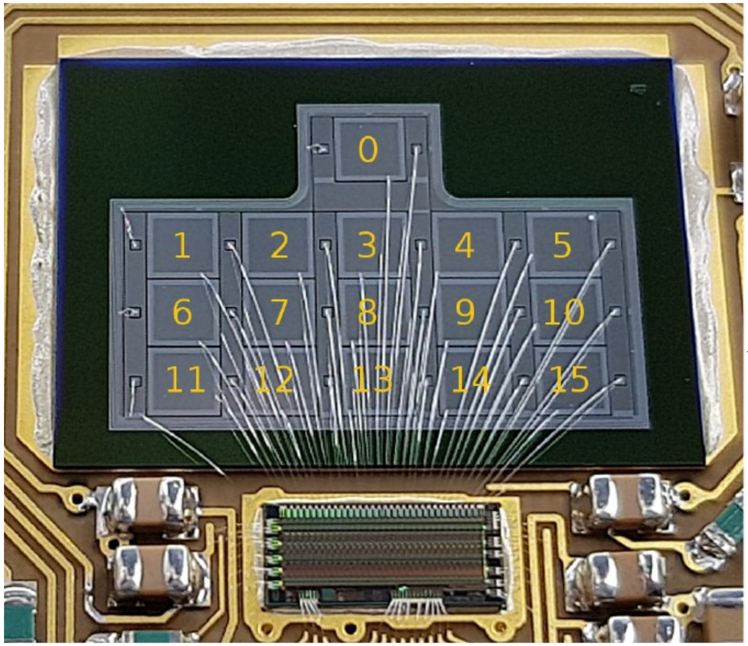

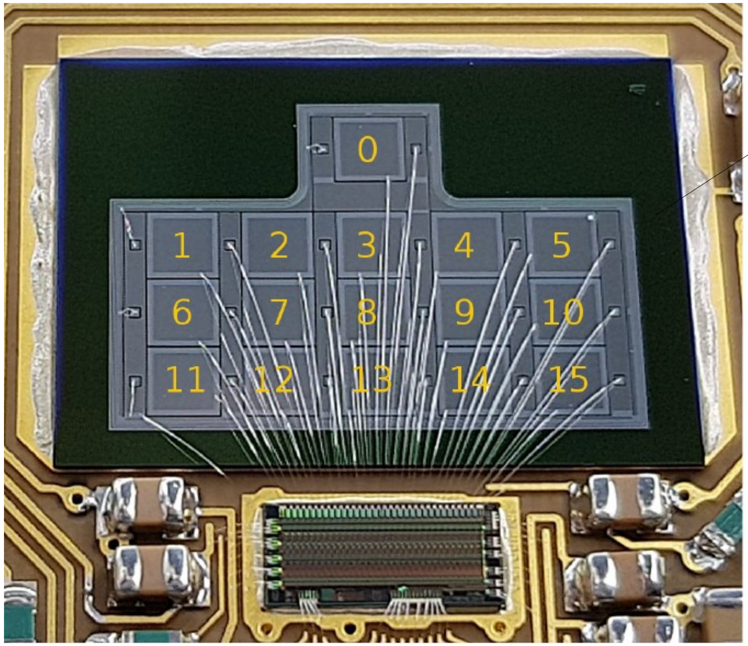

Integral channel:
Measures electrons & ions
Magnet channel:
Deflects electrons,
measures ions
„Int – Mag = electrons“

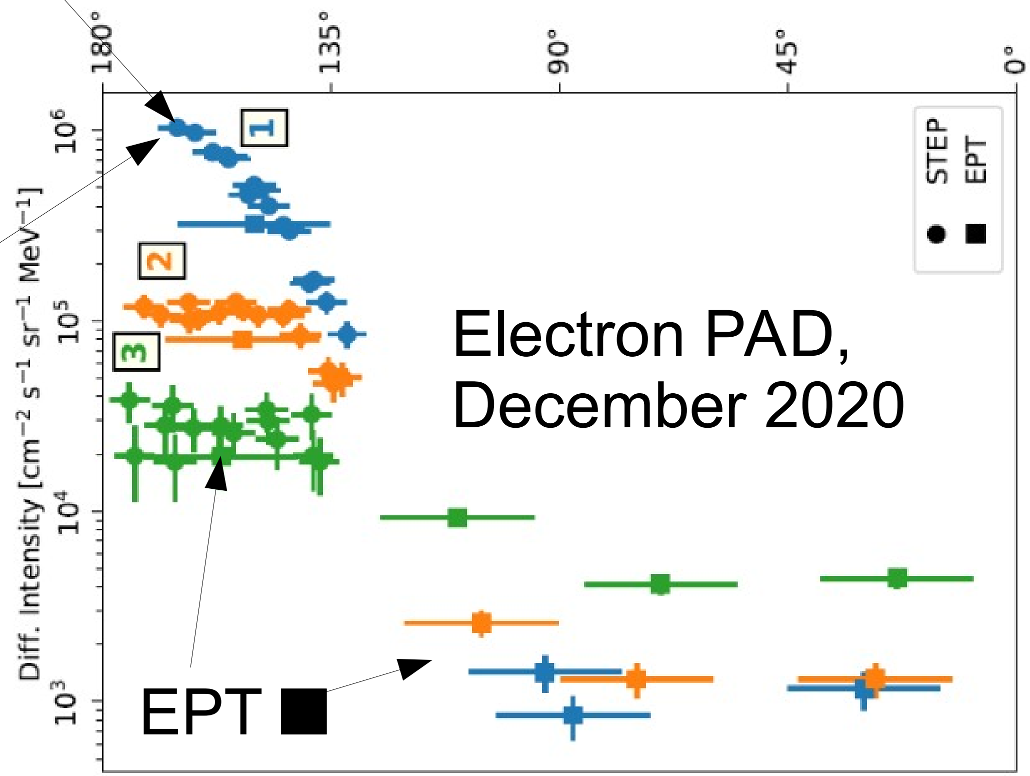

Summary suprathermal & energetic particles:

- injection

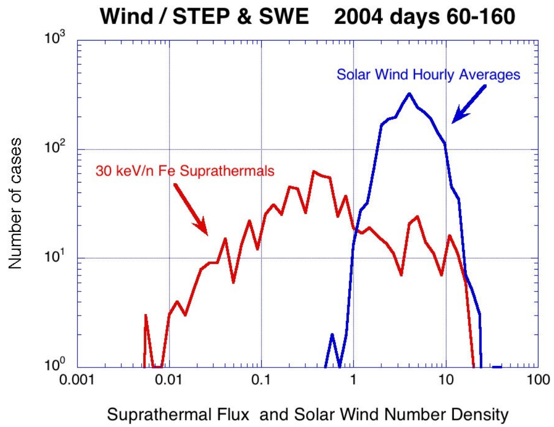

- acceleration

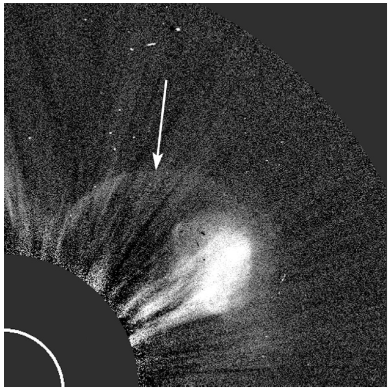

- transport

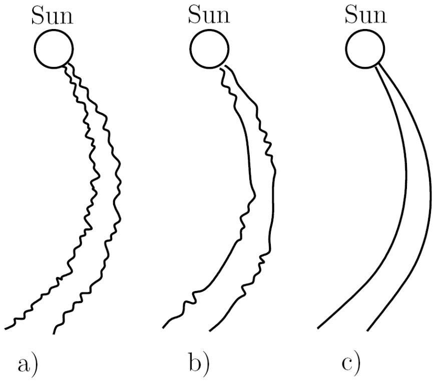

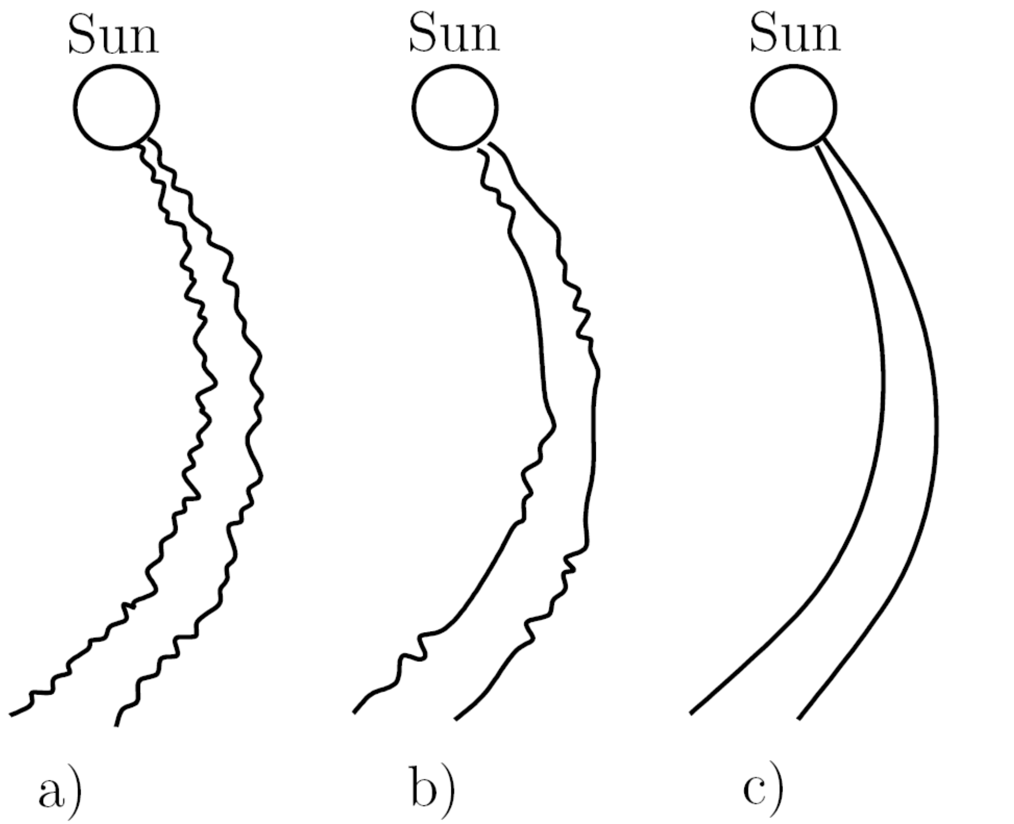

diffusive

focussed transport

scatter free

Part III

Interaction with Matter

–

Implications for Exploration!

Energy loss of charged particles in matter: Deposition profile – The Bragg Peak

$$\frac{\mathrm{d}E}{\mathrm{d}x} = -\frac{Z_1^2 e^4 n_e}{4\pi \cdot \varepsilon_0^2 v^2 m_e} \cdot \left[\ln\left(\frac{2 m_e v^2}{\langle E_B \rangle}\right) - \ln(1-\beta^2) - \beta^2 \right],$$ where $\beta = v/c$.

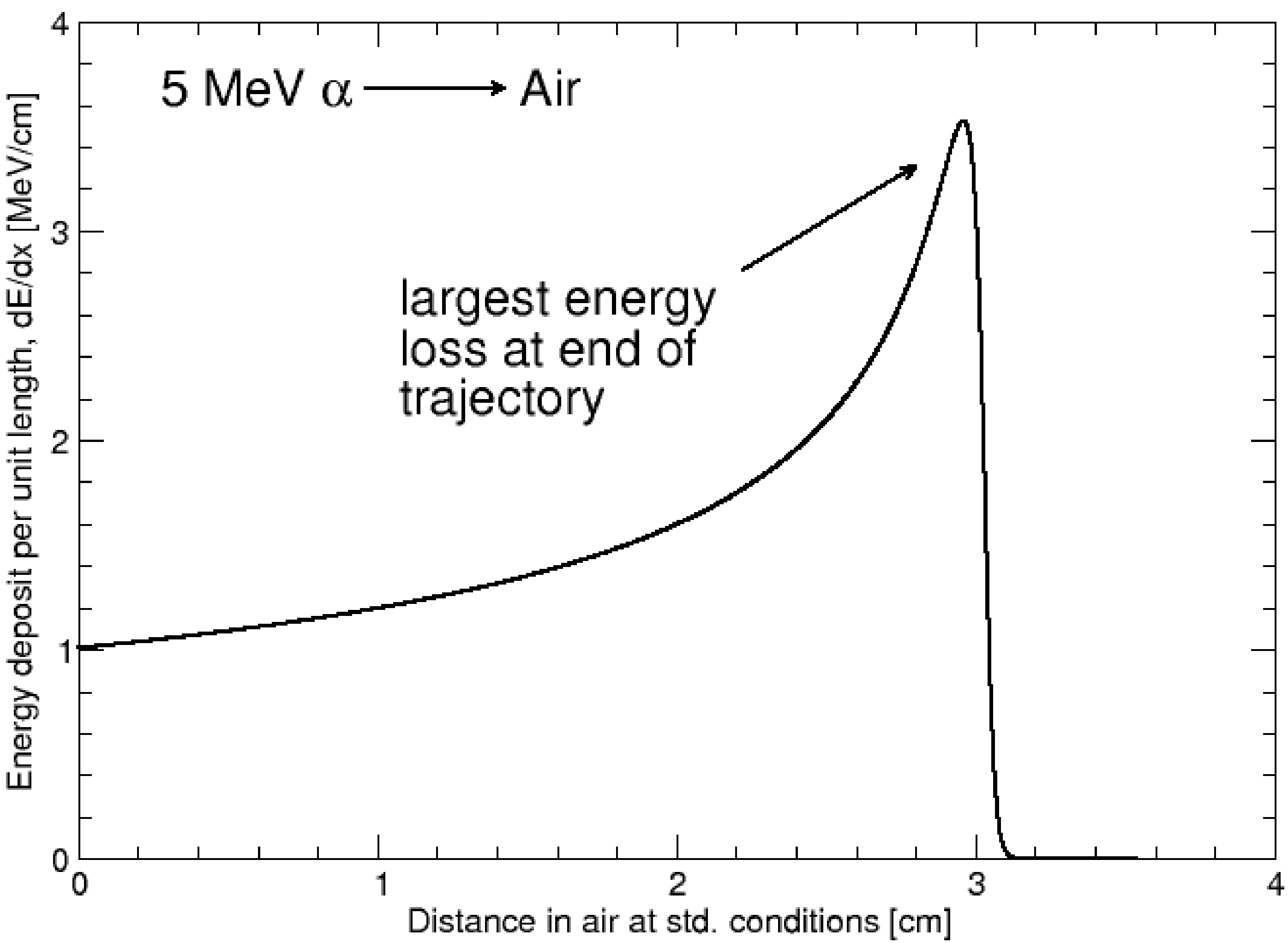

Because a particle looses more energy when it has less energy, it looses most of its energy at the end of its trajectory.

5 MeV ¬⅄ particle only penetrates few cm of air.

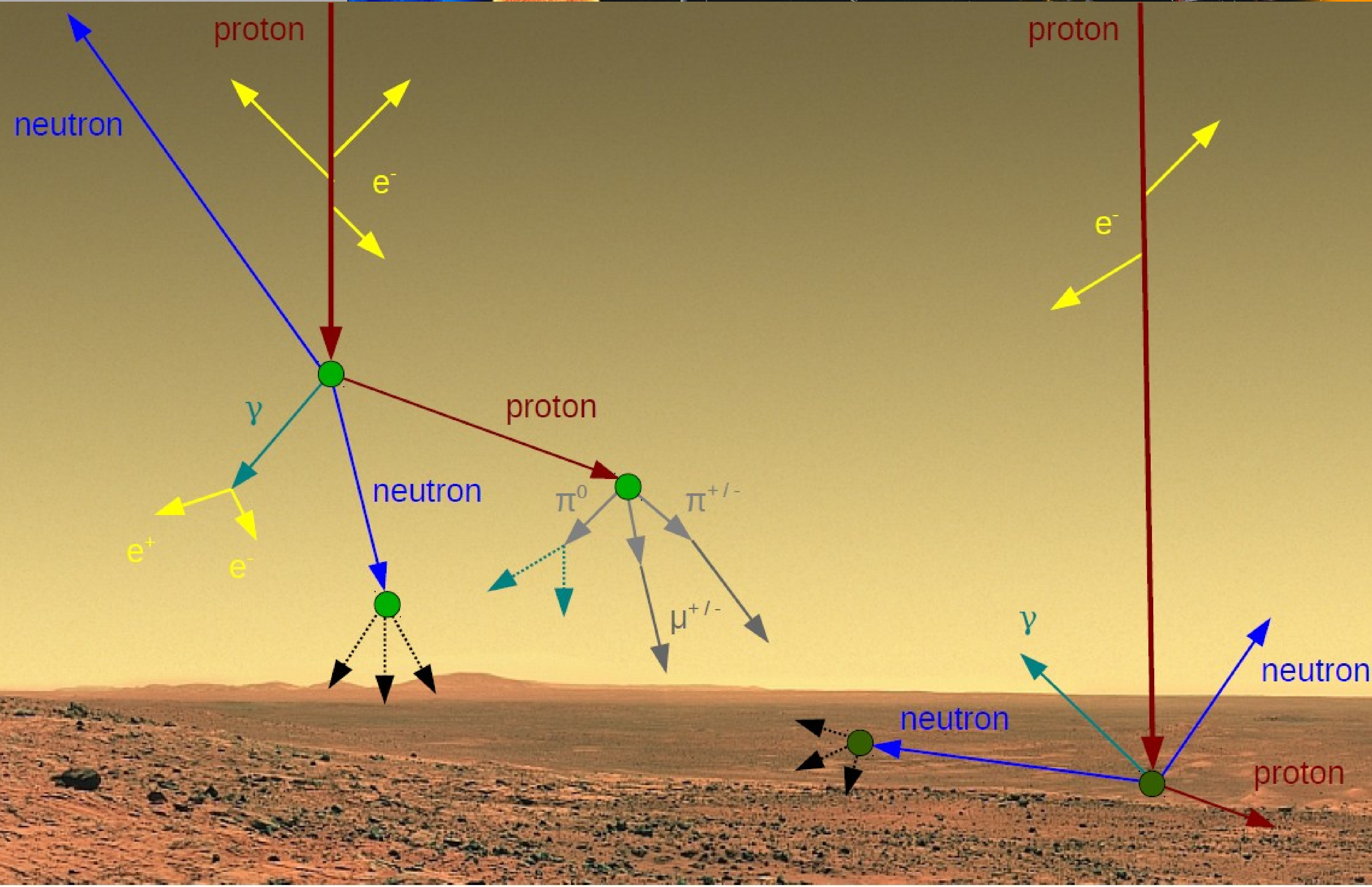

Secondary radiation (neutrals!) plays an important role! (Ehresmann, 2011)

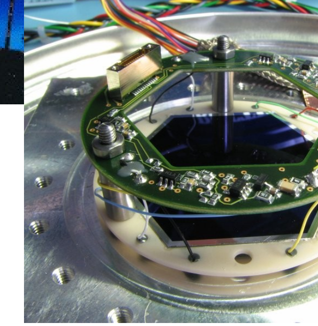

MSL's Radiation Assessment Detector (RAD)

Requirements:

- Charged particles (1 < Z < 27) up to 100 MeV/nuc
- Neutral particles (n, γ) up to 100 MeV
- LET
- Composition
- Time series
- Autonomous operations

Solution:

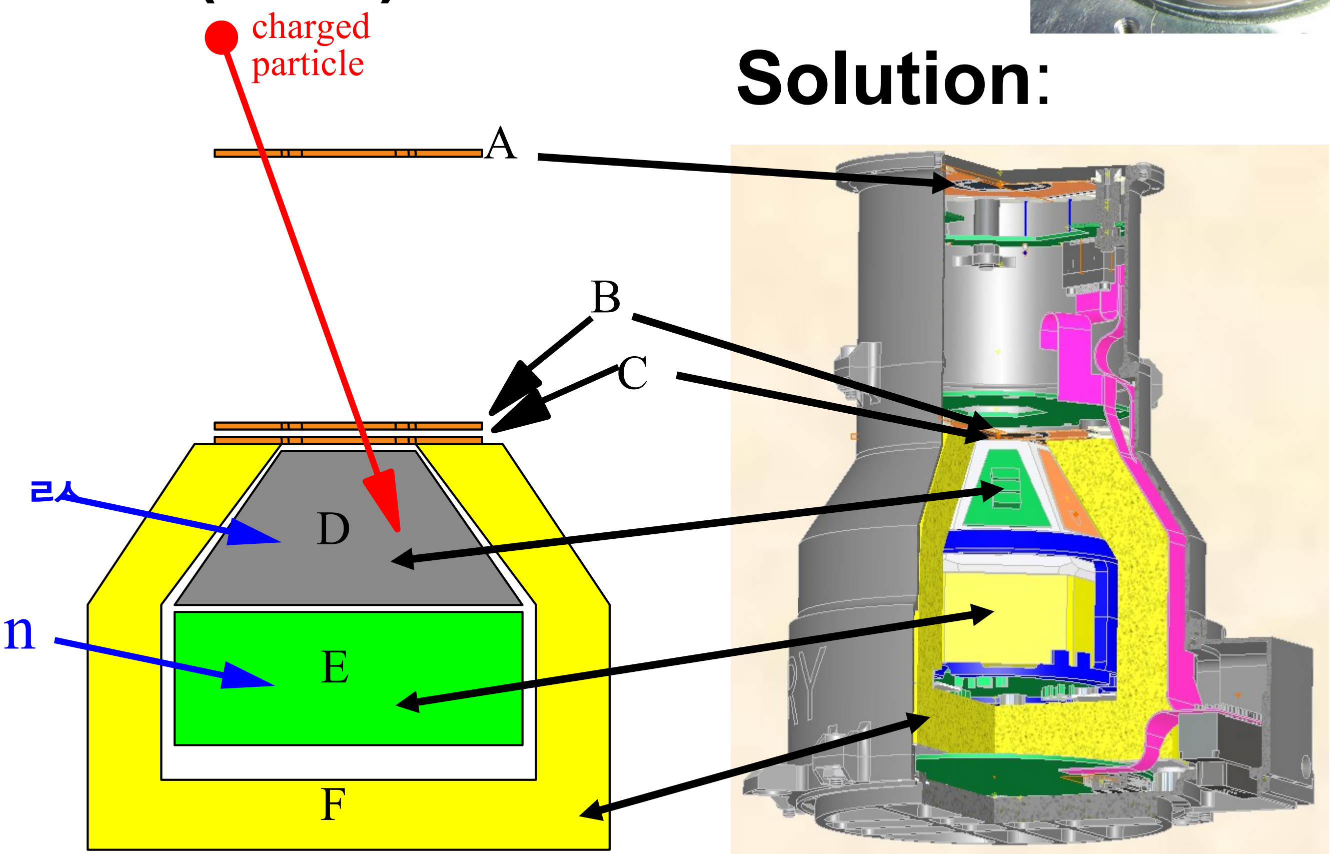

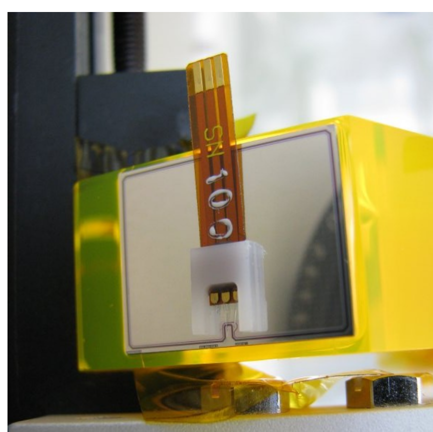

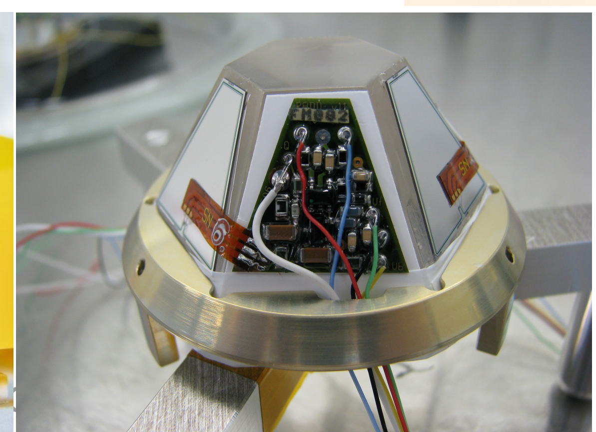

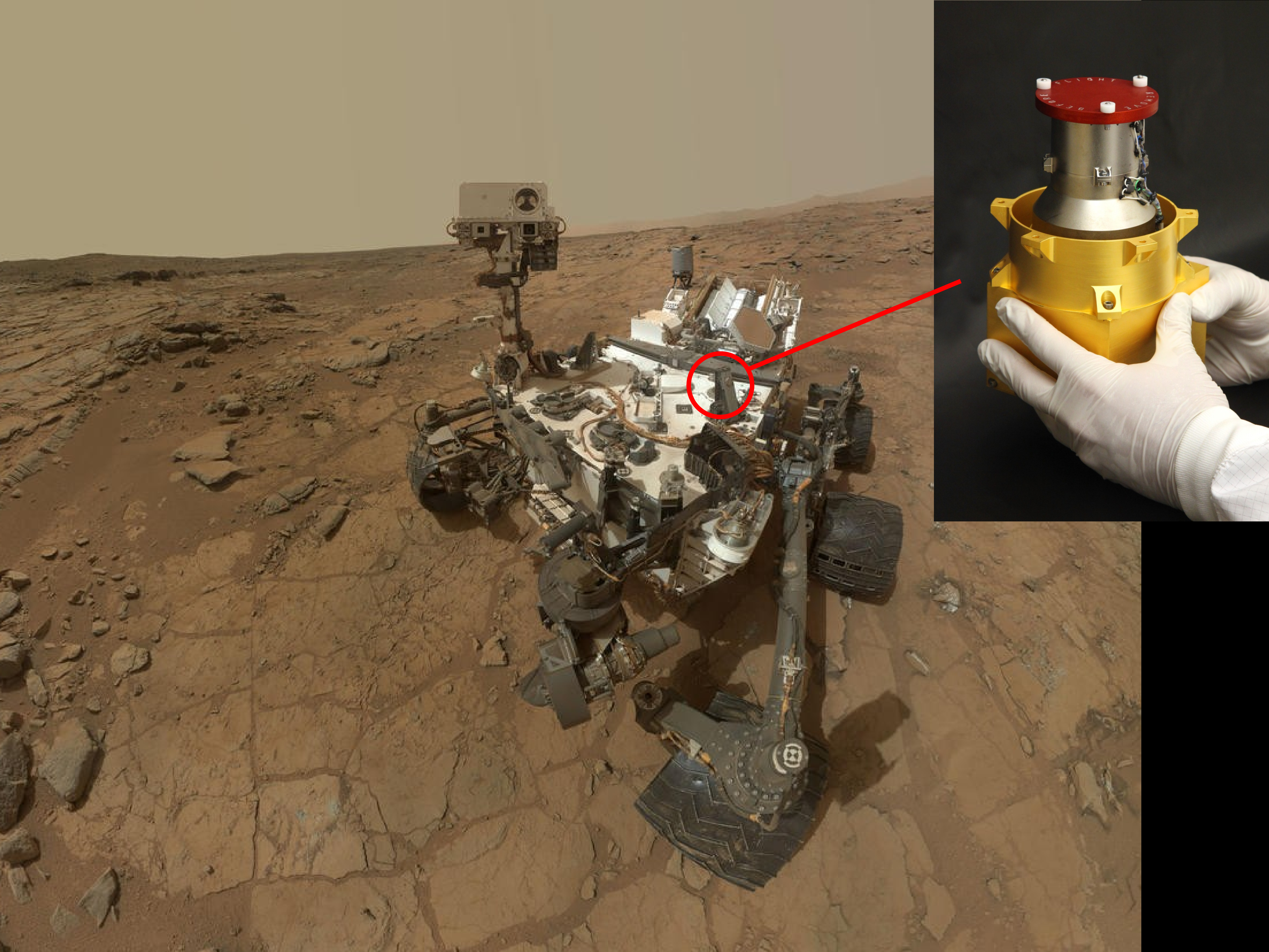

Age determination with cosmogenic isotopes

Nuclear reactions lead to creation of cosmogenic isotopes (here ^{3}He, ^{21}Ne, ^{36}Ar)

Their (relative) abundance is an indicator for the exposure age.

Sheepbed was exposed for only 80 ± 30 million years!

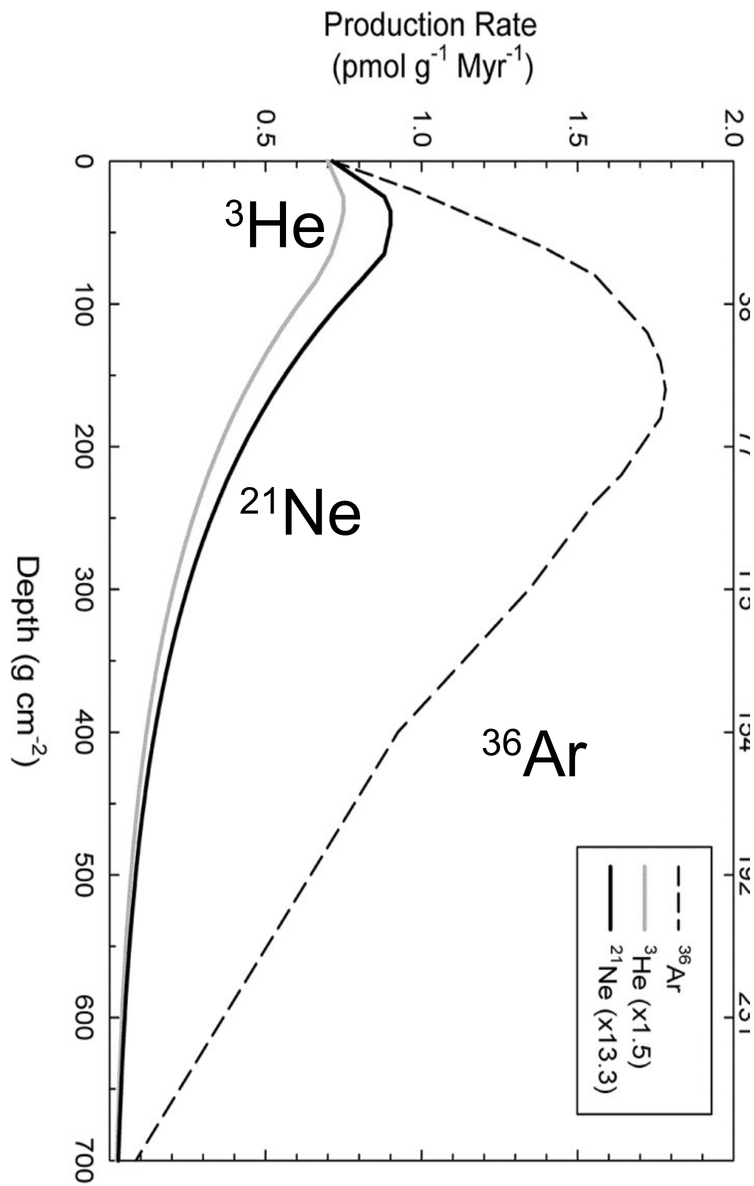

(Farley et al., Science, 2013)

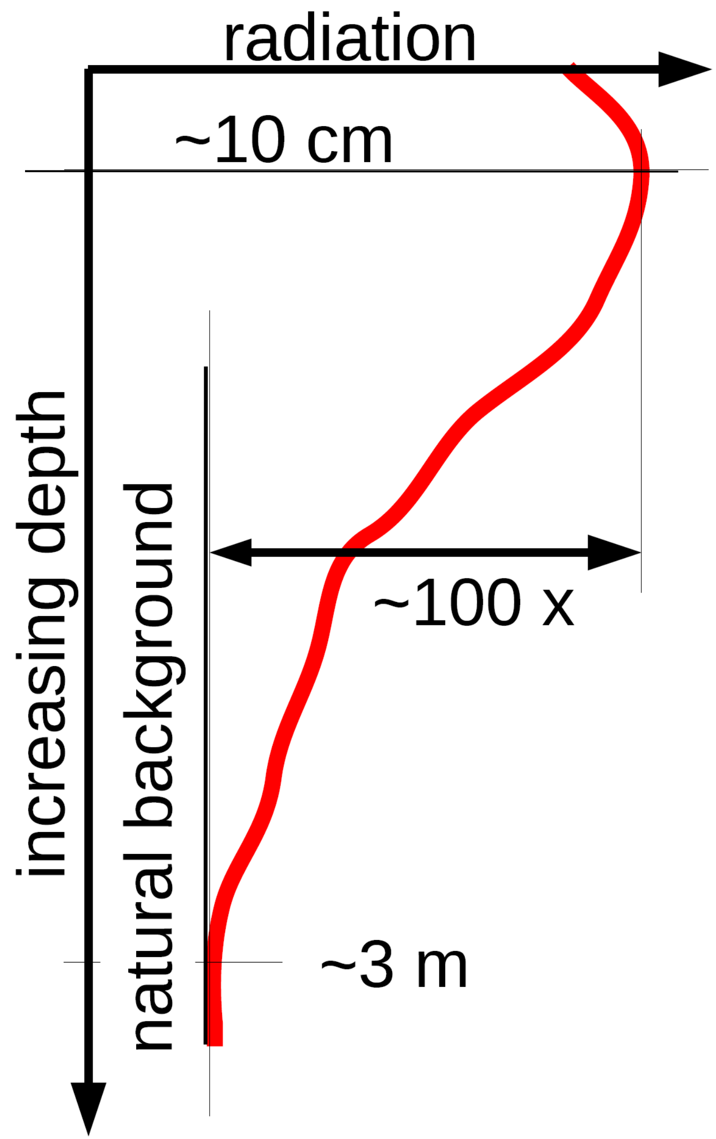

Destruction of Organic Compounds by Radiation

Ionizing radiation breaks chemical bonds and produces radicals and oxidants.

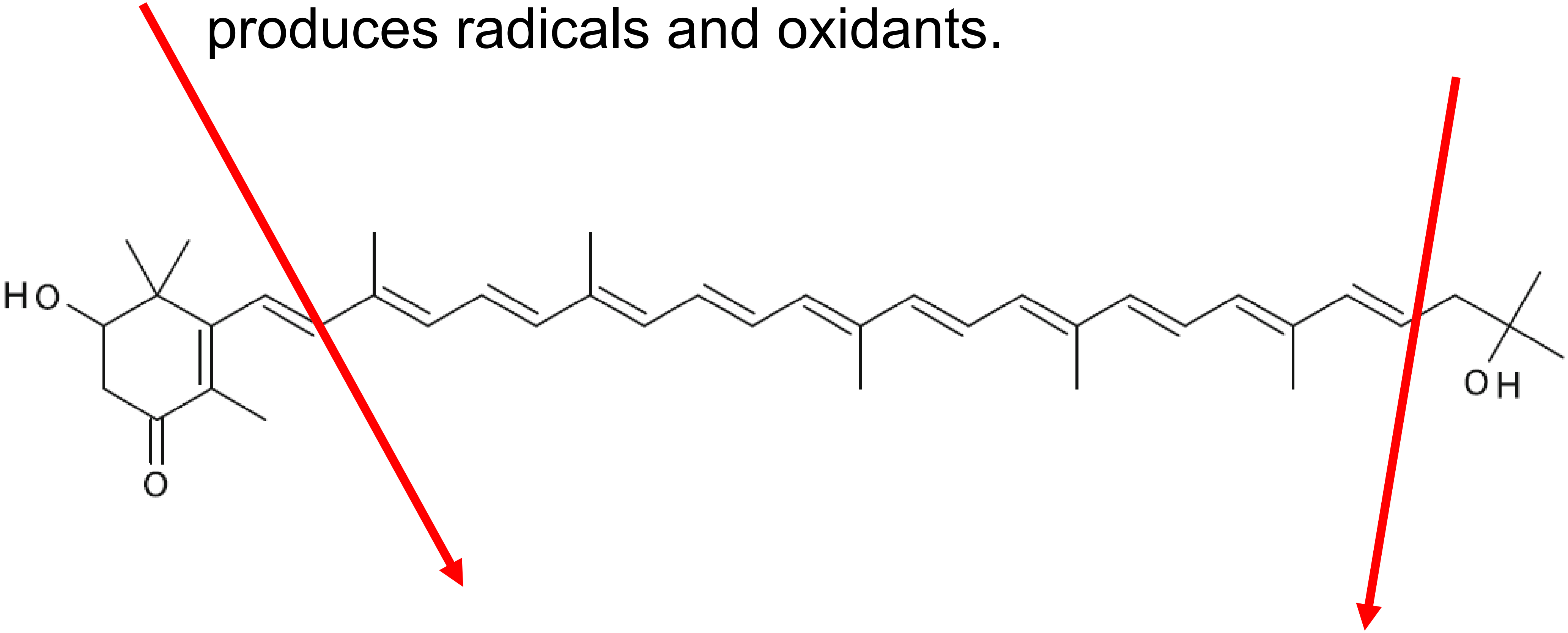

Result: Destruction of large organic molecules (if there is no repair mechanism)

How long could organic molecules survive ionizing radiation environment?

Previous models: 50 – 150 mGy/y
RAD measurements: 76 mGy/y

Organic molecules are efficiently destroyed at a depth of 4-5 cm. In 650 million years only 1/1000 survives.

How many after 3.8 Gy?

==> Half of the organics should still be around if the soil were only exposed for 65 million years.

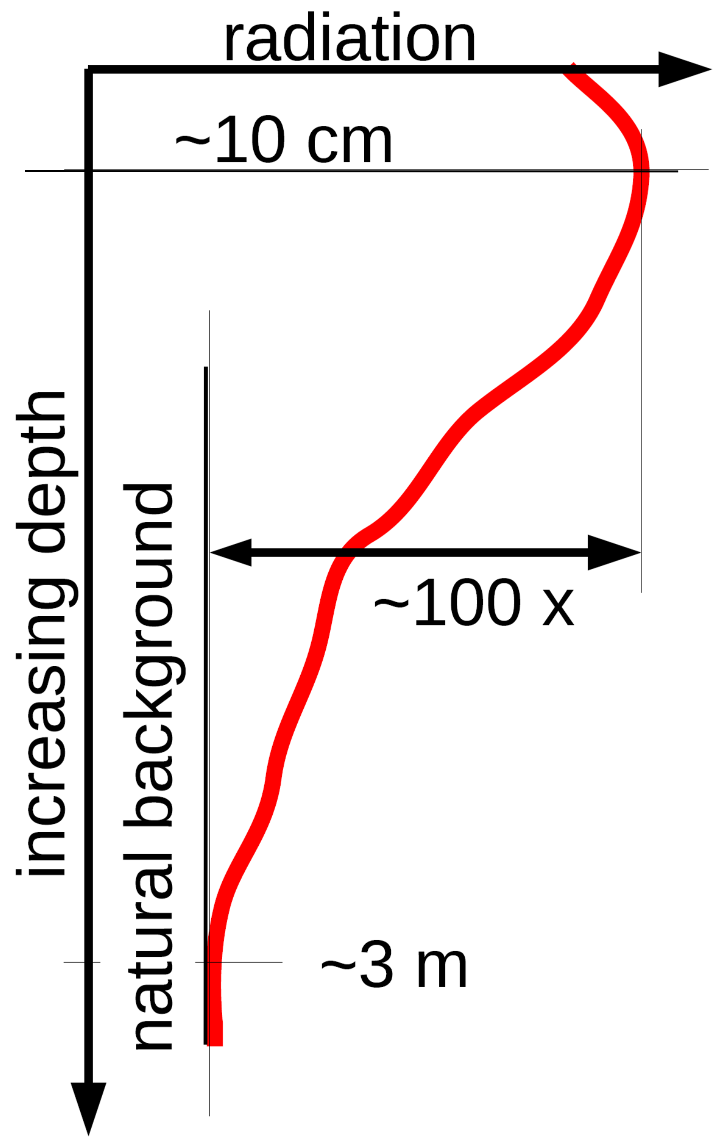

Drill results from SAM

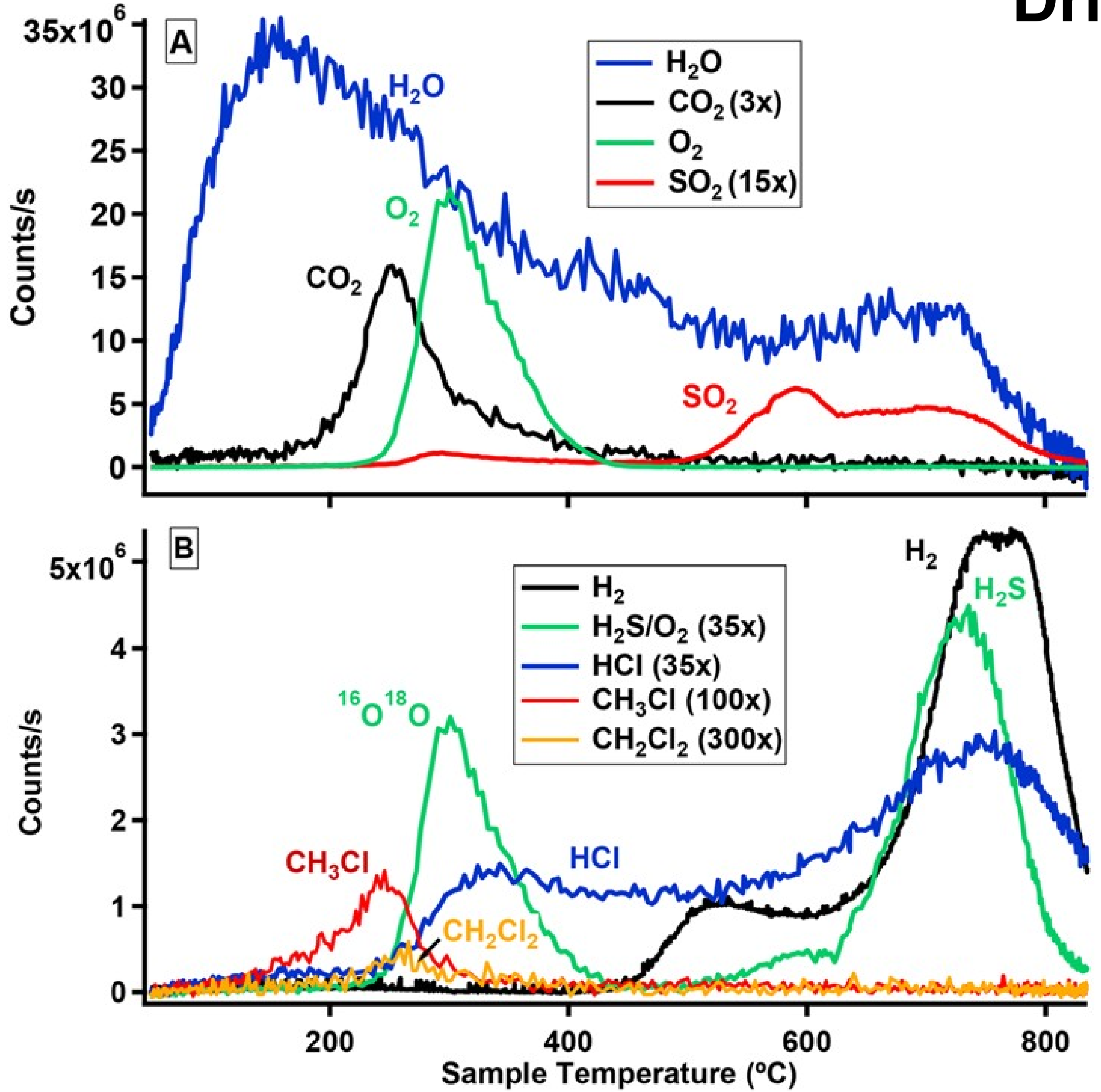

Measurements show that the drilled mudstone contained carbon, nitrogen, oxygen, and sulfur. These elements are needed for life to form.

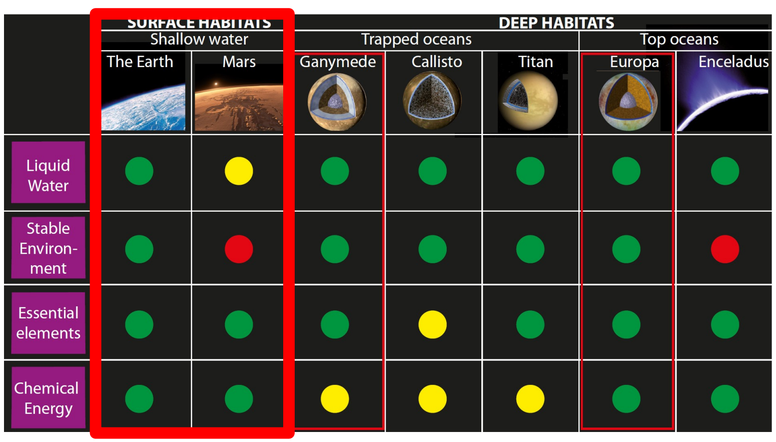

(Ming et al., Science, 2013)

PLANETARY SCIENCE

Science AAAS

NASA Curiosity rover hits organic pay dirt on Mars

Carbon molecules in rocks from ancient lakebed resemble kerogen, a “goopy” fossil fuel building block on Earth

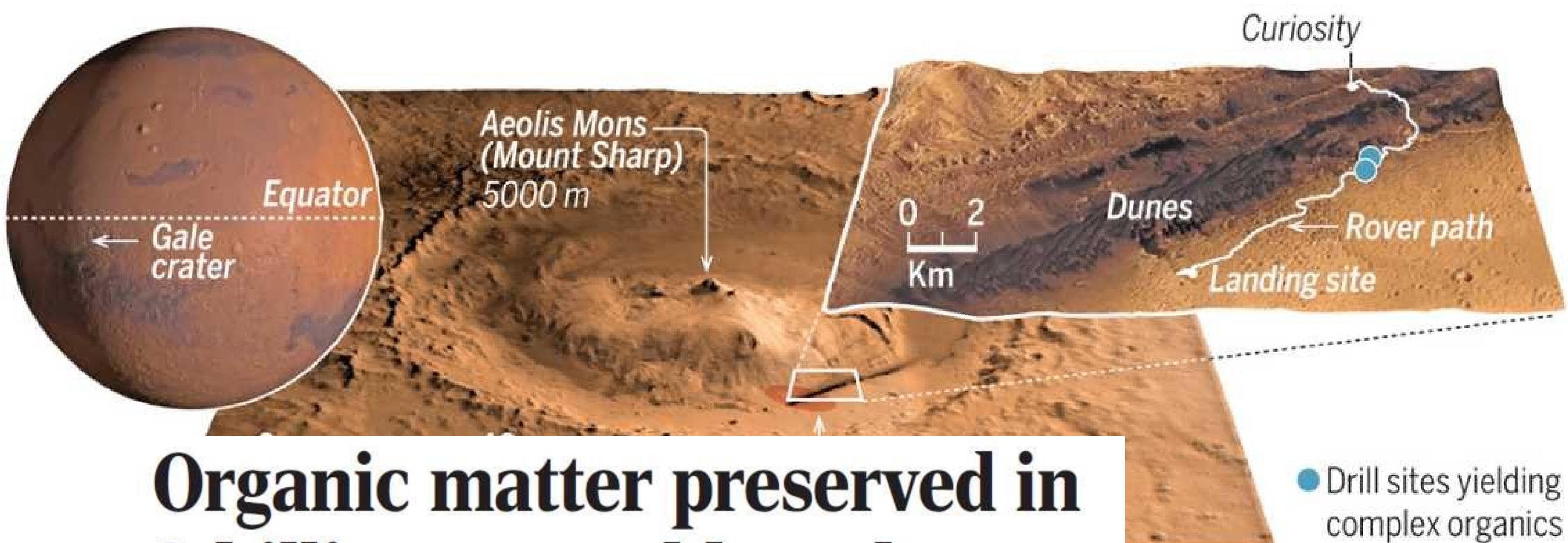

Organic matter preserved in 3-billion-year-old mudstones at Gale crater, Mars

Eigenbrode et al. Science 2018;360:1096

Detection of Methane (CH_4) on Mars

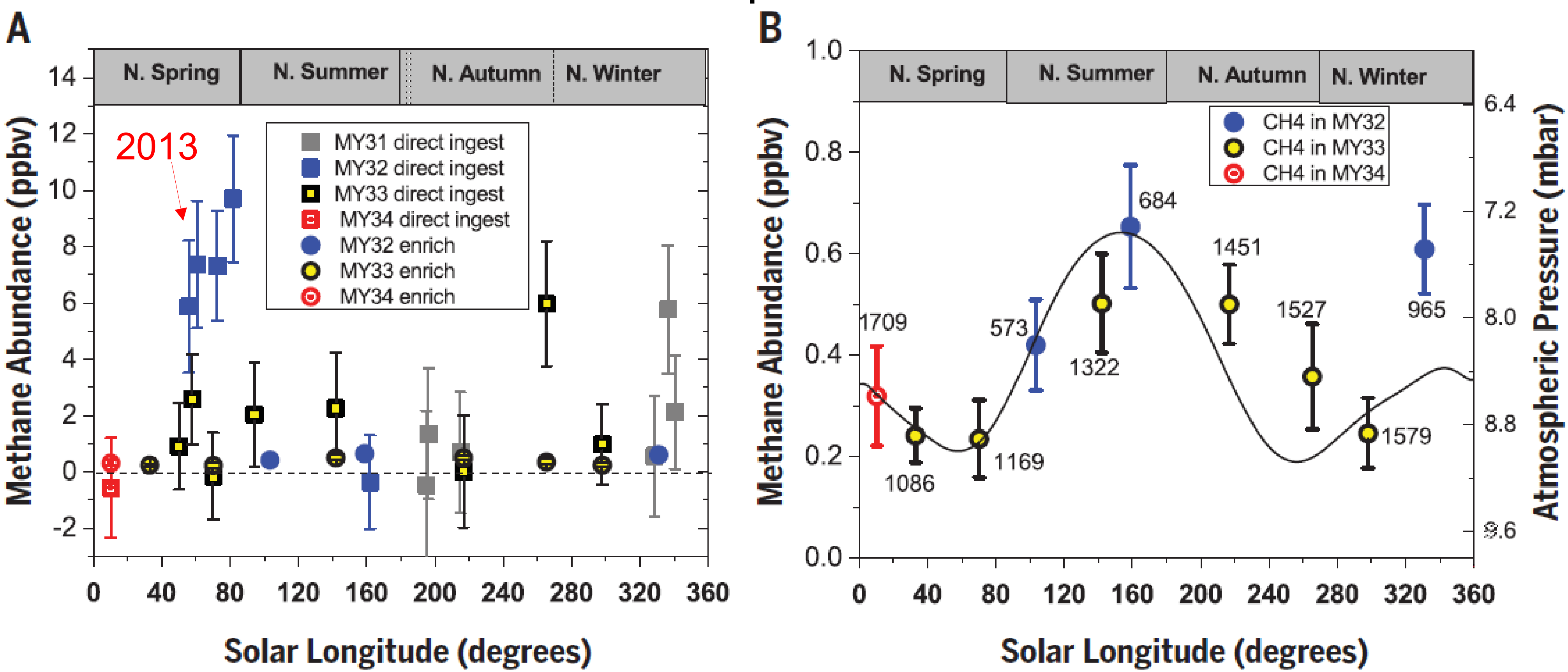

(Webster et al., 2018)

Methane had been detected by Formisano et al. (2004) with ESA‘s Mars Express. CH_4 was seen again in-situ by SAM on MSL in 2013. CH_4 background varies seasonally (Webster et al., 2018)

Detection of Methane (CH_4) on Mars – again!

- MSL-Measurements of 2013 were confirmed by MEX
- **MSL/TLS measured 21 ppbv CH4 on June 19, 2019**
- MEX was above Gale crater at that time
- Why is CH4 so variable on Mars?

For comparison: On Earth the CH4 concentration in pre-industrial times was ~ 700 ppbv, today (2019) it is 1866 ppbv.

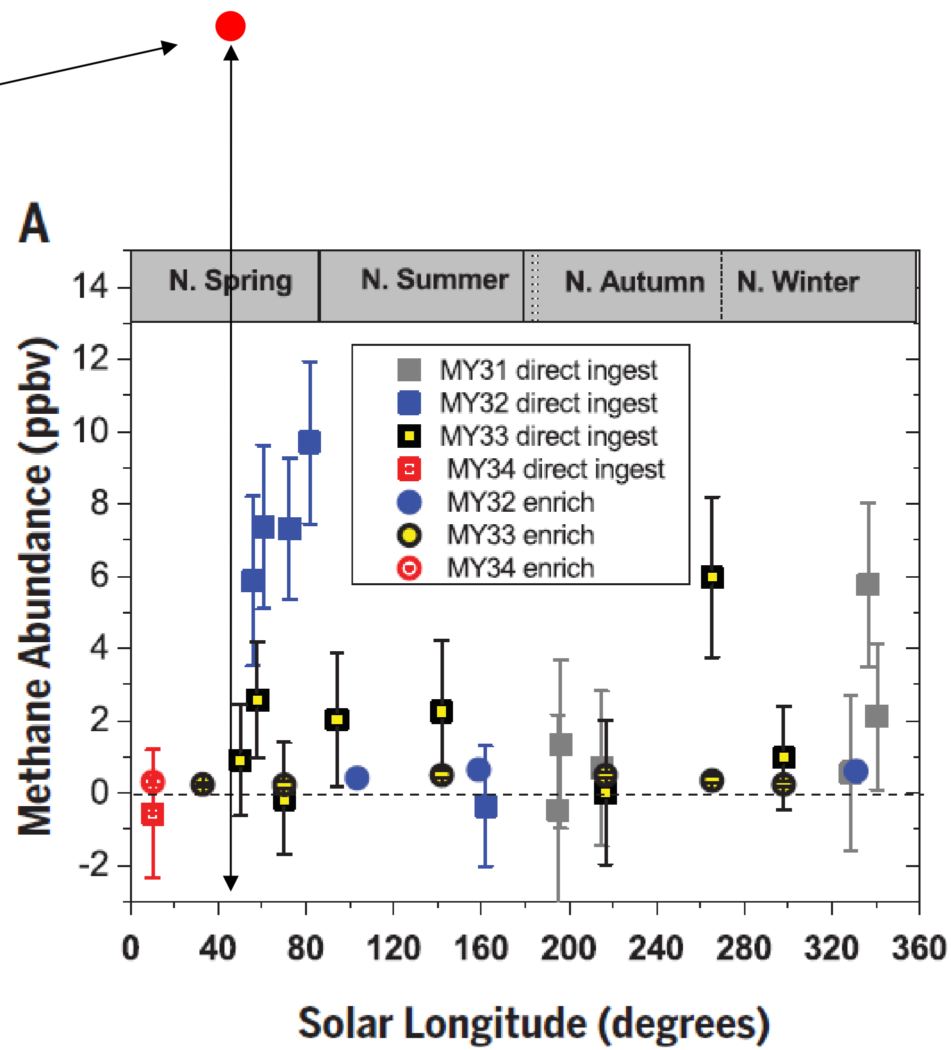

(Webster et al., 2018)

Back to radiation:

Summary of solar particle events seen by MSL/RAD during cruise

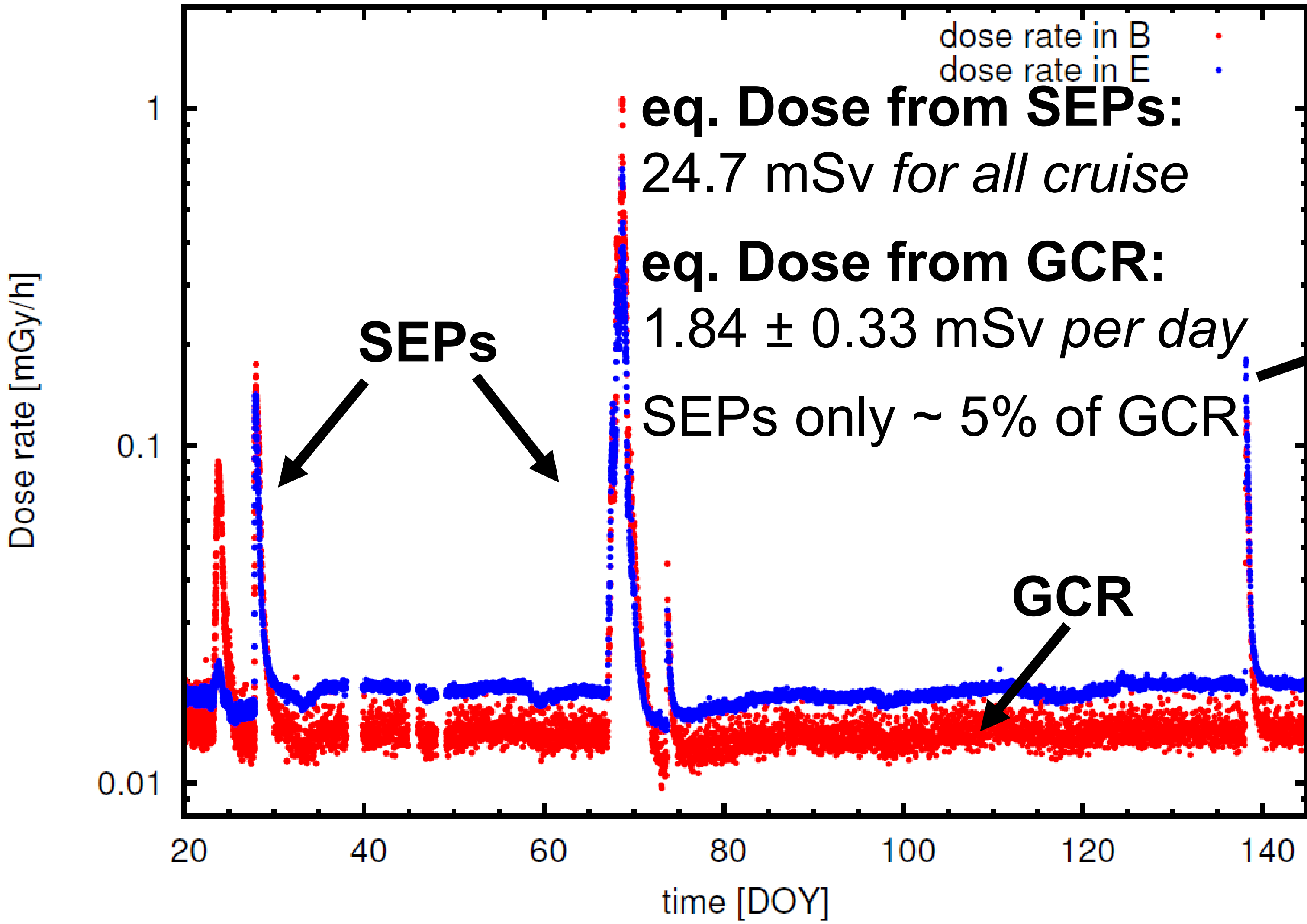

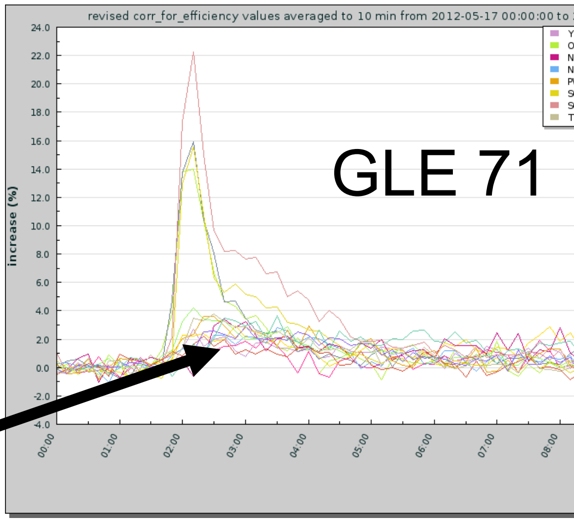

nmdb.eu

GCR dominates radiation exposure during RAD's cruise

Risks Assessments for all DRM*s (Jan 2015)

Human Spaceflight Risks	In Mission Risk - Operations						Post Mission Risk - Long Term Health					
Human Spaceflight Risks 01/12/15	Low Earth Orbit	Low Earth Orbit	Deep Space Sortie	Lunar Visit/Habitation	Deep Space Journey/Habitation	Planetary	Low Earth Orbit	Low Earth Orbit	Deep Space Sortie	Lunar Visit/Habitation	Deep Space Journey/ Habitation	Planetary
	6 Months	12 Months	30 Days	1 year	1 Year	3 years	6 Months	12 Months	30 Days	1 year	1 Year	3 years
VIIP	A	A	A	A	RM	RM	A	A	A	A	RM	RM
Renal Stone Formation	A	A	A	A	RM	RM	RM	RM	RM	RM	RM	RM
Inadequate food and nutrition	A	A	A	A	RM	RM	A	A	A	A	A	RM
Risk of Space Radiation Exposure	A	A	A	A	A	A	A	A	A	RM	RM	RM
Medications Long Term Storage	A	A	A	A	A	RM	A	A	A	A	A	RM
Acute and Chronic Carbon Dioxide	A	A	A	A	RM	RM	A	A	A	A	A	A
inflight Medical Conditions	A	A	A	RM	RM	RM	A	A	A	A	RM	RM
Cognitive or Behavioral Conditions	A	A	A	A	RM	RM	A	A	A	RM	RM	RM
Risk of Bone Fracture	A	A	A	A	A	A	A	A	A	A	A	RM
Team Performance Decrements#	A	A	A	A	RM	RM	A	A	A	A	A	A
Reduced Muscle Mass, Strength	A	A	A	A	A	RM	A	A	A	A	A	A
Reduced Aerobic Capacity	A	A	A	A	A	RM	A	A	A	A	A	A
Sensorimotor Alterations	A	A	A	A	A	RM	A	A	A	A	A	RM
Human-System Interaction Design#	A	A	A	RM	RM	RM	A	A	A	A	A	A
Injury from Dynamic Loads	A	A	RM	RM	RM	RM	A	A	RM	RM	RM	RM
Sleep Loss	A	A	A	A	RM	RM	A	A	A	A	RM	RM
Altered Immune Response	A	A	A	A	RM	RM	A	A	A	A	A	RM
Celestial Dust Exposure	N/A	N/A	A	TBD	TBD	TBD	N/A	N/A	A	TBD	TBD	TBD
Host-Microorganism Interactions	A	A	A	A	RM	RM	A	A	A	A	A	RM
Injury due to EVA Operations	A	A	A	RM	A	RM	A	A	A	RM	RM	RM
Decompression Sickness	A	A	A	A	RM	A	A	A	A	RM	A	RM
Toxic Exposure	A	A	A	A	A	A	A	A	A	A	A	A
Hypobaric Hypoxia	A	A	A	A	A	A	A	A	A	A	A	A
Space Adaptation Back Pain	A	A	A	A	A	A	N/A	N/A	N/A	N/A	N/A	N/A
Urinary Retention	A	A	A	A	A	A	A	A	A	A	A	A
Hearing Loss Related to Spaceflight	A	A	A	A	A	A	A	A	A	A	A	A
Orthostatic Intolerance	A	A	A	A	A	A	A	A	A	A	A	A
Injury from Sunlight Exposure - retired	A	A	A	A	A	A	A	A	A	A	A	A
Risk of electrical shock - Retired	A	A	A	A	A	A	A	A	A	A	A	A

A – Accepted RM- Requires Mitigation

Green – controlled Yellow - partially controlled Red uncontrolled

* Design Reference Mission

Summary of radiation exposure seen by MSL/RAD during cruise

Quantity	value	Estimated variability	Two 180-day legs return trip
RAD cruise measurement SEPs	**24.7 mSv (5% of all)**	**Orders of magnitude**	**?**
RAD cruise measurement GCR	**1.84 mSv/d**	**0.33 mSv/d ± 20%**	**= 662 ± 108 mSv ± 20%**
6-month stay of astronaut on ISS	75-90 mSv/(a/2)	20%	150-180 mSv
Radiation worker limit (ICRP)	20 mSv/a	n/a	
Average exposure of normal population	4 mSv/a	Wide range, radon!	
Allowable additional exposure norm. pop.	1 mSv/a	n/a	

Summary of radiation exposure for a manned mission to Mars based on MSL/RAD measurements

Radiation exposure on a mission to Mars:

Cruise: 662 +/- 108 mSv
Mars: 320 +/- 50 mSv

Total ~ 1000 mSv

For comparison:
6 months ISS: 75-90 mSv
radiation worker: 20 mSv/y
CT-scan: 8 mSv

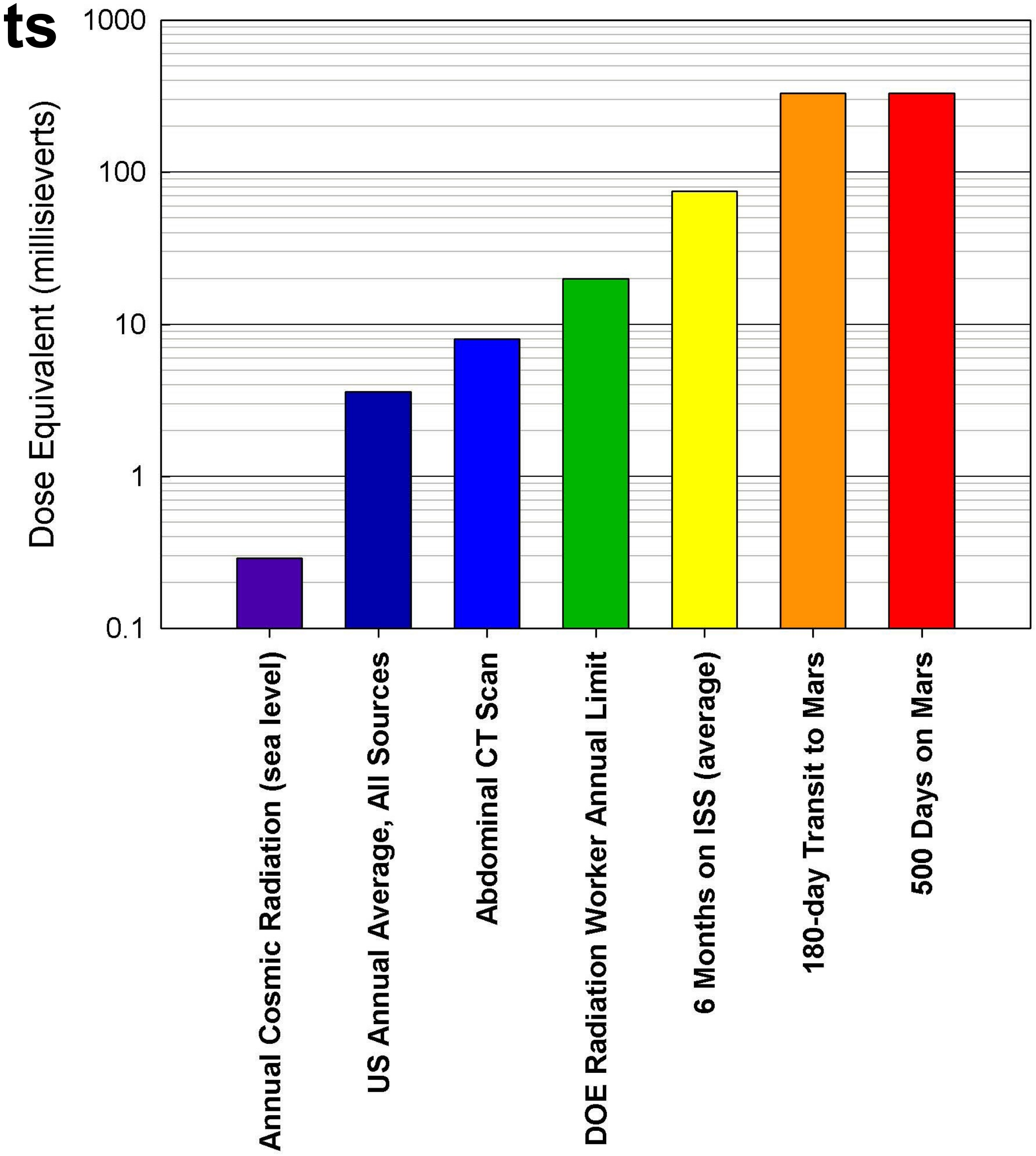

(Zeitlin et al., Science, 2013)

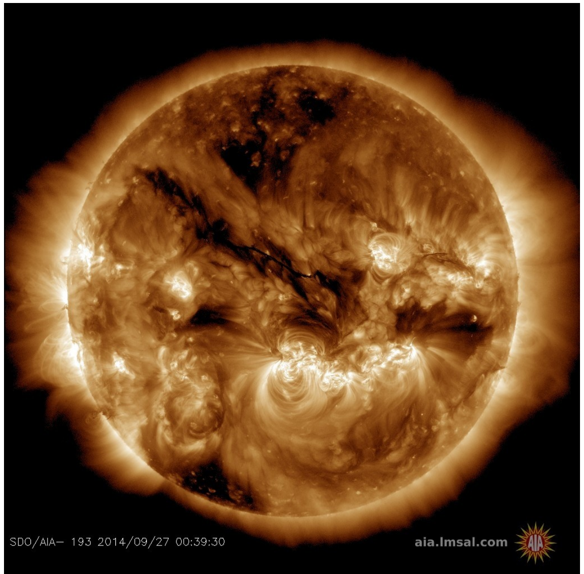

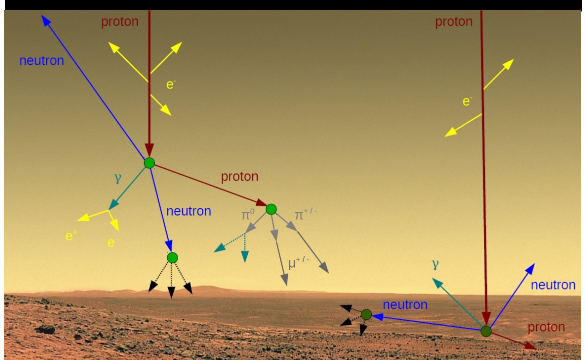

Implications for human exploration

- Particle radiation is complex!
- Space weather predictions are still very difficult
- Large variability (solar, heliospheric, seasonal, diurnal)
- Secondary radiation important (n/γ)
- Where should we live on Moon & Mars?
- Implications for non-terrestrial life? Exo-, astrobiology?

Conclusions:

Space radiation is influenced by a number of factors:
- solar corona
- solar wind
- transport phenomena
- heliosphere

Space radiation is important to
- understand the history of the solar system
- understand the habitability of (exo-) planets and moons
- prepare for human exploration of the solar system

謝謝